International Journal of Biological Macromolecules

Carboxymethyl chitosan Dopamine Conjugates: Synthesis and Evaluation for Intranasal anti Parkinson Therapy

--Manuscript Draft--

Manuscript Number:	IJBIOMAC-D-23-07156R2
Article Type:	Research Paper
Section/Category:	Carbohydrates, Natural Polyacids and Lignins
Keywords:	Polymeric conjugates; dopamine; storage stability
Corresponding Author:	Adriana Trapani University of Bari Department of Pharmacy and Pharmacology Bari, ITALY
First Author:	Adriana Trapani
Order of Authors:	Adriana Trapani
	Sante Di Gioia
	Giuseppe Fracchiolla
	Stefania Cometa
	Filippo Maria Perna
	Andrea Francesca Quivelli
	Concetta Nobile
	Massimo Conese
	Valeria Daniello
	MdNiamat Hossain
	Giuseppe Trapani
Abstract:	With respect to the Parkinson disease (PD), herein, we aimed at synthetizing and characterizing two novel macromolecular conjugates where dopamine (DA) was linked to N,O-carboxymethyl chitosan or O-carboxymethyl chitosan, being both conjugates obtained from an organic solvent free synthetic procedure. They were characterized by FT-IR, 1H-NMR spectroscopies, whereas thermal analysis (including Differential Scanning Calorimetry and Thermal Gravimetric Analysis) revealed good stability of the two conjugates after exposure at temperatures close to 300°C. Release studies in simulated nasal fluid elucidated that a faster release occurred since O-carboxymethyl chitosan-DA conjugate maybe due to the less steric hindrance exerted by the polymeric moiety. The CMCS-DA conjugates prepared in aqueous medium may self-assembly to form polymeric micelles and/or may form polymeric nanoparticles. TEM and Photon correlation spectroscopy lent support for polymeric nanoparticle formation. Moreover, such CMCS-DA conjugates showed antioxidant activity, as demonstrated by DPPH radical scavenging assay. Finally, cytocompatibility studies with neuroblastoma SH-SY5Y cells showed no cytotoxicity of both conjugates, whereas their uptake increased from 2.5 to 24 h and demonstrated in 40-66% of cells.
Suggested Reviewers:	Mariano Licciardi mariano.licciardi@unipa.it
	Alvaro Mata a.mata@qmul.ac.uk
	Carmen Gutierrez Millan carmen.gutierrez@usal.es
Opposed Reviewers:	
Response to Reviewers:	

DIPARTIMENTO DI FARMACIA-SCIENZE DEL FARMACO

Prof. Dr. Adriana Trapani

Università degli Studi di Bari

Via E. Orabona 4

70125 BARI (Italy)

Tel. +39-080-544-2114. Fax +39-080-5442724.

e-mail: adriana.trapani@uniba.it

August 30, 2023

To the Editor of

International Journal of Biological Macromolecules

Dr. Daniela Giacomazza

Institute of Biophysics Italian National Research Council

90121-Palermo,

Italy

Dear Editor,

Please find enclosed the manuscript entitled **"Carboxymethyl chitosan Dopamine Conjugates: Synthesis and Evaluation for Intranasal anti Parkinson Therapy"** by S. Di Gioia et al. submitted to *the International Journal of Biological Macromolecules*. This is the revised version of the manuscript number: IJBIOMAC-D-23-07156R1 according to your mail message of August 26, 2023. In the manuscript all changes referring to the decision of 26 August 2023 are highlighted in yellow in order to report them together with the previously revised version sent on August 18, 2023 written in red colour. In a separate document, the reply to the Reviewers' comments is also sent to the Editorial office.

We would like to thank the Reviewers for their useful comments which allowed us to improve the quality of the manuscript.

At this regard, the main changes are below listed:

1) Figures 2, 8, 9 and 10 were provided with higher resolution (as mentioned in the revised manuscript) and sent to the Editorial Office;
2) Figure 6 and Table 2 were edited;
3) In the Introduction section, the aims of the work were better pointed out;

4) Changes in the text occurred in the Results and Discussion Sections mainly concerning the models of *in vitro* release studies of the conjugates as well as the self-assembly process occurring in aqueous environment.
5) Three more references were added in the revised manuscript;
6) The revised Figure caption Section was also provided.

We hope that the manuscript is now suitable for publication in *International Journal of Biological Macromolecules*. All the co-authors and I confirm that neither the manuscript nor any parts of its content are currently under consideration or published in another Journal. All authors have approved such further revision of the manuscript to *International Journal of Biological Macromolecules*.

I look forward to hearing from you in the next future.

Sincerely yours,

Prof. Adriana Trapani

Corresponding author

Editor and Reviewer comments:

Q. One of the Reviewers is not satisfied of the response to her/his comments about a model to represent the release profile. So, I invite the Authors to go carefully through the previous referee comments, give more exhaustive and precise answers and revise accordingly the manuscript.

R. Being not clearly stated what is the specific reason for which one of the Reviewers was not satisfied about the model used by us to represent the release profile, we supposed that it could be due either to the unknown solubility of amide conjugates **2** and **3** or to the limited number of data points employed in these calculations. In the revised version, we have inserted on page 13 a paragraph where the release kinetic data of amide conjugates **2** and **3** are discussed in the light of the Juriga et al.'s work (Acta Biomater 76 (2018) 225-238.), considering these polymer-DA conjugates very soluble in water or, alternatively, poorly soluble in this last solvent. Thus, we provide two novel panels (i.e., panels c and d) in Figure 6 and the novel Table 2 to express appropriate drug release data and to provide a deeper interpretation from a mechanism/theory point of view of these data, to understand the use of the conjugates. The important conclusion of this release kinetic study was that conjugate **3** provides a DA release quicker and in greater extent than conjugate **2** since the k_1 (first order kinetic rate constant) or K_H (Higuchi diffusion parameter) values of the former are higher than the corresponding of the latter. It in both the circumstances examined i.e., whether they should be considered poorly- or, alternatively, very-soluble in water. Thus, such chitosan-based nanocarrier conjugate **3** possess promising properties for brain delivery by intranasal administration.

Q. Please improve the resolution of the figures.

R. In this revised version, we made any possible effort to improve the resolution of figures. In details, the resolution of Figures 2, 8, 9 and 10 was increased and the edited Figures were mentioned in the manuscript and also sent to the Editorial Office.

Reviewer's Responses to Questions
Note: In order to effectively convey your recommendations for improvement to the author(s), and help editors make well-informed and efficient decisions, we ask you to answer the following specific questions about the manuscript and provide additional suggestions where appropriate.

1. Are the objectives and the rationale of the study clearly stated?
Please provide suggestions to the author(s) on how to improve the clarity of the objectives and rationale of the study. Please number each suggestion so that author(s) can more easily respond.

Reviewer #1: I don't find any authors response wrt reviewers comments. Please provide the same so that the recommendation is possible and answers to the questions.
Our apologies for this inconvenient probably due to our limited experience with Reviewer's Responses by using a questionnaire.

R1. We thank the Reviewer for this comment since offer us the opportunity to improve the presentation and discussion of our results at level of drug release studies. In the revised version, we

have inserted on page 13 a paragraph where the release kinetic data of conjugates **2** and **3** are discussed in the light of the Juriga et al.'s work (Acta Biomater 76 (2018) 225-238.), considering these polymer-DA conjugates very soluble in water or, alternatively, poorly soluble in this last solvent. Thus, we provide two novel panels (i.e., panels c and d) in Figure 6 and the novel Table 2 to express appropriate drug release data and to provide a deeper interpretation from a mechanism/theory point of view of these data, to understand the use of the conjugates.
As for the objectives and the rationale of the study, besides to state that our aim was to evaluate whether it is possible to develop a synthetic approach employing water as solvent together with to assess whether the position of the carboxymethyl substituent on the chitosan backbone could influence the features of the resulting conjugates, in the Introduction section of the revised version (decision August, 26) we have added as follows. "In particular, our aim was also to evaluate from which conjugate a greater amount of DA release occurs since it is well known that amide bonds are hydrolyzed very slowly, resulting sometimes in excessively slow release and, therefore, unacceptable from a practical point of view. In addition, it was also our interest to know from which conjugate a higher internalization by cells occurs". It in order to improve the clarity of the objectives and rationale of the study.

Reviewer #2: Yes

---

2. If applicable, is the method/study reported in sufficient detail to allow for its replicability and/or reproducibility?

Please provide suggestions to the author(s) on how to improve the replicability/reproducibility of their study. Please number each suggestion so that the author(s) can more easily respond.

Reviewer #1: Mark as appropriate with an X:

Yes [] No [x] N/A []

Provide further comments here: I don't find any authors response wrt reviewers comments. Please provide the same so that the recommendation is possible and answers to the questions.

Please, find our apologies as mentioned above.

R2. We have made every effort to describe in sufficient detail any method/study reported in this manuscript to allow for its replicability/reproducibility. Actually, the description at level of drug release studies in the original version was partial and important aspects were neglected and missing at all. In the revised version, we have inserted on page 13 a paragraph where the release kinetic data of conjugates **2** and **3** are discussed in the light of the Juriga et al.'s work (Acta Biomater 76 (2018) 225-238.), considering these polymer-DA conjugates very soluble in water or, alternatively, poorly soluble in this last solvent. We think that in the last revision of the manuscript the mentioned gap has been filled considerably improving the quality of presentation of the same manuscript. We thank the Reviewer for this comment.

Reviewer #2: Mark as appropriate with an X: Yes [] No [] N/A [X]

Provide further comments here:

---

3. If applicable, are statistical analyses, controls, sampling mechanism, and statistical reporting (e.g., P-values, CIs, effect sizes) appropriate and well described?

Please clearly indicate if the manuscript requires additional peer review by a statistician. Kindly provide suggestions to the author(s) on how to improve the statistical analyses, controls, sampling mechanism, or statistical reporting. Please number each suggestion so that the author(s) can more easily respond.

Reviewer #1: Mark as appropriate with an X:

Yes [] No [x] N/A []

Provide further comments here: I don't find any authors response wrt reviewers comments. Please provide the same so that the recommendation is possible and answers to the questions.

Please, find our apologies as mentioned above.

R.3 We believe that statistical analyses, controls, sampling mechanism and statistical reporting are appropriate and well described. In the revised manuscript, we have also made it clear that multiple comparisons were based on one-way analysis of variance (ANOVA) with Bonferroni or Tukey post hoc test and differences were considered significant when $p < 0.05$.

Reviewer #2: Mark as appropriate with an X: Yes [] No [] N/A [X]

Provide further comments here:

---

4. Could the manuscript benefit from additional tables or figures, or from improving or removing (some of the) existing ones?

Please provide specific suggestions for improvements, removals, or additions of figures or tables. Please number each suggestion so that author(s) can more easily respond.

Reviewer #1: I don't find any authors response wrt reviewers comments. Please provide the same so that the recommendation is possible and answers to the questions.

Please, find our apologies as mentioned above.

R 4. The insertion of Table 2 and Figure 6 panels c) and d) markedly improved the quality of presentation and discussion of our results at level of drug release studies. Moreover, we made any possible effort to improve the resolution of some figures and in such a way the manuscript benefits, in our opinion.

Reviewer #2: The clarity of some figures is poor.

R.4 In this revised version, we made any possible effort to improve the resolution of some figures.

---

5. If applicable, are the interpretation of results and study conclusions supported by the data?

Please provide suggestions (if needed) to the author(s) on how to improve, tone down, or expand the study interpretations/conclusions. Please number each suggestion so that the author(s) can more easily respond.

Reviewer #1: Mark as appropriate with an X: Yes [] No [x] N/A []

Provide further comments here: I don't find any authors response wrt reviewers comments. Please provide the same so that the recommendation is possible and answers to the questions.

Please, find our apologies as mentioned above.

R.5 We believe that the interpretation of the results and corresponding conclusions relative to the study reported in this manuscript are based on sound methodology that is part of the expertise of the authors as a whole. Thus, as for the synthetic aspects of this study, they are based on spectroscopic findings (mainly ^{1}H NMR). The data of physical stability of CMCS-DA conjugates are supported by TGA and DSC outcomes, while the results concerning the storage stability are based on the hydrolysis of these CMCS-DA conjugates under strong conditions and successive determination of the free DA amount by HPLC to assess DS%. Thanks to a Reviewer comment we improved the presentation and discussion of the drug release studies. In the revised version, we have inserted on page 13 a paragraph where the release kinetic data of conjugates **2** and **3** are discussed in the light of the Juriga et al.'s work (Acta Biomater 76 (2018) 225-238.). Thus, the important conclusion has been deduced that the chitosan-based nanocarrier conjugate **3** possesses promising properties for brain delivery by intranasal administration. Most interesting are also the findings concerning the possibility that conjugates **2** and **3** can self-assemble to form nanosized structures and it is supported by TEM analysis and Photon Correlation Spectroscopy results. We have mentioned in the revised manuscript that in a successive work we wish to complete the characterization of these nanosized-structures by studying, in particular, their surface features (to assess, inter alia, the neurotransmitter localization in the nanosized structure) and mucoadhesive properties. The antioxidant activity of conjugates **2** and **3** has been demonstrated by the DPPH test most employed in literature for this purpose. As for the cytotoxicity towards SH-SY5Y cells and uptake of amide conjugates by SH-SY5Y cells, these studies have been performed by the well-established MTT test and Flow Cytometry measurements, respectively.

Reviewer #2: Mark as appropriate with an X: Yes [X] No [] N/A []

Provide further comments here:

---

6. Have the authors clearly emphasized the strengths of their study/methods?

Please provide suggestions to the author(s) on how to better emphasize the strengths of their study. Please number each suggestion so that the author(s) can more easily respond.

Reviewer #1: I don't find any authors response wrt reviewers comments. Please provide the same so that the recommendation is possible and answers to the questions.

Please, find our apologies as mentioned above.

R.6. In our opinion, we have appropriately pointed out in the manuscript that conjugate **3** provides a DA release quicker and in greater extent than conjugate **2**. These release kinetic features make the amide **3** promising candidate for neurotransmitter delivery by intranasal administration resulting the corresponding DA release not excessively long and, thus, acceptable from a practical point of view. Further favourable characteristics of conjugate **3** evidenced in the manuscript are its DPPH radical scavenging activity as well as its uptake increased compared with conjugate **2**.

Reviewer #2: Yes

---

7. Have the authors clearly stated the limitations of their study/methods?

Please list the limitations that the author(s) need to add or emphasize.

Please number each limitation so that author(s) can more easily respond.

Reviewer #1: I don't find any authors response wrt reviewers comments. Please provide the same so that the recommendation is possible and answers to the questions.

Please, find our apologies as mentioned above.

R. 7 In our opinion, we have appropriately pointed out in the manuscript also some limitations of our study. Thus, we have already mentioned above that in a successive work we wish to complete the characterization of the nanosized-structures formed by self-assembly of conjugate **2** and **3**. Moreover, also from a synthetic point of view, we need to optimize the polymer/neurotransmitter weight ratio in order to maximize the production yield of conjugates and the substitution degree and also these aspects we wish to complete in a successive work. On the other hand, we have clearly specified in the manuscript that the calculations relative to the release kinetic of DA from conjugates **2** and **3** are based on a limited number of data points and it was the consequence to follow the release for a long time (i.e., fifteen days). However, we evidenced in the manuscript that, even though these calculations are based on a limited number of data points, a certain trend may be deduced. Moreover, we have clearly stated in the manuscript that, being unknown the solubility features of conjugate **2** and **3**, we performed the mentioned calculations, considering them poorly or, alternatively, soluble enough in water.

Reviewer #2: Yes

---

8. Does the manuscript structure, flow or writing need improving (e.g., the addition of subheadings, shortening of text, reorganization of sections, or moving details from one section to another)?

Please provide suggestions to the author(s) on how to improve the manuscript structure and flow. Please number each suggestion so that author(s) can more easily respond.

Reviewer #1: I don't find any authors response wrt reviewers comments. Please provide the same so that the recommendation is possible and answers to the questions.

Please, find our apologies as mentioned above.

R.8 We think that the manuscript structure does not need improving. In particular, in our opinion it does not need addition of subheadings or shortening of text or reorganization of sections, or moving details from one section to another.

Reviewer #2: No

---

9. Could the manuscript benefit from language editing?

Reviewer #1: No

Reviewer #2: No

Reviewer #1: This field is optional. If you have any additional suggestions beyond those relevant to the questions above, please number and list them here.

I don't find any authors response wrt reviewers comments. Please provide the same so that the recommendation is possible and answers to the questions.

Please, find our apologies as mentioned above.

R.9 We agree with the Reviewer that the manuscript does not need language editing.

Reviewer #2: The authors have addressed most of the issues, and the quality of the manuscript is improved. But there are some minor issues should be addressed.

1. The quality of the some pictures should be improved.

2. What is the yield of the nanoparticles (micelles) ? The authors should provided it in the manuscript.

3. The manuscript is lack of information about the polysaccharides based drug delivery. Some more detailed information required need to be included.

For example: CARBOHYDRATE POLYMERS,DOI 10.1016/j.carbpol.2022.119509

R. 9.1. In this revised version, we made any possible effort to improve the resolution of figures. The resolution of Figures 2, 8, 9 and 10 was increased and the edited Figures were mentioned in the manuscript and also sent to the Editorial Office.

R. 9.2. As mentioned above, in a successive work we wish to complete the characterization of the nanosized-structures formed by self-assembly of conjugate **2** and **3** also including their production yield calculation.

R.9.3. We thank the Reviewer for this comment because offers the possibility to evidence the difference between the hydrophobic domains of the classical polymeric micelles with those proposed by us for the self-assembly process of *N,O*- or *O*-CMCS-DA conjugates **2** and **3**. In the revised version of the manuscript on page 18 a new paragraph has been included where we discuss about hydrophobic domains of the classical polymeric micelles compared with those proposed for the self-assembly process of conjugates **2** and **3**.

Abstract

With respect to the Parkinson disease (PD), herein, we aimed at synthetizing and characterizing two novel macromolecular conjugates where dopamine (DA) was linked to *N,O*-carboxymethyl chitosan or *O*-carboxymethyl chitosan, being both conjugates obtained from an organic solvent free synthetic procedure. They were characterized by FT-IR, ^{1}H-NMR spectroscopies, whereas thermal analysis (including Differential Scanning Calorimetry and Thermal Gravimetric Analysis) revealed good stability of the two conjugates after exposure at temperatures close to 300°C. Release studies in simulated nasal fluid elucidated that a faster release occurred since *O*-carboxymethyl chitosan-DA conjugate maybe due to the less steric hindrance exerted by the polymeric moiety. The CMCS-DA conjugates prepared in aqueous medium may self-assembly to form polymeric micelles and/or may form polymeric nanoparticles. TEM and Photon correlation spectroscopy lent support for polymeric nanoparticle formation. Moreover, such CMCS-DA conjugates showed antioxidant activity, as demonstrated by DPPH radical scavenging assay. Finally, cytocompatibility studies with neuroblastoma SH-SY5Y cells showed no cytotoxicity of both conjugates, whereas their uptake increased from 2.5 to 24 h and demonstrated in 40-66% of cells.

Carboxymethyl chitosan Dopamine Conjugates: Synthesis and Evaluation for Intranasal anti Parkinson Therapy

Sante Di Gioia[1], Giuseppe Fracchiolla[2], Stefania Cometa[3], Filippo Maria Perna[2], Andrea Francesca Quivelli[2], Giuseppe Trapani[2], Valeria Daniello[1], Concetta Nobile[4], Md Niamat Hossain[1], Adriana Trapani[2*], Massimo Conese[2]

[1]*Department of Clinical and Experimental Medicine, University of Foggia, 71122, Foggia, Italy*

[2]*Department of Pharmacy-Drug Sciences, University of Bari "Aldo Moro", Consorzio C.I.N.M.P.I.S., via E. Orabona, 4-70125 Bari, Italy*

[3]*Jaber Innovation s.r.l., 00144 Rome, Italy*

[4]*CNR-NANOTEC Institute of Nanotechnology, Via Monteroni, 73100 Lecce, Italy*

[*]Corresponding Author: Prof. Adriana Trapani

Department of Pharmacy-Drug Sciences

University of Bari "Aldo Moro", Bari, Italy

Tel.: +39-0805442114. Fax: +39-0805442724.

Email: adriana.trapani@uniba.it

Abstract

With respect to the Parkinson disease (PD), herein, we aimed at synthetizing and characterizing two novel macromolecular conjugates where dopamine (DA) was linked to *N,O*-carboxymethyl chitosan or *O*-carboxymethyl chitosan, being both conjugates obtained from an organic solvent free synthetic procedure. They were characterized by FT-IR, ^{1}H-NMR spectroscopies, whereas thermal analysis (including Differential Scanning Calorimetry and Thermal Gravimetric Analysis) revealed good stability of the two conjugates after exposure at temperatures close to 300°C. Release studies in simulated nasal fluid elucidated that a faster release occurred since *O*-carboxymethyl chitosan-DA conjugate maybe due to the less steric hindrance exerted by the polymeric moiety. The CMCS-DA conjugates prepared in aqueous medium may self-assembly to form polymeric micelles and/or may form polymeric nanoparticles. TEM and Photon correlation spectroscopy lent support for polymeric nanoparticle formation. Moreover, such CMCS-DA conjugates showed antioxidant activity, as demonstrated by DPPH radical scavenging assay. Finally, cytocompatibility studies with neuroblastoma SH-SY5Y cells showed no cytotoxicity of both conjugates, whereas their uptake increased from 2.5 to 24 h and demonstrated in 40-66% of cells.

***Keywords*:** Polymeric conjugates, Dopamine, Storage stability, Cytotoxicity, Uptake

List of chemical compounds studied in the article: Dopamine hydrochloride (Compound CID: 65340), Chitosan (Compound CID: 129662530), *N,O*-carboxymethyl chitosan–Dopamine amide conjugate, *O*-carboxymethyl chitosan–Dopamine amide conjugate.

1. Introduction

Neurodegenerative diseases (NDs) are characterized by progressive loss of neuron function whose occurrence increases with the age of the patient [1]. Thus, it has been even predicted that NDs will become the second leading cause of death after cardiovascular diseases in developed countries by 2040 due, at least in part, to the progressively aging of population [2]. Among the NDs, including Alzheimer's disease (AD), Parkinson's disease (PD), Huntington's disease, amyotrophic lateral sclerosis, frontotemporal dementia and the spinocerebellar ataxias, PD is the second widespread disorder after AD and it is endowed with the increasing impairment of dopaminergic neurons in the Substantia Nigra as well as with significant decrease in concentration of dopamine (DA) in the striatum [3]. From a symptomatic point of view, PD is characterized by movement disorders like tremors, rigidity, bradykinesia, memory loss and hesitant speech as well as by several non-motor symptoms such as sleep disorders and gastrointestinal ones [4, 5]. The current pharmacological treatment of PD is only symptomatic and it is based on the "dopamine replacement strategy", involving the oral administration of the DA precursor levodopa (L-DOPA) in order to restore acceptable levels of the neurotransmitter in the brain. However, long-term administration of L-DOPA brings about adverse effects including motor complications and dyskinesia [6]. Thus, even though many preclinical studies have been carried out to find new therapeutic agents for PD, the majority of new drug candidates failed in clinical trials mainly because they are unable to cross the blood brain barrier (BBB) in therapeutic amounts. Hence, as occurs also for other NDs, there is a huge need to

develop both symptomatic and disease-modifying treatments for PD [7]. However, even though the main cause(s) of PD is (are) still not fully understood, new therapeutic targets useful to limit the loss of DAergic neurons have been evidenced including alpha-synuclein aggregation and phosphorylation, proteasome and lysosome approach, mitochondrial disruptions and oxidative stress as well as glial environment and neuroinflammation [7].

In the last decade, an interesting and non-invasive approach to bypass the BBB in NDs has been extensively investigated. It consists in the use of the intranasal (IN) administration which allows a direct access to the brain using the olfactory and/or trigeminal connections between the nose and the brain [8-11]. Such nose-to-brain delivery possesses not only the advantage to overcome the BBB but also to avoid hepatic and gastrointestinal metabolism as well as to decrease systemic side effects since the plasma exposure is reduced [12]. Despite these advantages, however, nose-to-brain delivery has some limitations that must be taken into account when this approach is followed for the treatment of neurological disorders including NDs. This delivery route, indeed, is difficult when high doses of drug are to be administered due to the limited volume of each nostril in humans, moreover the residence times of formulations within the nasal cavity may be short due to mucociliary clearance with important consequences on drug absorption. Again, it should be taken into account the presence of enzymes in the nasal cavity and, consequently, the need to protect sensitive drugs from enzymatic degradation and, finally, it should be considered that the nasal formulation does not cause irritation in the nasal cavity [12].

In the field of nose-to-brain delivery, several studies showed that the encapsulation of the drugs in nanocarriers can improve drug transport across BBB enhancing the bioavailability at brain level. Thus, nanoparticles prepared from chitosan and its derivatives have been shown better nose-to-brain delivery properties perhaps due to the temporarily opening capability of intercellular tight junctions of these polymers and/or to their mucoadhesive characteristics which would prolong the residence time of the formulation within the nasal cavity [12]. Again, advances in nanotechnology led to the synthesis of nanoparticles of small size (< 100 nm) by laser ablation even with application in BBB crossing [13, 14]. Also lipid based nanocarriers, including solid lipid nanoparticles (SLNs), nanostructured lipid carriers (NLC) and liposomes of small size (< 100 nm) have a good potential for nose-to-brain delivery since they can encapsulate hydrophilic or hydrophobic drugs with good efficiency [15-18]. Moreover, they can easily squeeze through intercellular spaces between olfactory cells and their mucoadhesive/mucopenetration properties can be appropriately tailored to prolong the residence time in the nasal cavity facilitating nose-to-brain transport [15, 17].

In this context, recently we have developed *N,O*-carboxymethyl chitosan-DA ester and amide conjugates (ester or amide *N,O*-CMCS-DA) and evaluated both their in vitro mucoadhesive properties in simulated nasal fluid (SNF) and their uptake by Olfactory Ensheating Cells (OECs) for potential application in nose-to-brain delivery of the neurotransmitter to restore acceptable levels of DA in the brain of parkinsonian patients [19, 20]. These macromolecular conjugates could possess several advantages including prolonged circulation, controlled release and improved mucoadhesive properties. Moreover, such conjugates could offer the relevant possibility to formulate polymeric nanoparticles with limited premature leakage of the biologically active substance (i.e., DA) since it is linked to the polymeric backbone by a covalent chemical bond. The premature leakage of the cargo encapsulated in nanocarriers is an important drawback to be considered particularly for most potent substances as DA. Among the conjugates studied, the *N,O* CMCS ester **1** and the corresponding *N,O*-CMCS amide conjugates **2** were evaluated (Figure 1) [19, 20]. These conjugates were prepared according to synthetic procedures involving organic solvent (DMF) and coupling reagents. The main

results of the previous studies were the observed higher stability of *N,O*-CMCS-DA amide conjugate compared to the ester ones as well as the high internalization of this amide conjugate by OECs.
Following these studies, we considered of interest to synthesize both conjugate **2** and the new amide macromolecular conjugate of the neurotransmitter **3** (Figure 1), resulting from the conjugation of the primary amino group of neurotransmitter with the –COOH function of *O*-CMCS polymer, following eco-friendly procedures of synthesis in pharmaceutical laboratories. This last carboxymethyl chitosan derivative is soluble in a wide range of pH due to the introduction of carboxymethyl group and it is characterized by the presence of the carboxymethyl substituent on the primary –OH group in position-6 of the glucose nucleus. Chitosan, indeed, possesses three reactive groups in the molecule and namely a primary hydroxyl group, a secondary hydroxyl group and an amino group. Depending on the reaction conditions used, *N*-carboxymethyl chitosan (*N*-CMCS), *O*-carboxymethyl chitosan (*O*-CMCS) or *N,O*-carboxymethyl chitosan (*N,O*-CMCS) may be prepared [21, 22]. Thus, our working hypotheses for these novel conjugates were to evaluate whether *i*) it is possible to develop a synthetic approach employing, in agreement with green chemistry principles, water as solvent and the elimination of organic reagents not absolutely necessary. It in order to minimize the toxicity potential of conjugates **2** and **3** and, hence, to improve their performance for DA replacement in anti-Parkinson therapy; *ii*) the position of the carboxymethyl substituent on the chitosan backbone could influence the features of the resulting conjugates including release of the neurotransmitter and uptake by neuronal SH-SY5Y cell model line.

Hence, in the present paper, we describe the procedure we used for the synthesis of *N,O*-CMCS-DA **2** and *O*-CMCs-DA **3** conjugates in aqueous buffered medium (Figure 1). The new amide conjugates were characterized by FT-IR, ^{1}H-NMR spectroscopies and thermal analysis (Thermogravimetric Analysis (TGA) and Differential Scanning Calorimetry (DSC)), DA release kinetic as well as it was examined the possibility that CMCS conjugates **2** and **3** could self-assembly forming micelles or further nanosized structures in the aqueous medium. In order to consider the biocompatibility and translational capability of the two amide conjugates, cell viability and uptake tests were carried out in neuroblastoma SHSY-5Y cells.

2. Materials and Methods

2.1. Materials

N,O-Carboxymethyl Chitosan (*N,O*-CMCS, Molecular weight in the range of 30-500 kDa, deacetylation degree, 94.2%; viscosity 22 mPa sec, according to the provider's instructions) was purchased from Heppe Medical Chitosan GmbH (Halle, Germany). *O*-Carboxymethyl Chitosan (*O*-CMCS, Molecular weight in the range of 100-300 kDa, deacetylation degree, 90%; substitution degree 88 %, according to the supplier's instructions) was purchased from DBA (Milan, Italy). Ethyl-dimethyl-aminopropylcarbodiimide (EDC), dopamine hydrochloride (DA), 2,2-diphenyl-1-picrylhydrazyl (DPPH), fluorescein 5(6)-isothiocyanate (FITC), and PBS were purchased from Sigma-Aldrich (Milan, Italy). Dialysis tubes with a MWCO 12-14 kDa were purchased from Spectra Labs (Milan, Italy). Throughout this work, double distilled water was used. All other chemicals used were of reagent grade.

[Insert Figure 1]

2.2. Apparatus

The conjugates **2** and **3** were prepared following the synthetic procedure summarized in Scheme 1 and characterized by Proton nuclear magnetic resonance (^{1}H NMR) spectroscopy and Fourier transform infrared (FT-IR) spectroscopy as well as by thermogravimetric Analysis (TGA) and differential scanning calorimetry (DSC).

^{1}H NMR spectra were recorded on a Brüker spectrometer (Billerica, Massachusetts, US) operating at 600 MHz and the analyses were performed at 293 °K on dilute solutions of each conjugate using D_2O as solvent. In particular, to allow the determination of the substitution degree of *N,O*-CMCS-DA **2** and *O*-CMC-DA **3** via ^{1}H-NMR spectrometry, dispersions in D_2O were prepared for both conjugates at a concentration of 4 mg/mL and heated at 40°C for few minutes before the analysis. Chemical shifts are reported in parts per million (δ). Spectra were processed using Mnova (Mestrelab Research, A Coruña, Spain).

FT-IR spectra were obtained in KBr discs using a Perkin Elmer 1600 FT-IR spectrometer (Perkin Elmer, Milan, Italy). The range examined was 4,000–400 cm^{-1} with a resolution of 1 cm^{-1}.

Thermogravimetric analysis (TGA) was performed on a PerkinElmer TGA-400 instrument (PerkinElmer Inc, Waltham, MA), heating samples (5-10 mg) in the range 30-600°C under inert nitrogen flow at the heating rate of 20°C/min. For each sample, thermograms (TG) and derivative curves (DTG) were acquired and elaborated with the TGA Pyris software (version 13.3.1.0014, Waltham, USA).

Differential scanning calorimetry (DSC) thermograms were obtained using a Mettler Toledo DSC 822e STARe 202 System (Mettler Toledo, Milan, Italy), equipped with a DSC MettlerSTARe Software. For DSC analysis, aliquots of about 10 mg of both freeze-dried conjugates **1** and **2**, pure *O*-CMCS, pure *N,O*-CMCS were placed in an aluminium pan and hermetically sealed. The scanning rate was 5°C/min under a nitrogen flow of 20 cm^3/min and the temperature range was from 25 to 300°C and 25 to 275°C for DA and pure polymers/conjugates, respectively. The calorimetric system was calibrated using indium (purity 99.9%) and following the procedure of the MettlerSTARe Software. Each experiment was carried out in triplicate.

Transmission Electron Microscopy (TEM) images of samples containing both conjugates were recorded on a JEOL Jem1011 microscope (Tokyo, Japan) operating at an accelerating voltage of 100 kV.

The hydrodynamic diameters, polydispersity and zeta potential values of *N,O*-CMCS-DA **2** and *O*-CMCS-DA conjugates **3** self-assembled into nanoparticles were determined by using a Zetasizer NanoZS, ZEN 3600 (Malvern Instruments, Worcestershire, U.K.) instrument according to photon correlation spectroscopy (PCS) mode.

2.3 Synthesis of DA amide conjugates

To prepare conjugate **2** and **3**, the Fan's protocol for the preparation of the gelatin-DA conjugate in aqueous environment based on the carbodiimide (EDC) chemistry was followed with significant modifications [23]. In particular, besides the use of aqueous medium, we also avoided the use of *N*-hydroxysuccinimide or *N*-hydroxysulfosuccinimide, well-known agents increasing the efficiency of EDC-mediated coupling reactions. This in order to minimize the toxicity potential of the resulting conjugates due to the presence of traces of organic solvent and reagents not absolutely necessary.

Thus, the reaction conditions used for the synthesis of this conjugate **2** and **3** resulted quite different from those used by Fan et al. [23].

*2.3.1. Synthesis of N,O-Carboxymethyl Chitosan-DA amide conjugate **2** in aqueous buffered medium*

To a solution of *N,O*-CMCS (0.2 g) in diluted HCl (0.1 N-50 mL) showing pH= 6, DA (0.1 g, 0.57 x 10^{-3} mol) was added together with 32 mg of EDC and the mixture was left to react under magnetic stirring in argon atmosphere for 48 h at room temperature (r.t.). The polymer/neurotransmitter weight ratio used was that employed by Fan et al. [23]. Afterwards, the reaction mixture was dialyzed in distilled water for three days and then lyophilized (Lio Pascal 5P, Milan Italy). The obtained product (*N,O*-Carboxymethyl Chitosan-DA amide conjugate **2**, *N,O*-CMCS-DA) was collected in good yield (about 37%) and characterized by FT-IR, ^{1}H NMR, TGA and DSC.

N,O-CMCS-DA amide conjugate **2**: FT-IR (KBr) ν (cm^{-1}): 3246 (NH, OH), 1629 (C=O), 1110 (OH).

*2.3.2. Synthesis of O-Carboxymethyl Chitosan-DA conjugate **3***

In a solution composed of 10 mL of diluted HCl (0.1N) and 40 mL of distilled water, 0.15 g of *O*-CMCS were poured, so achieving pH = 6 and, afterwards, 0.21 g of DA and 38 mg of EDC were added. Unlike the conjugate **2** synthesis, in this case the polymer/neurotransmitter weight ratio was that used in our previous work on the synthesis of the *N,O*-Carboxymethyl Chitosan-DA amide conjugate [20]. The resulting mixture was left under magnetic stirring in argon atmosphere for 48 h at r.t. Afterwards, the product was dialyzed in distilled water for three days and then lyophilized (Lio Pascal 5P, Milan Italy). The obtained product (*O*-Carboxymethyl Chitosan-DA amide conjugate **3**, *O*-CMCS-DA) was collected in good yield (about 24%) and, as above, characterized by FT-IR, ^{1}H NMR TGA and DSC. *O*-CMCS-DA amide conjugate **3**: FT-IR ν (cm^{-1}): 3412 (NH, OH), 2923 (CH aliphatic), 1639, 1617 (C=O), 1071 (OH).

2.3.3 Determination of substitution degree (DS) of DA-CMCS amide conjugates by titrations or hydrolysis under strong acidic conditions

The substitution (DS) of *N,O*-CMCS-DA **2** and *O*-CMCS-DA **3** conjugates was determined by potentiometric titration after alkaline hydrolysis according to a procedure previously described by us with slight modification [19, 20]. A weighted amount of each conjugate sample (50 mg) was dissolved in a solution of NaOH (0.25 N) in ethanol (5 mL) and the mixture was stirred at reflux for 24 h. Then, at room temperature a potentiometric titration on the dark-yellow mixture (1 mL) degree was carried out using the automatic titrator (TITREX-1000, Wertheim, Germany) with a pH meter. Each potentiometric titration was carried out in triplicate.

During titration, two equivalent points were determined using a standardized solution of HCl (0.1 N). The first point referred headline in excess of NaOH (V1 equivalent point); the second equivalent point referred to the neutralization of the acid salt present (V2 equivalent point). The moles of HCl occurring between the first and the second equivalent point corresponding to the moles of free amide and the DS% were, therefore, determined by the following Equation (1):

$$DS\% = [\text{mass (sample)} - \text{mass (free amide)}]x100/\text{mass (sample)} \quad (1)$$

where mass (sample) corresponds to 1 mL (10 mg) of each conjugate sample before alkaline hydrolysis; moles of free amide or ester are equal to:

(V2 equivalent point - V1 equivalent point) x [HCl] determined by potentiometric titration as the average of three titrations.

The DS% concerning DA of each CMCS-DA amide conjugate was also measured according to hydrolysis under strong acidic conditions previously described [24]. Briefly, 2 mg of CMCS-DA amide conjugate were weighed and dissolved in HCl 1 N (pH 1) under stirring and light protection at r.t. for 3 h. Afterwards, the solution was centrifuged (16,000× g, for 45 min, Eppendorf 5415D,

Germany) and the obtained supernatant was analysed by HPLC to assess the DA amounts (Section 2.2). The DS% was calculated as mg DA/mg CMCS-DA amide conjugate x 100 [24].

2.3.4 Preparation of FITC-N,O-CMCS-DA and FITC-O-CMCS-DA conjugates

For cellular uptake studies, *N,O*-carboxymethyl chitosan-DA conjugate **2** and *O*-carboxymethyl chitosan-DA conjugate **3** were labelled with fluoresceine isothiocyanate (FITC) by using a previously reported protocol with slight modifications [19, 20]. Briefly, for *N,O*-CMCS-DA amide conjugate **2**, (70 mg) were dissolved in 0.1 N HCl (3.2 mL) and then the pH was adjusted to 6.5 with 0.1 N NaOH (0.01 mL). For *O*-CMCS-DA amide conjugate **3**, (70 mg) was dissolved in double distilled water (4.5 mL) and then the pH was adjusted to 6.5 with 0.1 N HCl (0.37 mL). For both labelling procedures, FITC was dissolved at 20 mg/mL concentration in ethanol and 0.75 mL of this solution were added to amide conjugates **2** and **3**, under magnetic stirring at r.t. for 72 h under light protection. Afterwards, the fluorescent mixtures were dialyzed against double distilled water for 3 days and freeze-dried for 72 h. The labelling efficiencies of FITC-*N,O*-CMCS-DA and FITC-*O*-CMCS DA amide conjugates were determined calibrating the fluorometer (Perkin Elmer, Milan, Italy) in the range 1-140 ng/mL of FITC obtained by diluting 100 μg/mL of a methanol solution of FITC with phosphate buffer at pH 8.0 (excitation wavelength: 488 nm; emission wavelength: 525 nm; slits: 2.5 nm). Furthermore, to determine the substitution degree (DS), the FITC-CMCS-DA amide conjugate underwent acid hydrolysis [25]. Two mg of the FITC-CMCS-DA amide conjugate were weighed and dissolved in 2 mL of HCl 1 N (pH 1), stirred and protected from light, at r.t. for 3 h. Then, the resulting mixture was centrifuged (16,000× g, for 45 min, Eppendorf 5415D, Hamburg, Germany) and the supernatant was analyzed by HPLC to assess the DA amounts. The DS was calculated as mg DA/mg FITC-CMCS-DA amide conjugate [25].

2.4. Quantitative determination of dopamine

DA quantification was carried out by HPLC as previously reported [26]. Briefly, the mobile phase consisted of 0.02 M potassium phosphate buffer, pH 2.8: CH_3OH 70:30 (v/v), and the elution of the column in isocratic mode occurred at the flow rate of 0.7 mL/min. Under such chromatographic conditions, DA retention time was equal to 5.5 min, whereas retention time of both conjugates was equal to 4.9 min.

2.5. Storage Stability of DA-CMCS conjugates at low temperature

With the aim to check the storage stability at -20°C, aliquots of 3-5 mg of each freeze-dried DA-CMCS-conjugate were stored in the freezer at the above mentioned temperature.

Sampling was done at 1, 2, 4 and 8 weeks in order to verify DS of DA over the time. In each sampling time, the aliquot of the DA-CMCS-conjugate was incubated with 1 mL HCl (0.1N) for 30 min to allow the cleavage of the amide linkage polymer-DA and, afterwards, the resulting mixture was centrifuged (16,000 × g, 45 min, Eppendorf 5415D, Hamburg, Germany).

In the supernatant the DA content was determined by HPLC as described in Section 2.4.

*2.6. In vitro neurotransmitter release from conjugates **2** and **3** in Simulated Nasal Fluid*

The neurotransmitter DA release in SNF [19] (pH 6.0, without enzymes) from *N,O*-CMCS-DA or *O*-CMCS-DA conjugates was carried out starting from a weighted amount of conjugate corresponding to 1-1.2 mg of DA and dispersing it in 2.5 mL of SNF containing 0.05% (v/v) of DMSO and thermostated at 37 ± 0.1°C in an agitated (40 rpm/min) water bath (Julabo, Milan, Italy). At scheduled time points, 0.25 mL of the receiving medium were withdrawn and replaced with 0.25 mL of fresh

medium Then, each sample was centrifuged at 16,000 × g for 45 min, (Eppendorf 5415D, Germany), and the amounts of the neurotransmitter delivered were quantified in the resulting supernatants by HPLC, as above described, and plotted against the time. All the release experiments in SNF were carried out in triplicate.

*2.7. Self-aggregation of CMCS-DA conjugates **2** and **3** to form nanosized structures*

Dilute stock suspensions of conjugates **2** and **3** were prepared by dispersion of 2 mg of each conjugate in 200 μL of PBS (pH 7.4). Centrifugation of the samples at 13,200 rpm for 45 min (Eppendorf 5415D, Germany) allowed to discard the pellet and isolating the corresponding supernatant from which 25 μL were dropped onto carbon-coated copper grids and then stained with 1% (w/v) phosphotungstic acid solution for 1 min. Afterwards, the grids were rinsed with deionized water and left to dry under air overnight. Then, TEM observations of the resulting nanoparticles (NPs) were performed in order to obtain their morphology and an average TEM size. TEM images of both conjugates were recorded on a JEOL Jem1400 microscope (Tokyo, Japan) operating at an accelerating voltage of 120 kV. Particle size data arising from TEM analysis were also compared with the ones acquired according to Photon Correlation Spectroscopy (PCS) of the Zetasizer NanZS (ZEN 3600, Malvern, UK) apparatus after treatment with a probe sonication with a Vibra-cell sonicator (Sonics and Materials, U.K.) for 15 min at the output of energy equal to 750W in an ice water bath. The particle size and polydispersion (PDI) values were measured at 25 °C after dilution in double distilled water (1:1, v/v). For ζ-potential measurements laser Doppler anemometry technique was adopted (ZetasizerNanoZS, ZEN 3600, Malvern, UK) after dilution 1:20 (v.v) with KCl (1 mM, pH 7.0).

2.8. In vitro evaluation of antioxidant activity: Assay of DPPH radical scavenging activity

The in vitro antioxidant activity of the pure polysaccharides, *O*-CMCS-DA and *N,O*-CMCS-DA and the two corresponding conjugates (*N,O*-CMCS-DA **2** and *O*-CMCS-DA **3**) was evaluated using the DPPH test reported in literature slightly edited [27]. Firstly, ethanol was used as solvent for DPPH test to obtain a stock solution at the concentration of 0.001% w/v and, then, diluted to 8 x 10^{-4}% (w/v). Dispersion of 5 mg of each sample in 0.5 mL of double distilled water was reacted with 2.5 mL of the diluted DPPH solution for 60 min at room temperature in the dark. The corresponding absorbances were recorded at the wavelength of 514 nm by using PerkinElmer Lambda Bio 20 spectrophotometer (PerkinElmer, Milan, Italy). Blanks were obtained by filling the cuvettes with 0.5 mL of ethanol and 2.5 mL of the 8 x 10^{-4}% (w/v) solution in DPPH. For all formulations under investigation, antioxidant activity (AA) was calculated from Equation (2) and expressed in percentages:

$$AA\ (\%) = (1 - As/Ab) \times 100 \qquad (2)$$

where As is the sample absorbance, and Ab the absorbance of the radical. All the experiments were carried out in triplicate.

However, it is now accepted that the results obtained by Equation (2) are useful only for qualitative but not for accurate quantitative evaluations which should be made considering the IC_{50} values defined as the concentration of the sample that caused 50% inhibition of DPPH radical formation [28].

2.9. Cytotoxicity evaluation in SH-SY5Y cell model line

SH-SY5Y cells were grown as previously described [24]. Briefly, cells were plated in a 96-well plate (BD, USA) at a density of 1×10^4 per well in 100 μL of complete medium and incubated overnight

to allow cell attachment. Then, the culture medium was replaced with 100 µL of fresh medium containing different dilutions of *N,O*-CMCS-DA conjugate **2** (final concentration of dopamine: 18.75 µM and 4 µM, corresponding to 1336 µg/mL and 334 µg/mL) and *O*-CMCS-DA conjugate **3** (final concentrations of dopamine: 75 µM, 18.75 µM, 4 µM, corresponding to 11.5 µg/mL, 2.9 µg/mL, 0.7 µg/mL). Volumes of *O*-CMCS without DA were chosen to obtain the same CMCS amounts of the *O*-CMCS-DA conjugate **3** (11.5 µg/ml, 2.9 µg/ml, 0.7 µg/ml). Under these conditions cells were grown at 37 °C for 24 h. 1% Triton-X100-treated cells were used as a positive control. After treatments, cell viability was evaluated by MTT (3-(4,5-dimethylthiazol-2-yl)-2,5 diphenyl tetrazolium bromide), as previously described [20]. The cell viability was calculated as follows:
% viability = [(Optical density {OD} of treated cell − OD of blank)/(OD of vehicle control − OD of blank) × 100], considering untreated cells as 100%.

2.10. Uptake of amide conjugates by SH-SY5Y cells

SH-SY5H cells were plated at the number of 80,000 per each well of a 24-well plate. Cells were incubated with 500 µL of fresh medium containing different dilutions of *O*-CMCS-DA conjugate **3** (final concentrations of dopamine: 75 µM, 18.75 µM, 4 µM, corresponding to 11.5 µg/mL, 2.9 µg/mL, 0.7 µg/mL) and *N,O*-CMCS-DA conjugate **2** (final concentration of dopamine: 75 µM, 18.75 µM and 4 µM, corresponding to 5344 µg/mL, 1336 µg/mL and 334 µg/mL). After 2.5 or 24 h, each well was treated with 0.05% trypan blue in PBS (in order to quench extracellular fluorescence), trypsinized, resuspended in 0.5 mL of PBS, and analysed by the BD FACSLyric™ Flow Cytometry (BD Biosciences, Franklin Lakes, NJ, USA). Fluorescence for FITC was measured at the wavelength of 488 nm, determining the percentage of FITC-positive cells after setting the gating on 99% (excluding cell debris) and by subtracting the fluorescence of untreated control cells. Ten thousand cells were examined in each experiment, evaluating the percentage of positive cells for FL1H fluorescence and the relative mean fluorescence per cell (MFI).

2.11. Statistics

Statistical analyses were carried out by Prism v. 5, GraphPad Software Inc., USA. Results were expressed as mean ± SD. Multiple comparisons were based on one-way analysis of variance (ANOVA) with Bonferroni or Tukey post hoc test and differences were considered significant when $p < 0.05$.

3. Results

[Insert Scheme 1]

*3.1. Synthesis and structural characterization of the amide conjugates **2** and **3***

EDC mediated coupling reaction between *N,O*-CMCS or *O*-CMCS and DA was used to prepare *N,O*-CMCS-DA amide conjugate **2** and *O*-CMCS-DA amide conjugate **3**, respectively (Scheme 1). In particular, the condensation reaction was carried out by stirring the reagents in aqueous buffered medium at pH 6.0 for 48 h at r. t. and the reaction products were purified by dialysis in distilled water for three days and lyophilisation. Conjugates **2** and **3** were structurally characterized by spectroscopic

methods i.e., FT-IR and ^{1}H NMR. In the FT-IR spectrum of *N,O*-CMCS-DA amide conjugate **2** a characteristic absorption band centered at 1629 cm^{-1} was present and it was attributed to the carbonyl groups of the conjugate **2** (Figure 2a). In the FT-IR spectrum of *O*-CMCS-DA amide conjugate **3**, the splitted band at 1639 cm^{-1} and 1617 cm^{-1} was diagnostic of the amide carbonyl group (Figure 2b). Notably, in the FT-IR spectra of both *N,O*-CMCS-DA conjugate **2** and *O*-CMCS-DA conjugate **3**, no absorption band at 1730 cm^{-1} occurs suggesting that in these chitosan derivatives the carboxymethyl substituent is present in –COONa form [22].

[Insert Figure 2]

In Figure 3, the ^{1}H NMR spectrum of the polysaccaride *O*-CMCS in D_2O (Figure 3a), showed multiplets from 3.91 to 3.27 ppm that were assigned to protons H3, H4, H5, H6 and the signal at 4.41 to methylene protons H7, in accordance with Du and Hsieh's peak attribution [29]. In Figure 3b, the ^{1}H NMR spectrum of the reaction product after functionalization of *O*-CMCS with DA is reported. Two new sets of signals, located at 6.26, 6.41, 6.51, 6.59, 6.66 ppm, were shown corresponding to the aromatic protons of DA, covalently-bonded to the polymer by an amide bond, probably due to two conformers of *O*-CMCS-DA conjugate **3**. The signals at 6.26 and 6.41 ppm belong to two aromatic protons of the majority signal set, those at 6.51 and 6.59 ppm belong to the minority one, while the third aromatic dopamine proton gives a single signal, for both conformers, to 6.66 ppm.The percentage of monomeric units substituted with DA (*DA-subst*) was determined comparing the integral of the signal at 6.66 ppm with that of the multiplets from 3.83 ppm to 3.22 ppm, which takes into account the H3, H4, H5, 2 x H6 protons, using the Equation: $DA\text{-}subst = I_{H\text{-}Ar} \times 5 / I_{H3,H4,H5,H6}$, where $I_{H\text{-}Ar}$ is intensity of the signal for the aromatic proton at 6.66 ppm and $I_{H3,H4,H5,H6}$ is intensity of the signal for H3, H4, H5 and both H6 protons, and it turns out to be 11%.

[Insert Figure 3]

Similarly, in Figure 4, the ^{1}H NMR spectra *of N,O*-CMCS, conjugate **2** (Figure 4a), in D_2O and after its functionalization with DA (Figure 4b) are shown. In this case, comparing the integral of the signals of the aromatic protons (6.50-6.64 ppm) with that of the multiplets 3.71-3.28 ppm (corresponding to H3, H4, H5, H6 protons [29]), the percentage of incorporated DA turns out to be 7%, calculated by the equation $DA\text{-}subst = I_{H\text{-}Ar} \times 5 / I_{H3,H4,H5,H6} \times 3$, where $I_{H\text{-}Ar}$ is the sum of the intensity of the signal for the aromatic protons and $I_{H3,H4,H5,H6}$ is intensity of the signal for H3, H4, H5 and both H6 protons. However, the analysis of the ^{1}H-NMR spectrum does not allow to distinguish between DA bound in position 2 and 6 of the six-term ring.

[Insert Figure 4]

The amounts of DA covalently bound to *N,O*-CMCS-DA and *O*-CMCS-DA amide conjugates **2** and **3**, respectively, were also determined by chemical means following the procedures reported in Section 2.2.3. From titration data focusing on quantification of -COOH groups, the DS% of *N,O*-CMCS-DA conjugate **2** was 5.36% corresponding to 536 μg (-COO derivatized)/10 mg *N,O*-CMCS-DA conjugate **2**. The DS% of *O*-CMCS-DA conjugate **3** was 12.65% corresponding to 1.265 mg (-COO derivatized)/10 mg *O*-CMCS-DA conjugate **3**. From hydrolysis under strong acidic conditions the DS% values were found equal to 2.3 ± 0.8% for *N,O*-CMCS-DA conjugate **2** and 6 ± 0.9% for *O*-CMCS-DA conjugate **3**. Comparing these data it appears that the DS% values of conjugates **2** and **3** measured by spectroscopic (^{1}H-NMR spectrum) and titration methods are in good agreement, while those obtained by hydrolysis under strong conditions are underestimated enough. This outcome may suggest that the conditions used for such hydrolysis under strong acidic conditions (mixture at pH 1 stirred at r.t. for 3 h) are not appropriate to obtain complete hydrolysis of the starting conjugate.
As for the FITC-*N,O*-CMCS-DA and FITC-*O*-CMCS DA amide conjugates the measured DS% values of the neurotransmitter were 0.7 ± 0.05% for the former conjugate and 2.2 ± 0.9% for the latter conjugate, respectively. The labelling efficiency referred to FITC (mg FITC/mg FITC-DA-conjugate) for the FITC-*N,O*-CMCS-DA and FITC-*O*-CMCS DA amide conjugates were 13 ± 0.4% and 5 ± 0.6%, respectively.

3.2. Thermal analysis

Thermal analysis on the herein examined conjugates included both studies of TGA and DSC.

3.2.1. Thermo-Gravimetric Analysis (TGA)

TGA thermograms and derivative traces are reported in Figure 5 panel (a) and in the relevant inset, respectively, whereas all the main events are summarized in Table 1.

[Insert Figure 5]

In all the analysed samples for TGA, excluding DA, the water content was in the range of 10-13%, which is typical for polysaccharides. DA degraded under one thermal event centred at 327°C, with a residue at 600°C of 29%. Pure *N,O*-CMCS polymer exhibited two main decompositions peaks at 295°C and 307.4°C, while the residue at 600°C was equal to 51% (Figure 5), as also reported in a previous work [30]. As far as pure *O*-CMCS is concerned, a single sharp decomposition step was recorded, centred at 290°C, corresponding to a weight loss of 30.7%, while the residue at 600°C was equal to 57.2%. Finally, as far as the two conjugates **2** and **3** are concerned, after a first step relevant to the moisture/volatiles loss, a broad decomposition step, centred at 307.7°C and 304.9°C (weight losses of 30.7%, and 56.3% respectively) occurred for *N,O*-CMCS-DA and *O*-CMCS-DA, respectively. The residue at 600°C was equal to 26.8% and 30.5% and for *N,O*-CMCS-DA conjugate **2** and *O*-CMCS-DA conjugate **3**, respectively.

3.2.2. Differential Scanning Calorimetry (DSC)

In Figure 5 panel (b), DSC thermal curves of different polymers/conjugates were shown. For both polymers *N,O*-CMCS and *O*-CMCS, (i.e., Figure 5 panel (b), curves b and d, respectively), a semi-crystalline solid state was deduced from DSC thermograms referring to both polymers with melting

point of 153°C and 159°C for *N,O*-CMCS and *O*-CMCS, respectively. An amorphous state was observed for both *N,O*-CMCS-DA conjugate **2** and *O*-CMCS-DA conjugate **3** (Figure 5, panel (b), curves c and e), with the disappearance for both of them of the melting point peak of the corresponding polymer. Furthermore, none of the conjugates showed the melting point peak, as such or shifted, of the pure neurotransmitter DA, confirming the existence of an amorphous solid state for these CMCS conjugates (Figure 5 panel (b), curves c and e).

[Insert Table 1]

3.3. Storage Stability of DA-CMCS-conjugates at T= -20°C

To estimate the storage stability of conjugates herein studied, both powders of *N,O*-CMCS-DA conjugate **2** and *O*-CMCS-DA conjugate **3** were stored in a freezer at T = -20°C up to eight weeks and the DS% over the time are shown in Figure 6 panel (a). We chose to use the method of hydrolysis under strong conditions because a faster determination of DS% takes place, even though we knew that in this way an underestimated value of DS% is deduced. In particular, *O*-CMCS-DA conjugate **3** reduced DS %, starting from one week where DS% collapsed to 40% and after 8 weeks 32% was found (Figure 6 panel (a)). Moreover, in the corresponding HPLC chromatograms, the peak of DA maintained its shape, typical retention time value and no further peaks appeared. In contrast, for *N,O*-CMCS-DA conjugate **2**, HPLC chromatograms showed an enlarged peak with an increase of few min in the retention time value than in the case of intact DA and such behaviour occurred since one week of storage (Figure 6 panel (a)).

3.4. In vitro drug release from conjugates

In Figure 6 panel (b) the in vitro release profiles of *N,O*-CMCS-DA conjugate **2** and *O*-CMCS-DA conjugate **3** in SNF (pH 6.0 without enzymes) are shown. While after 2 days only about 10% of the neurotransmitter was delivered from conjugate **2**, DA release from the amide **3** was quicker being after 2 days 24% of DA released in the SNF receiving medium. Notably, it should be considered that under the conditions used (pH 6.0 without enzymes) during release test of the *N,O*-CMCS-DA conjugate **2** further degradation products of the neurotransmitter were detected as additional HPLC peaks showed in the corresponding chromatograms since 3 days up to 14 days [31]. For *O*-CMCS-DA conjugate **3**, such additional peaks appeared only when HPLC chromatograms were recorded from 10 to 14 days.

[Insert Figure 6]

3.5. CMCS-DA conjugates can self-assemble to form nanosized structures

An interesting property of the CMCS-DA conjugates herein studied is that they can self-assembly to form nanosized structures. Thus, by dispersing each conjugate (2 mg) in 200 μL of PBS (pH 7.4) followed by centrifugation and by dropping 25 μL of the resulting supernatant onto grids for TEM and then stained with phosphotungstic acid, TEM analysis clearly demonstrated the nanostructured assembly of conjugates with NP formation. Figure 7(a) and 7(b) show NPs obtained from *N,O*-CMCS-DA conjugate **2** and *O*-CMCS-DA conjugate **3**, respectively. In particular, from conjugate **3** smaller and spherical NPs were obtained, whereas from conjugate **2** larger particles (average TEM size of 187 ± 41 nm) probably due to the fusion of individual particles (see the inset of Figure 7(a)) were detected. On the other hand, besides a negligible amount of microsized structures, by PCS

analysis a bimodal distribution was detected in both cases with a little quantity having a particle size < 100 nm and a prevalent one with a particle size > 100 nm (Figure 7(c) and 7(d)).
In Table 2, the hydrodynamic diameters, polydispersity and zeta potential values of conjugates **2** and **3** self-assembled into NPs determined by Zetasizer NanoZS, ZEN 3600 instrument are shown.

[Insert Figure 7]

[Insert Table 2]

*3.6 In vitro antioxidant activity of conjugates **2** and **3***

The antioxidant activity of *N,O*-CMCS-DA conjugate **2** and *O*-CMCS-DA conjugate **3** was studied according to a slightly modified spectrophotometric assay based on the use of 2,2-diphenyl-1-picrylhydrazyl (DPPH) free radical enabling us to assess the ability of studied chemical substances to act as free radical scavengers [27, 32]. In this assay, antioxidants are able to reduce the stable DPPH radical (purple) to non-radical form DPPH-H (yellow). Polymers as such, namely *N,O*-CMCS and *O*-CMCS in our hands showed negligible DPPH radicals scavenging activity since they did not produce any yellow mixture. Instead, the DA conjugates **2** and **3** resulted to be in vitro capable to elicit DPPH radicals scavenging activity evidenced by yellow mixture formation and, hence, possess an antioxidant effect. On the other hand, even the neurotransmitter DA is endowed with radical scavenging ability which is reported to be 86% at 0.1 mM [33]. Thus, it can be stated that the DPPH radical scavenging activity of starting polymer and corresponding conjugates herein studied decreased in the following rank order: DA > *O*-CMCS-DA conjugate **3** > *N,O*-CMCS-DA conjugate **2** **>>>>** *O*-CMCS ~ *N,O*-CMCS.

3.7. MTT assay

In order to verify the cyto/biocompatibility of conjugates **2** and **3** with the target neuronal cells, SH-SY5Y cells were treated with *N,O*-CMCS or *O*-CMCS based conjugates at the indicated concentrations. *O*-CMCS was used also as a formulation not carrying DA. None of these formulations was cytotoxic, although a nonsignificant decrease in cell viability was observed with 75 μM of *N,O*-CMCS-DA conjugate **2** and *O*-CMCS-DA conjugate **3** (Figure 8).

[Insert Figure 8]

3.8. Uptake studies

For uptake studies fluorescent *O*-CMCS-DA conjugate **3** or *N,O*-CMCS-DA conjugate **2** were prepared by covalent linkage of FITC (see Materials and Methods). Cell uptake was studied in SH-SY5Y cells following incubation for either 2.5 or 24 h. Fig. 9 illustrates the cytofluorimetric gating (panels a and c) and overlay analysis (panels b and d) made on the total population that have been used for cells incubated with *N,O*-CMCS-DA conjugate **2** only as an example. Overlay of gated cells demonstrated that cells took up FITC-conjugated conjugate in a dose- and time-dependent manner (Figure 9b and d). Figure 10 shows these data as histograms. As expected, the uptake was a time-dependent process with more conjugates internalised at 24 h than at 2 h. Specifically, after 2.5 h there was a steep increase of percentages of FITC-positive cells with both conjugates, reaching ~34% and ~39% with *N,O*-CMCS-DA conjugate **2** and *O*-CMCS-DA conjugate **3**, respectively (Figure 10a). At

24 h of incubation, the percentage of FITC-positive cells arose to ~66% with *O*-CMCS-DA conjugate **3** and ~40% with *N,O*-CMCS-DA conjugate **2** at the highest concentration of 75 μM (Fig. 10b). MFI showed also a dose-dependent increase at 2.5 h, in particular with *N,O*-CMCS-DA conjugate **2** (Figure 10c); however, there was not an increment at 24 h, except for *O*-CMCS-DA conjugate **3** at 75 μM (Figure 10d). Overall, these data indicate that the two conjugates are taken up by a high number of cells in a time-dependent fashion although the average number of conjugates remained similar, with the notable exception of *O*-CMCS-DA conjugate **3** at the highest DA concentration.

[Insert Figure 9]

[Insert Figure 10]

4. Discussion

There is great interest for developing new and more effective therapeutic strategies as disease-modifying treatments for PD based on polymeric and lipid nanocarriers able to cross the BBB and to combat this rapidly rising in incidence and harmful disease. In this context, we are involved in a project aimed at developing polymer-DA conjugates which should possess the advantage of limited premature leakage of cargo (i.e., DA) during manipulations and administration due to the presence of a covalent chemical bond between polymeric backbone and neurotransmitter. The polymer we studied was *N,O*-CMCS, a water-soluble derivative of chitosan, endowed with several properties such as biocompatibility, biodegradability, mucoadhesion and non-toxicity [34]. We have previously described the synthesis by using DMF as solvent of the ester and amide conjugates **1** and **2**, respectively, as well as the high internalization of conjugate **2** by OECs (Figure 1) [19, 20]. The main aim of the present work was to develop a synthetic procedure of the amide conjugates **2** and **3** (Figure 1) carried out in aqueous medium in order to minimize the toxicity potential of the resulting conjugates as well as to follow eco-friendly procedures of synthesis in pharmaceutical laboratories. In addition, a further aim was to evaluate the effect of the carboxymethyl substituent position onto glucose nucleus of chitosan in order to gain insights into this structural modification. To this end, we included in this study also the polymer O-CMCS characterized by the presence of the carboxymethyl substituent exclusively on the primary –OH group in position-6 of the parent polymer chitosan.

We succeeded in reaching these goals following a modified reported procedure based on carbodiimide (EDC) chemistry [23]. As for the EDC mediated coupling reaction between *N,O*-CMCS or *O*-CMCS and DA to prepare the amide conjugates **2** and **3**, the coupling reagent EDC can react with the carboxyl groups of the carbohydrate polymers to form an *O*-acylisourea intermediate which, in turn, provides the required amide conjugate by reaction with the NH_2 group of the neurotransmitter as outlined in Scheme 1.

When the backbones of *N,O*-CMCS and *O*-CMCS were subjected to the amidification with DA in water as solvent, the yield values of the corresponding conjugates were 37% and 24% for *N,O*-CMCS-DA conjugate **2** and *O*-CMCS-DA conjugate **3**, respectively. It should be noted that the amide conjugate *N,O*-CMCS-DA **2** previously prepared employing organic solvent (DMF) was obtained in 70% yield [20]. On the other hand, comparing the yields in water as solvent, it resulted that conjugate **3,** even though prepared in lower yield, it is characterized by a higher DS% (12.65% vs 5.36% determined by potentiometric titration for **3** and **2**, respectively). This result could be rationalized

580 considering that in *O*-CMCS the carboxymethyl group substituent on the primary –OH group in position-6 of the glucose nucleus is available for the reaction with EDC and NH_2 group of the neurotransmitter more than that occurs for the carboxymethyl group substituents of *N*,*O*-CMCS polymer.

The thermal stability of DA, *N,O*-CMCS, *O*-CMCS, and corresponding conjugates with DA was 585 investigated by TGA to give a quantitative measure of their mass changes on increasing the temperature (Figure 5). Both the developed DA-conjugates from TGA thermograms evidenced thermal stability (up to about 190°C) which are acceptable for pharmaceutical applications [35]. In details, from TGA curves (Figure 5a), the main thermal events ascribable to both the chitosan derivatives under investigation could consist of deacetylation and decomposition of the parent 590 chitosan's main chains [36]. Moreover, it can be hypothesized that the cleavage of substituent groups in the carboxymethylated derivatives fell in the same temperature range (270-330°C). In any case, comparing with unmodified chitosan, the thermal stability of chitosan derivatives slightly decreased, as also reported [37]. While in the case of pure substances, a sharp weight loss was observed, starting at higher temperatures, in the case of conjugates a slow weight loss occurred at lower temperatures. 595 Indeed, broader peaks are observed in DTGA profiles of both the DA-conjugates, probably due to the overlapping of the decomposition steps relevant to CMCS (*N,O*- and *O*-) moieties and DA. Overall, TGA has been already employed to determine the thermostability of delivery systems targeting brain diseases, as reported in literature [30, 38] and information arising from such methodology has been combined with data obtained from DSC analysis. DSC thermograms reported in Figure 5b evidenced 600 the amorphous state of both *N,O*-CMCS-DA **2** and *O*-CMCS-DA **3**, without any endothermal/esothermal event occurring in the range of temperatures explored, whereas the thermogram of pure *N,O*-CMCS showed an endothermic peak at 150°C and the thermogram of *O*-CMCS showed an endothermic peak at 153°C.

Some information on the physical stability of *N,O*- and *O*-CMCS-DA conjugates on storage at -20°C 605 can be gained from Figure 6 panel (a). As can be seen, conjugate **2** possess higher stability under storage at T= -20°C than *O*-CMCS-DA conjugate **3**. Moreover, a further different behaviour noted between the two conjugates refers to the shape and retention time of the peak corresponding to the neurotransmitter in HPLC chromatograms. This peak maintained its shape, typical retention time value and no further peaks appeared in the case of *O*-CMCS-DA conjugate **3** suggesting that no DA 610 autoxidation occurred during storage frame time. Instead, for *N,O*-CMCS-DA **2**, HPLC chromatograms showed an enlarged peak with a little increase in retention time of DA signal together with the apparent increase of DS % occurring since four up to eight weeks. It may be probably due to DA autoxidation induced by air oxygen which was demonstrated to be a very slow process unlike the aerobic and anaerobic DA autoxidation in solution [39].

615 Consistent enough with the physical stability on storage data were also those from in vitro DA release from conjugates (Figure 6 panel (b)). The general trend showed in both release profiles, indeed, was of a prompt DA release (burst effect) within the first two days followed by a sustained release period. However, the bust effect noted for conjugate **3** was more intense than that showed by conjugate **2**, just as deduced by physical stability on storage data and, moreover, unlike that occurs for *O*-CMCS-620 DA, it was noted the complete disappearance of the neurotransmitter in the release profile of *N,O*-CMCS-DA **2**. This last outcome may support the above made hypothesis to explain the apparent increase of DS % of conjugate **2** occurring since four up to eight weeks of storage.

Several recent literature suggestions pointed out the self-aggregation of phenolic compounds conjugated with polysaccharides including *N,O*- or *O*-CMCS [28, 40, 41]. It prompted us to verify

whether also the conjugates **2** and **3** prepared in aqueous medium could similarly self-assembly into nanoscale structures as NPs. We succeeded in this task as demonstrated by TEM analysis after dispersion of each conjugate in PBS (pH 7.4) and following the procedure reported in Section 2.7. However, a different behaviour between the two conjugates was noted. In detail, while from conjugate **3** smaller and spherical NPs were observed by PCS (average size of 292 ± 2 nm), from conjugate **2** larger particles (average size of 459 ±7 nm) were detected. Moreover, by comparing the average diameters observed by TEM it was noted that they were smaller than the corresponding deduced by PCS (i.e., 187 ±7 nm by TEM compared with 459 ±7 nm by PCS). This discrepancy is a well-documented outcome in literature and it has been ascribed to the procedure involved in preparation of samples for which, due to solvent effect, the diameter measured by PCS (hydrodynamic diameter) results larger than that determined by TEM. As for the self-assembly process of *N,O*- or *O*-CMCS-DA conjugates **2** and **3**, it can be rationalized taking into account that both these conjugates may be considered amphiphilic polymers just as occurs for other phenolic compounds conjugated with polysaccharides [28, 40, 41]. In both conjugates, indeed, hydrophobic domains can be envisaged due to specific π–π- as well as hydrogen bonding-interactions between the catechol moieties of these conjugates (Figure S1). These hydrophobic domains may form the internal core of polymeric micelles with an external shell constituted by CMCS hydrophilic moieties [41]. Hence, the self-assembly process of conjugates **2** and **3** may involve polymeric micelle formation in DA-grafted CMCSs. The observed better quality of NPs from conjugate **3** in terms of size may be due to the uniform introduction of the CH_2-CO-NH-$(CH_2)_2$-Aryl-substituent on the C-6 hydroxyl of the glucose nucleus which allows the formation of regular and more effective π–π interactions between the mentioned aromatic regions than those occurring in conjugate **2** (Figure S1). In this last conjugate, indeed, the mentioned Aryl-substituents occur either at C-6 hydroxyl group or at the NH_2 moiety, making the mentioned interactions even at long-range and, hence, less regular and effective hydrophobic domains. Hence, it can be stated that the position of the carboxymethyl substituent on the CMCS backbone is quite important in determining the features of the resulting nanocarrier. A peculiar property of micelles is that they are stable at concentration higher than the Critical Micellar Concentration (CMC) while they disassemble by dilution at concentration below the CMC. In our case, however, even the disassembled conjugates **2** and **3** may be nano-structured leading to NP formation. It is already known, indeed, that grafted chitosans bearing aryl-groups can form polymeric NPs [42]. Hence, besides polymeric micelles, conjugates **2** and **3** may form polymeric NPs as nanosized structures. Considering that often polymeric micelles are smaller than 100 nm in size, at present it cannot be excluded that particles in little amount with a particle size < 100 nm detected in size distribution plots (Figure 7 (c) and 7 (d)) are constituted by polymeric micelles, while those in predominant amount with a particle size > 100 nm are represented by NPs. The negative zeta potentials of these nanocarriers (Table 2) are consistent with the absence of any absorption at 1730 cm^{-1} in FT-IR spectra of both conjugates suggesting the presence of free carboxymethyl substituents in –COONa form. Moreover, the observed PDI values suggest a satisfactory polydispersion. However, further characterization and evaluation of such nanocarriers as delivery systems of the neurotransmitter is in progress and the results of these studies will be reported in due course.

As mentioned in introduction section, mitochondrial disruptions and oxidative stress have been suggested to play an important role in the loss of DAergic neurons occurring in parkinsonian patients and such processes are mediated by ROS (reactive oxygen species) and free radicals like H_2O_2 and OH^- [7]. It induced us to evaluate the significant antioxidant potential of conjugates **2** and **3** measured by DPPH, unlike the starting polymers *N,O*-CMCS and *O*-CMCS. This is also supported by a

literature report showing that the DPPH scavenging activity of *O*-CMCS is only 2.98% at 2.5 mg/mL [28]. Following the literature hints reported for phenolic compounds conjugated with polysaccharides, *N*,*O*- or *O*-CMCS-DA could react with DPPH radical by donating hydrogen atom to form stable DPPH-H and *N*,*O*- or *O*-CMCS-DA radicals. Next, *N*,*O*- or *O*-CMCS-DA radical could be further withdrawn hydrogen atom to form stable *N*,*O*- or *O*-CMCS-DA quinone compounds as shown in Figure S2 [43]. Hence the DPPH radical scavenging activity of *N*,*O*- or *O*-CMCS-DA conjugates **2** and **3** may be mainly due to the catechol moieties occurring in these macromolecular substances and, therefore, possess an antioxidant effect with the latter conjugate at a higher extent than the former.

For uptake studies, fluorescent conjugates were obtained and for both FITC-*O*-CMCS-DA conjugate **3** and FITC- *N*,*O*-CMCS-DA conjugate **2** the DS in the dye FITC was found to be equal to 5 and 13 μg FITC/mg of fluorescent conjugate, namely significantly lower than the previously studied FITC-*N*,*O*-CMCS-DA **1** exhibiting 100 μg FITC/mg of FITC-*N*,*O*-CMCS-DA [20]. However, while in our previous work, FITC-*N*,*O*-CMCS-DA **1** was taken up by ~70% of OECs already at 2 h, neuroblastoma cells were less permissive to uptake at 2.5 h, reaching a good level of internalisation only at 24 h. Whether these results are due to less FITC molecules associated with conjugates or to a different cell line, it is difficult to discern. The lower MFI (~8000 verso ~2000 arbitrary units) may indicate that the lower FITC content may have given these results. Nevertheless, the therapeutic dose of DA (i.e. 75 μM, corresponding to 11.5 μg/mL, with Tang et al. [44] showing that DA-carrying nanoparticles was effective in alleviating motor symptoms in a rat model of PD at the dose of ~ 7.4 μg/mL) was taken up by a good number of cells, (i.e. up to 66% with *O*-CMCS-DA **3**), indicating that further experiments would clarify if these percentages allows for an efficacious arrival of DA into the relevant neuronal cells of the subcortical nuclei.

Overall, it seems that *N*,*O*- or *O*-CMCS-DA conjugates **2** and **3** may constitute an example of the so called "multifunctional nanomedicines" that combine multiple biological functions into a single nanosystem and whose usefulness in brain diseases has been recently evidenced [45]. Thus, conjugates **2** and **3** can provide neurotransmitter DA useful for "dopamine replacement strategy" and an antioxidant effect which limits the ROS production.

5. Conclusions

We succeeded to conjugate the primary amino group of neurotransmitter DA with the –COOH function of *N*,*O*-CMS or *O*-CMCS leading to amide conjugates **2** and **3** in aqueous environment following eco-friendly procedures of synthesis trying to minimize the toxicity potential of the conjugates obtained. From a structural point of view, conjugates **2** and **3** were characterized by spectroscopic means (i.e., FT-IR and ^{1}H-NMR) and percentage of substitution degree. Thermal analysis showed that **2** and **3** are endowed with thermal stability and an amorphous state was observed for both, unlike the starting polymers *N*,*O*-CMS and *O*-CMCS. Interestingly, it was found that CMCS-DA conjugates may self-assembly to form polymeric micelles and/or NPs, these last supported by TEM observations. The better quality in size of NPs from conjugate **3** may be due to more efficient π–π- and hydrogen bonding- interactions between aromatic regions than those occurring in conjugate **2.** Moreover, DA release from conjugate **3** was quicker in the SNF receiving medium as well as its uptake increased of ~66% with *O*-CMCS-DA conjugate **3** at the highest concentration of 75 μM compared with~40% for conjugate **2**. Hence, the obtained results indicate that the position of the carboxymethyl group on the CMCS backbone plays an important role in

determining the features of the resulting nanocarrier confirming so our starting hypothesis. Further characterization and evaluation of such NPs as DA delivery systems are in progress and the results will be reported in due course. Besides this, a further interesting conclusion is that conjugates **2** and **3** show antioxidant activity, with the latter conjugate at a higher extent than the former, as demonstrated by DPPH radical scavenging assay. Thus, such new examples of chitosan-based nanocarriers to be used by intranasal administration possess promising properties for brain delivery as "multifunctional nanomedicines" [45, 46].

5. Author contribution section

Sante Di Gioia: Writing—review and editing; supervision, **Giuseppe Fracchiolla**: Investigation and methodology **Stefania Cometa:** Investigation; **Filippo Perna**: Investigation and methodology; **Andrea Francesca Quivelli**: Investigation and software; **Giuseppe Trapani**: Supervision; **Valeria Daniello:** Investigation; **Concetta Nobile:** Investigation; **Md Niamat Hossain**: Investigation; **Adriana Trapani**: Conceptualization, investigation; writing—original draft preparation, writing—review and editing; funding acquisition and Supervision; **Massimo Conese**: Conceptualization, methodology, supervision; writing—original draft preparation, writing—review and editing.

Declaration of competing interests

The authors declare that they have no known competing financial interests or personal relationships that could have appeared to influence the work reported in this paper.

Acknowledgement

A.T. would like to acknowledge Dr. Sergio Cellamare (University of Bari, Aldo-Moro, Italy) and Dr. Alessandra Quarta (University of Salento, Italy) for their technical help. S.D.G and M.C. would like to thank Dr. Nicoletta Mangialetto (Hematology Unit, Policlinico Riuniti of Foggia, Foggia, Italy) for her help with cytofluorimetric analysis.

References

[1] A.D. Gitler, P. Dhillon, J. Shorter, Neurodegenerative disease: models, mechanisms, and a new hope, Dis Model Mech 10(5) (2017) 499-502.
[2] Y. Esmaeili, Z. Yarjanli, F. Pakniya, E. Bidram, M.J. Los, M. Eshraghi, D.J. Klionsky, S. Ghavami, A. Zarrabi, Targeting autophagy, oxidative stress, and ER stress for neurodegenerative disease treatment, J Control Release 345 (2022) 147-175.
[3] C. Spuch, O. Saida, C. Navarro, Advances in the treatment of neurodegenerative disorders employing nanoparticles, Recent Pat Drug Deliv Formul 6(1) (2012) 2-18.
[4] M. Pandya, C.S. Kubu, M.L. Giroux, Parkinson disease: not just a movement disorder, Cleve Clin J Med 75(12) (2008) 856-64.
[5] E. Wollmer, S. Klein, A review of patient-specific gastrointestinal parameters as a platform for developing in vitro models for predicting the in vivo performance of oral dosage forms in patients with Parkinson's disease, Int J Pharm 533(1) (2017) 298-314.
[6] K.R. Chaudhuri, A. Rizos, K.D. Sethi, Motor and nonmotor complications in Parkinson's disease: an argument for continuous drug delivery?, J Neural Transm (Vienna) 120(9) (2013) 1305-20.

[7] C. Rodriguez-Nogales, E. Garbayo, M.M. Carmona-Abellan, M.R. Luquin, M.J. Blanco-Prieto, Brain aging and Parkinson's disease: New therapeutic approaches using drug delivery systems, Maturitas 84 (2016) 25-31.
[8] V. Bourganis, O. Kammona, A. Alexopoulos, C. Kiparissides, Recent advances in carrier mediated nose-to-brain delivery of pharmaceutics, Eur J Pharm Biopharm 128 (2018) 337-362.
[9] M. Conese, R. Cassano, E. Gavini, G. Trapani, G. Rassu, E. Sanna, S. Di Gioia, A. Trapani, Harnessing Stem Cells and Neurotrophic Factors with Novel Technologies in the Treatment of Parkinson's Disease, Curr Stem Cell Res Ther 14(7) (2019) 549-569.
[10] C. Riccardi, F. Napolitano, D. Montesarchio, S. Sampaolo, M.A.B. Melone, Nanoparticle-Guided Brain Drug Delivery: Expanding the Therapeutic Approach to Neurodegenerative Diseases, Pharmaceutics 13(11) (2021).
[11] D. Lee, T. Minko, Nanotherapeutics for Nose-to-Brain Drug Delivery: An Approach to Bypass the Blood Brain Barrier, Pharmaceutics 13(12) (2021).
[12] Z. Wang, G. Xiong, W.C. Tsang, A.G. Schatzlein, I.F. Uchegbu, Nose-to-Brain Delivery, J Pharmacol Exp Ther 370(3) (2019) 593-601.
[13] A. Ancona, M. Sportelli, A. Trapani, R.A. Picca, C. Palazzo, E. Bonerba, F. Mezzapesa, G. Tantillo, G. Trapani, N. Cioffi, Synthesis and Characterization of Hybrid Copper-Chitosan Nano-antimicrobials by Femtosecond Laser-Ablation in Liquids, Material Letters 136 (2014) 397-400.
[14] A. Singh, H.L. Kutscher, J.C. Bulmahn, S.D. Mahajan, G.S. He, P.N. Prasad, Laser ablation for pharmaceutical nanoformulations: Multi-drug nanoencapsulation and theranostics for HIV, Nanomedicine 25 (2020) 102172.
[15] T.T. Nguyen, H.J. Maeng, Pharmacokinetics and Pharmacodynamics of Intranasal Solid Lipid Nanoparticles and Nanostructured Lipid Carriers for Nose-to-Brain Delivery, Pharmaceutics 14(3) (2022).
[16] T. Kurano, T. Kanazawa, A. Ooba, Y. Masuyama, N. Maruhana, M. Yamada, S. Iioka, H. Ibaraki, Y. Kosuge, H. Kondo, T. Suzuki, Nose-to-brain/spinal cord delivery kinetics of liposomes with different surface properties, J Control Release 344 (2022) 225-234.
[17] R. Maher, A. Moreno-Borrallo, D. Jindal, B.T. Mai, E. Ruiz-Hernandez, A. Harkin, Intranasal Polymeric and Lipid-Based Nanocarriers for CNS Drug Delivery, Pharmaceutics 15(3) (2023).
[18] V. De Leo, S. Ruscigno, A. Trapani, S. Di Gioia, F. Milano, D. Mandracchia, R. Comparelli, S. Castellani, A. Agostiano, G. Trapani, L. Catucci, M. Conese, Preparation of drug-loaded small unilamellar liposomes and evaluation of their potential for the treatment of chronic respiratory diseases, Int J Pharm 545(1-2) (2018) 378-388.
[19] R. Cassano, A. Trapani, M.L. Di Gioia, D. Mandracchia, R. Pellitteri, G. Tripodo, S. Trombino, S. Di Gioia, M. Conese, Synthesis and characterization of novel chitosan-dopamine or chitosan-tyrosine conjugates for potential nose-to-brain delivery, Int J Pharm 589 (2020) 119829.
[20] S. Di Gioia, A. Trapani, R. Cassano, M.L. Di Gioia, S. Trombino, S. Cellamare, I. Bolognino, M.N. Hossain, E. Sanna, G. Trapani, M. Conese, Nose-to-brain delivery: A comparative study between carboxymethyl chitosan based conjugates of dopamine, Int J Pharm 599 (2021) 120453.
[21] X.-G. Chen, H.-J. Park, Chemical characteristics of O-carboxymethyl chitosans related to the preparation conditions, Carbohydrate Polymers 53(4) (2003) 355-359.
[22] V.K. Mourya, N. Inamdara, N. Ashutosh Tiwari, Carboxymethyl Chitosan And Its Applications, Advanced Materials Letters 1(1) (2010) 11-33.
[23] C. Fan, J. Fu, W. Zhu, D.A. Wang, A mussel-inspired double-crosslinked tissue adhesive intended for internal medical use, Acta Biomater 33 (2016) 51-63.
[24] A. Trapani, F. Corbo, G. Agrimi, N. Ditaranto, N. Cioffi, F. Perna, A. Quivelli, E. Stefano, P. Lunetti, A. Muscella, S. Marsigliante, A. Cricenti, M. Luce, C. Mormile, A. Cataldo, S. Bellucci, Oxidized Alginate Dopamine Conjugate: In Vitro Characterization for Nose-to-Brain Delivery Application, Materials (Basel) 14(13) (2021).

[25] A. Trapani, F. Corbo, E. Stefano, L. Capobianco, A. Muscella, S. Marsigliante, A. Cricenti, M. Luce, D. Becerril, S. Bellucci, Oxidized Alginate Dopamine Conjugate: A Study to Gain Insight into Cell/Particle Interactions, J Funct Biomater 13(4) (2022).
[26] A. Trapani, D. Mandracchia, G. Tripodo, S. Cometa, S. Cellamare, E. De Giglio, P. Klepetsanis, S.G. Antimisiaris, Protection of dopamine towards autoxidation reaction by encapsulation into non-coated- or chitosan- or thiolated chitosan-coated-liposomes, Colloids Surf B Biointerfaces 170 (2018) 11-19.
[27] M. Fir, L. Milivojevic, M. Prosek, A. Smidovnik, Properties Studies of Coenzyme Q10-Cyclodextrins complexes. , Acta Chim Slov. 56 (2009) 885.891.
[28] R. Bai, H. Yong, X. Zhang, J. Liu, J. Liu, Structural characterization and protective effect of gallic acid grafted O-carboxymethyl chitosan against hydrogen peroxide-induced oxidative damage, Int J Biol Macromol 143 (2020) 49-59.
[29] J. Du, Y.L. Hsieh, Nanofibrous membranes from aqueous electrospinning of carboxymethyl chitosan, Nanotechnology 19(12) (2008) 125707.
[30] A. Trapani, S. Cometa, E. De Giglio, F. Corbo, R. Cassano, M.L. Di Gioia, S. Trombino, M.N. Hossain, S. Di Gioia, G. Trapani, M. Conese, Novel Nanoparticles Based on N,O-Carboxymethyl Chitosan-Dopamine Amide Conjugate for Nose-to-Brain Delivery, Pharmaceutics 14(1) (2022).
[31] N. Umek, B. Gersak, N. Vintar, M. Sostaric, J. Mavri, Dopamine Autoxidation Is Controlled by Acidic pH, Front Mol Neurosci 11 (2018) 467.
[32] A. Trapani, L. Guerra, F. Corbo, S. Castellani, E. Sanna, L. Capobianco, A.G. Monteduro, D.E. Manno, D. Mandracchia, S. Di Gioia, M. Conese, Cyto/Biocompatibility of Dopamine Combined with the Antioxidant Grape Seed-Derived Polyphenol Compounds in Solid Lipid Nanoparticles, Molecules 26(4) (2021) 916.
[33] D. Hadjipavlou-Litina, G.E. Magoulas, S.E. Bariamis, D. Drainas, K. Avgoustakis, D. Papaioannou, Does conjugation of antioxidants improve their antioxidative/anti-inflammatory potential?, Bioorg Med Chem 18(23) (2010) 8204-17.
[34] Z. Shariatinia, Carboxymethyl chitosan: Properties and biomedical applications, Int J Biol Macromol 120(Pt B) (2018) 1406-1419.
[35] M.I. Yoshida, E.C. Gomes, C.D. Soares, A.F. Cunha, M.A. Oliveira, Thermal analysis applied to verapamil hydrochloride characterization in pharmaceutical formulations, Molecules 15(4) (2010) 2439-52.
[36] S.F. Wang, L. Shen, Y.J. Tong, L. Chen, I.Y. Phang, P.Q. Lim, T.X. Liu, Biopolymer chitosan/montmorillonite nanocomposites: Preparation and characterization, Polymer Degradation and Stability 90(1) (2005) 123-131.
[37] M. Ziegler-Borowska, D. Chełminiak, H. Kaczmarek, A. Kaczmarek-Kędziera, Effect of side substituents on thermal stability of the modified chitosan and its nanocomposites with magnetite, Journal of Thermal Analysis and Calorimetry 124(3) (2016) 1267-1280.
[38] S. Cometa, M.A. Bonifacio, G. Trapani, S. Di Gioia, L. Dazzi, E. De Giglio, A. Trapani, In vitro investigations on dopamine loaded Solid Lipid Nanoparticles, J Pharm Biomed Anal 185 (2020) 113257.
[39] M. Salomaki, T. Ouvinen, L. Marttila, H. Kivela, J. Leiro, E. Makila, J. Lukkari, Polydopamine Nanoparticles Prepared Using Redox-Active Transition Metals, J Phys Chem B 123(11) (2019) 2513-2524.
[40] J. Liu, J.F. Lu, J. Kan, Y.Q. Tang, C.H. Jin, Preparation, characterization and antioxidant activity of phenolic acids grafted carboxymethyl chitosan, Int J Biol Macromol 62 (2013) 85-93.
[41] F.Q. Hu, L.N. Liu, Y.Z. Du, H. Yuan, Synthesis and antitumor activity of doxorubicin conjugated stearic acid-g-chitosan oligosaccharide polymeric micelles, Biomaterials 30(36) (2009) 6955-63.
[42] R.R. Gadkari, S. Suwalka, M.R. Yogi, W. Ali, A. Das, R. Alagirusamy, Green synthesis of chitosan-cinnamaldehyde cross-linked nanoparticles: Characterization and antibacterial activity, Carbohydr Polym 226 (2019) 115298.

[43] J. Liu, C.G. Meng, Y.H. Yan, Y.N. Shan, J. Kan, C.H. Jin, Protocatechuic acid grafted onto chitosan: Characterization and antioxidant activity, Int J Biol Macromol 89 (2016) 518-26.
[44] S. Tang, A. Wang, X. Yan, L. Chu, X. Yang, Y. Song, K. Sun, X. Yu, R. Liu, Z. Wu, P. Xue, Brain-targeted intranasal delivery of dopamine with borneol and lactoferrin co-modified nanoparticles for treating Parkinson's disease, Drug Deliv 26(1) (2019) 700-707.
[45] P. Faria, C. Pacheco, R.P. Moura, B. Sarmento, C. Martins, Multifunctional nanomedicine strategies to manage brain diseases, Drug Deliv Transl Res 13(5) (2023) 1322-1342.
[46] C. Pacheco, F. Sousa, B. Sarmento, Chitosan-based nanomedicine for brain delivery: Where are we heading?, Reactive and Functional Polymers 146 (2020) 104430.

Carboxymethyl chitosan Dopamine Conjugates: Synthesis and Evaluation for Intranasal anti Parkinson Therapy

Sante Di Gioia[1], Giuseppe Fracchiolla[2], Stefania Cometa[3], Filippo Maria Perna[2], Andrea Francesca Quivelli[2], Giuseppe Trapani[2], Valeria Daniello[1], Concetta Nobile[4], Md Niamat Hossain[1], Adriana Trapani[2*], Massimo Conese[1]

[1]Department of Clinical and Experimental Medicine, University of Foggia, 71122, Foggia, Italy

[2]Department of Pharmacy-Drug Sciences, University of Bari "Aldo Moro", Consorzio C.I.N.M.P.I.S., via E. Orabona, 4-70125 Bari, Italy

[3]Jaber Innovation s.r.l., 00144 Rome, Italy

[4]CNR-NANOTEC Institute of Nanotechnology, Via Monteroni, 73100 Lecce, Italy

[*]Corresponding Author: Prof. Adriana Trapani

Department of Pharmacy-Drug Sciences

University of Bari "Aldo Moro", Bari, Italy

Tel.: +39-0805442114. Fax: +39-0805442724.

Email: adriana.trapani@uniba.it

Abstract

With respect to the Parkinson disease (PD), herein, we aimed at synthetizing and characterizing two novel macromolecular conjugates where dopamine (DA) was linked to *N,O*-carboxymethyl chitosan or *O*-carboxymethyl chitosan, being both conjugates obtained from an organic solvent free synthetic procedure. They were characterized by FT-IR, ^{1}H-NMR spectroscopies, whereas thermal analysis (including Differential Scanning Calorimetry and Thermal Gravimetric Analysis) revealed good stability of the two conjugates after exposure at temperatures close to 300°C. Release studies in simulated nasal fluid elucidated that a faster release occurred since *O*-carboxymethyl chitosan-DA conjugate maybe due to the less steric hindrance exerted by the polymeric moiety. The CMCS-DA conjugates prepared in aqueous medium may self-assembly to form polymeric micelles and/or may form polymeric nanoparticles. TEM and Photon correlation spectroscopy lent support for polymeric nanoparticle formation. Moreover, such CMCS-DA conjugates showed antioxidant activity, as demonstrated by DPPH radical scavenging assay. Finally, cytocompatibility studies with neuroblastoma SH-SY5Y cells showed no cytotoxicity of both conjugates, whereas their uptake increased from 2.5 to 24 h and demonstrated in 40-66% of cells.

Keywords**:** Polymeric conjugates, Dopamine, Storage stability, Cytotoxicity, Uptake

List of chemical compounds studied in the article: Dopamine hydrochloride (Compound CID: 65340), Chitosan (Compound CID: 129662530), *N,O*-carboxymethyl chitosan–Dopamine amide conjugate, *O*-carboxymethyl chitosan–Dopamine amide conjugate.

1. Introduction

Neurodegenerative diseases (NDs) are characterized by progressive loss of neuron function whose occurrence increases with the age of the patient [1]. Thus, it has been even predicted that NDs will become the second leading cause of death after cardiovascular diseases in developed countries by 2040 due, at least in part, to the progressively aging of population [2]. Among the NDs, including Alzheimer's disease (AD), Parkinson's disease (PD), Huntington's disease, amyotrophic lateral sclerosis, frontotemporal dementia and the spinocerebellar ataxias, PD is the second widespread disorder after AD and it is endowed with the increasing impairment of dopaminergic neurons in the Substantia Nigra as well as with significant decrease in concentration of dopamine (DA) in the striatum [3]. From a symptomatic point of view, PD is characterized by movement disorders like tremors, rigidity, bradykinesia, memory loss and hesitant speech as well as by several non-motor symptoms such as sleep disorders and gastrointestinal ones [4, 5]. The current pharmacological treatment of PD is only symptomatic and it is based on the "dopamine replacement strategy", involving the oral administration of the DA precursor levodopa (L-DOPA) in order to restore acceptable levels of the neurotransmitter in the brain. However, long-term administration of L-DOPA brings about adverse effects including motor complications and dyskinesia [6]. Thus, even though many preclinical studies have been carried out to find new therapeutic agents for PD, the majority of new drug candidates failed in clinical trials mainly because they are unable to cross the blood brain barrier (BBB) in therapeutic amounts. Hence, as occurs also for other NDs, there is a huge need to develop both symptomatic and disease-modifying treatments for PD [7]. However, even though the main cause(s) of PD is (are) still not fully understood, new therapeutic targets useful to limit the loss

of DAergic neurons have been evidenced including alpha-synuclein aggregation and phosphorylation, proteasome and lysosome approach, mitochondrial disruptions and oxidative stress as well as glial environment and neuroinflammation [7].

In the last decade, an interesting and non-invasive approach to bypass the BBB in NDs has been extensively investigated. It consists in the use of the intranasal (IN) administration which allows a direct access to the brain using the olfactory and/or trigeminal connections between the nose and the brain [8-11]. Relationships between epithelial/vascular structures and nerve endings in the nasal cavity indicate that the olfactory nerve, comprised of bipolar neurons projecting through the olfactory epithelium and he cribriform plate, is the preferential route for central nervous system (CNS) transport with less systemic absorption. Intracellular and paracellular mechanisms allow drugs/nanocarriers to enter into the subarachnoid space and eventually in the CNS tissues using cerebrospinal fluid convectional transport [12]. Evidences in animal models report that intranasally administered drugs reach the olfactory bulb as soon as 10 min post-administration and the striatum and other distal locations in 30 min [13]. Such nose-to-brain delivery possesses not only the advantage to overcome the BBB but also to avoid hepatic and gastrointestinal metabolism as well as to decrease systemic side effects since the plasma exposure is reduced [14]. The use of intranasal administration route sometimes allows to gain pharmacodynamic effects even superior when compared with the administration of the same drug by oral route which offers the advantage of patient acceptance and endorsement of pharmaceutical industry [14, 15]. Despite these advantages, however, nose-to-brain delivery has some limitations that must be taken into account when this approach is followed for the treatment of neurological disorders including NDs. This delivery route, indeed, is difficult when high doses of drug are to be administered due to the limited volume of each nostril in humans, moreover the residence times of formulations within the nasal cavity may be short due to mucociliary clearance with important consequences on drug absorption. Again, it should be taken into account the presence of enzymes in the nasal cavity and, consequently, the need to protect sensitive drugs from enzymatic degradation and, finally, it should be considered that the nasal formulation does not cause irritation in the nasal cavity [14].

In the field of nose-to-brain delivery, several studies showed that the encapsulation of the drugs in nanocarriers can improve drug transport across BBB enhancing the bioavailability at brain level. Thus, nanoparticles prepared from chitosan and its derivatives have been shown better nose-to-brain delivery properties perhaps due to the temporarily opening capability of intercellular tight junctions of these polymers and/or to their mucoadhesive characteristics which would prolong the residence time of the formulation within the nasal cavity [14]. Again, advances in nanotechnology led to the synthesis of nanoparticles of small size (< 100 nm) by laser ablation even with application in BBB crossing [16, 17]. Also lipid based nanocarriers, including solid lipid nanoparticles (SLNs), nanostructured lipid carriers (NLC) and liposomes of small size (< 100 nm) also have a good potential for nose-to-brain delivery since they can encapsulate hydrophilic or hydrophobic drugs with good efficiency [18-21]. Moreover, they can easily squeeze through intercellular spaces between olfactory cells and their mucoadhesive/mucopenetration properties can be appropriately tailored to prolong the residence time in the nasal cavity facilitating nose-to-brain transport [18, 20].

In this context, recently we have developed *N,O*-carboxymethyl chitosan-DA ester and amide conjugates (ester or amide *N,O*-CMCS-DA) and evaluated both their in vitro mucoadhesive properties in simulated nasal fluid (SNF) and their uptake by Olfactory Ensheating Cells (OECs) for potential application in nose-to-brain delivery of the neurotransmitter to restore acceptable levels of DA in the brain of parkinsonian patients [22, 23]. These macromolecular conjugates could possess several

advantages including prolonged circulation, controlled release and improved mucoadhesive properties. Moreover, such conjugates, unlike those with low molecular weight moieties [24], could offer the relevant possibility to formulate polymeric nanoparticles with limited premature leakage of the biologically active substance (i.e., DA) since it is linked to the polymeric backbone by a covalent chemical bond. The premature leakage of the cargo encapsulated in nanocarriers is an important drawback to be considered particularly for most potent substances as DA. Among the conjugates studied, the *N,O* CMCS ester **1** and the corresponding *N,O*-CMCS amide conjugates **2** were evaluated (Figure 1) [22, 23]. These conjugates were prepared according to synthetic procedures involving organic solvent (DMF) and coupling reagents. The main results of the previous studies were the observed higher stability of *N,O*-CMCS-DA amide conjugate compared to the ester ones as well as the high internalization of this amide conjugate by OECs.

Following these studies, we considered of interest to synthesize both conjugate **2** and the new amide macromolecular conjugate of the neurotransmitter **3** (Figure 1), resulting from the conjugation of the primary amino group of neurotransmitter with the –COOH function of *O*-CMCS polymer, following eco-friendly procedures of synthesis in pharmaceutical laboratories. This last carboxymethyl chitosan derivative is soluble in a wide range of pH due to the introduction of carboxymethyl group and it is characterized by the presence of the carboxymethyl substituent on the primary –OH group in position-6 of the glucose nucleus. Chitosan, indeed, possesses three reactive groups in the molecule and namely a primary hydroxyl group, a secondary hydroxyl group and an amino group. Depending on the reaction conditions used, *N*-carboxymethyl chitosan (*N*-CMCS), *O*-carboxymethyl chitosan (*O*-CMCS) or *N,O*-carboxymethyl chitosan (*N,O*-CMCS) may be prepared [25, 26]. Thus, our working hypotheses for these novel conjugates were to evaluate whether *i*) it is possible to develop a synthetic approach employing, in agreement with green chemistry principles, water as solvent and the elimination of organic reagents not absolutely necessary. It in order to minimize the toxicity potential of conjugates **2** and **3** and, hence, to improve their performance for DA replacement in anti-Parkinson therapy; *ii*) the position of the carboxymethyl substituent on the chitosan backbone could influence the features of the resulting conjugates including release of the neurotransmitter and uptake by neuronal SH-SY5Y cell model line. In particular, our aim was to evaluate from which conjugate a greater amount of DA release occurs since it is well known that amide bonds are hydrolyzed very slowly, resulting sometimes in excessively slow release and, thus, unacceptable from a practical point of view. In addition, it was also our interest to know from which conjugate a higher internalization by cells occurs.

Hence, in the present paper, we describe the procedure we used for the synthesis of *N,O*-CMCS-DA **2** and *O*-CMCs-DA **3** conjugates in aqueous buffered medium (Figure 1). The new amide conjugates were characterized by FT-IR, ^{1}H-NMR spectroscopies and thermal analysis (Thermogravimetric Analysis (TGA) and Differential Scanning Calorimetry (DSC)), DA release kinetic as well as it was examined the possibility that CMCS conjugates **2** and **3** could self-assembly forming micelles or further nanosized structures in the aqueous medium. In order to consider the biocompatibility and translational capability of the two amide conjugates, cell viability and uptake tests were carried out in neuroblastoma SHSY-5Y cells. The results show that it is possible to prepare conjugates **2** and **3** in organic solvent free environment, limiting so their potential toxicity and that the position of the carboxymethyl substituent on the chitosan backbone plays an important role in determining the features including the neurotransmitter release kinetic and uptake by neuronal SH-SY5Y cells.

2. Materials and Methods

2.1. Materials

N,O-Carboxymethyl Chitosan (*N,O*-CMCS, Molecular weight in the range of 30-500 kDa, deacetylation degree, 94.2%; viscosity 22 mPa sec, according to the provider's instructions) was purchased from Heppe Medical Chitosan GmbH (Halle, Germany). *O*-Carboxymethyl Chitosan (*O*-CMCS, Molecular weight in the range of 100-300 kDa, deacetylation degree, 90%; substitution degree 88 %, according to the supplier's instructions) was purchased from DBA (Milan, Italy). Ethyl-dimethyl-aminopropylcarbodiimide (EDC), dopamine hydrochloride (DA), 2,2-diphenyl-1-picrylhydrazyl (DPPH), fluorescein 5(6)-isothiocyanate (FITC), and PBS were purchased from Sigma-Aldrich (Milan, Italy). Dialysis tubes with a MWCO 12-14 kDa were purchased from Spectra Labs (Milan, Italy). Throughout this work, double distilled water was used. All other chemicals used were of reagent grade.

[Insert Figure 1]

2.2. Apparatus

The conjugates **2** and **3** were prepared following the synthetic procedure summarized in Scheme 1 and characterized by Proton nuclear magnetic resonance (^{1}H NMR) spectroscopy and Fourier transform infrared (FT-IR) spectroscopy as well as by thermogravimetric Analysis (TGA) and differential scanning calorimetry (DSC).

^{1}H NMR spectra were recorded on a Brüker spectrometer (Billerica, Massachusetts, US) operating at 600 MHz and the analyses were performed at 293 °K on dilute solutions of each conjugate using D_2O as solvent. In particular, to allow the determination of the substitution degree of *N,O*-CMCS-DA **2** and *O*-CMC-DA **3** via ^{1}H-NMR spectrometry, dispersions in D_2O were prepared for both conjugates at a concentration of 4 mg/mL and heated at 40°C for few minutes before the analysis. Chemical shifts are reported in parts per million (δ). Spectra were processed using Mnova (Mestrelab Research, A Coruña, Spain).

FT-IR spectra were obtained in KBr discs using a Perkin Elmer 1600 FT-IR spectrometer (Perkin Elmer, Milan, Italy). The range examined was 4,000–400 cm^{-1} with a resolution of 1 cm^{-1} [27].

Thermogravimetric analysis (TGA) was performed on a PerkinElmer TGA-400 instrument (PerkinElmer Inc, Waltham, MA), heating samples (5-10 mg) in the range 30-600°C under inert nitrogen flow at the heating rate of 20°C/min. For each sample, thermograms (TG) and derivative curves (DTG) were acquired and elaborated with the TGA Pyris software (version 13.3.1.0014, Waltham, USA).

Differential scanning calorimetry (DSC) thermograms were obtained using a Mettler Toledo DSC 822e STARe 202 System (Mettler Toledo, Milan, Italy), equipped with a DSC MettlerSTARe Software. For DSC analysis, aliquots of about 10 mg of both freeze-dried conjugates **1** and **2**, pure *O*-CMCS, pure *N,O*-CMCS were placed in an aluminium pan and hermetically sealed. The scanning rate was 5°C/min under a nitrogen flow of 20 cm^3/min and the temperature range was from 25 to 300°C and 25 to 275°C for DA and pure polymers/conjugates, respectively. The calorimetric system was calibrated using indium (purity 99.9%) and following the procedure of the MettlerSTARe Software. Each experiment was carried out in triplicate.

Transmission Electron Microscopy (TEM) images of samples containing both conjugates were recorded on a JEOL Jem1011 microscope (Tokyo, Japan) operating at an accelerating voltage of 100 kV.

The hydrodynamic diameters, polydispersity and zeta potential values of *N,O*-CMCS-DA **2** and *O*-CMCS-DA conjugates **3** self-assembled into nanoparticles were determined by using a Zetasizer NanoZS, ZEN 3600 (Malvern Instruments, Worcestershire, U.K.) instrument according to photon correlation spectroscopy (PCS) mode.

2.3 Synthesis of DA amide conjugates

To prepare conjugate **2** and **3**, the Fan's protocol for the preparation of the gelatin-DA conjugate in aqueous environment based on the carbodiimide (EDC) chemistry was followed with significant modifications [28]. In particular, besides the use of aqueous medium, we also avoided the use of *N*-hydroxysuccinimide or *N*-hydroxysulfosuccinimide, well-known agents increasing the efficiency of EDC-mediated coupling reactions. This in order to minimize the toxicity potential of the resulting conjugates due to the presence of traces of organic solvent and reagents not absolutely necessary. Thus, the reaction conditions used for the synthesis of this conjugate **2** and **3** resulted quite different from those used by Fan et al. [28].

*2.3.1. Synthesis of N,O-Carboxymethyl Chitosan-DA amide conjugate **2** in aqueous buffered medium*

To a solution of *N,O*-CMCS (0.2 g) in diluted HCl (0.1 N-50 mL) showing pH= 6, DA (0.1 g, 0.57 x 10^{-3} mol) was added together with 32 mg of EDC and the mixture was left to react under magnetic stirring in argon atmosphere for 48 h at room temperature (r.t.). The polymer/neurotransmitter weight ratio used was that employed by Fan et al. [28]. Afterwards, the reaction mixture was dialyzed in distilled water for three days and then lyophilized (Lio Pascal 5P, Milan Italy). The obtained product (*N,O*-Carboxymethyl Chitosan-DA amide conjugate **2**, *N,O*-CMCS-DA) was collected in good yield (about 37%) and characterized by FT-IR, ^{1}H NMR, TGA and DSC.

N,O-CMCS-DA amide conjugate **2**: FT-IR (KBr) ν (cm^{-1}): 3246 (NH, OH), 1629 (C=O), 1110 (OH).

*2.3.2. Synthesis of O-Carboxymethyl Chitosan-DA conjugate **3***

In a solution composed of 10 mL of diluted HCl (0.1N) and 40 mL of distilled water, 0.15 g of *O*-CMCS were poured, so achieving pH = 6 and, afterwards, 0.21 g of DA and 38 mg of EDC were added. Unlike the conjugate **2** synthesis, in this case the polymer/neurotransmitter weight ratio was that used in our previous work on the synthesis of the *N,O*-Carboxymethyl Chitosan-DA amide conjugate [23]. The resulting mixture was left under magnetic stirring in argon atmosphere for 48 h at r.t. Afterwards, the product was dialyzed in distilled water for three days and then lyophilized (Lio Pascal 5P, Milan Italy). The obtained product (*O*-Carboxymethyl Chitosan-DA amide conjugate **3**, *O*-CMCS-DA) was collected in good yield (about 24%) and, as above, characterized by FT-IR, ^{1}H NMR TGA and DSC. *O*-CMCS-DA amide conjugate **3**: FT-IR ν (cm^{-1}): 3412 (NH, OH), 2923 (CH aliphatic), 1639, 1617 (C=O), 1071 (OH).

2.3.3 Determination of substitution degree (DS) of DA-CMCS amide conjugates by titrations or hydrolysis under strong acidic conditions

The substitution degree (DS) of *N,O*-CMCS-DA **2** and *O*-CMCS-DA **3** conjugates was determined by potentiometric titration after alkaline hydrolysis according to a procedure previously described by us with slight modification [22, 23]. A weighted amount of each conjugate sample (50 mg) was dissolved in a solution of NaOH (0.25 N) in ethanol (5 mL) and the mixture was stirred at reflux for 24 h. Then, at room temperature a potentiometric titration on the dark-yellow mixture (1 mL) degree

was carried out using the automatic titrator (TITREX-1000, Wertheim, Germany) with a pH meter. Each potentiometric titration was carried out in triplicate.

During titration, two equivalent points were determined using a standardized solution of HCl (0.1 N). The first point referred headline in excess of NaOH (V1 equivalent point); the second equivalent point referred to the neutralization of the acid salt present (V2 equivalent point). The moles of HCl occurring between the first and the second equivalent point corresponding to the moles of free amide and the DS% were, therefore, determined by the following Equation (1):

$$DS\% = [\text{mass (sample)} - \text{mass (free amide)}]x100/\text{mass (sample)} \quad (1)$$

where mass (sample) corresponds to 1 mL (10 mg) of each conjugate sample before alkaline hydrolysis; moles of free amide or ester are equal to:

(V2 equivalent point - V1 equivalent point) x [HCl] determined by potentiometric titration as the average of three titrations.

The DS% concerning DA of each CMCS-DA amide conjugate was also measured according to hydrolysis under strong acidic conditions previously described [29]. Briefly, 2 mg of CMCS-DA amide conjugate were weighed and dissolved in HCl 1 N (pH 1) under stirring and light protection at r.t. for 3 h. Afterwards, the solution was centrifuged (16,000× g, for 45 min, Eppendorf 5415D, Germany) and the obtained supernatant was analysed by HPLC to assess the DA amounts (Section 2.2). The DS% was calculated as mg DA/mg CMCS-DA amide conjugate x 100 [29].

2.3.4 Preparation of FITC-N,O-CMCS-DA and FITC-O-CMCS-DA conjugates

For cellular uptake studies, *N,O*-carboxymethyl chitosan-DA conjugate **2** and *O*-carboxymethyl chitosan-DA conjugate **3** were labelled with fluoresceine isothiocyanate (FITC) by using a previously reported protocol with slight modifications [22, 23]. Briefly, for *N,O*-CMCS-DA amide conjugate **2**, (70 mg) were dissolved in 0.1 N HCl (3.2 mL) and then the pH was adjusted to 6.5 with 0.1 N NaOH (0.01 mL). For *O*-CMCS-DA amide conjugate **3**, (70 mg) was dissolved in double distilled water (4.5 mL) and then the pH was adjusted to 6.5 with 0.1 N HCl (0.37 mL). For both labelling procedures, FITC was dissolved at 20 mg/mL concentration in ethanol and 0.75 mL of this solution were added to amide conjugates **2** and **3**, under magnetic stirring at r.t. for 72 h under light protection. Afterwards, the fluorescent mixtures were dialyzed against double distilled water for 3 days and freeze-dried for 72 h. The labelling efficiencies of FITC-*N,O*-CMCS-DA and FITC-*O*-CMCS DA amide conjugates were determined calibrating the fluorometer (Perkin Elmer, Milan, Italy) in the range 1-140 ng/mL of FITC obtained by diluting 100 μg/mL of a methanol solution of FITC with phosphate buffer at pH 8.0 (excitation wavelength: 488 nm; emission wavelength: 525 nm; slits: 2.5 nm). Furthermore, to determine the substitution degree (DS), the FITC-CMCS-DA amide conjugate underwent acid hydrolysis [30]. Two mg of the FITC-CMCS-DA amide conjugate were weighed and dissolved in 2 mL of HCl 1 N (pH 1), stirred and protected from light, at r.t. for 3 h. Then, the resulting mixture was centrifuged (16,000× g, for 45 min, Eppendorf 5415D, Hamburg, Germany) and the supernatant was analyzed by HPLC to assess the DA amounts. The DS was calculated as mg DA/mg FITC-CMCS-DA amide conjugate [30].

2.4. Quantitative determination of dopamine

DA quantification was carried out by HPLC as previously reported [31]. Briefly, the mobile phase consisted of 0.02 M potassium phosphate buffer, pH 2.8: CH_3OH 70:30 (v/v), and the elution of the column in isocratic mode occurred at the flow rate of 0.7 mL/min. Under such chromatographic

conditions, DA retention time was equal to 5.5 min, whereas retention time of both conjugates was equal to 4.9 min.

2.5. Storage Stability of DA-CMCS conjugates at low temperature

With the aim to check the storage stability at -20°C, aliquots of 3-5 mg of each freeze-dried DA-CMCS-conjugate were stored in the freezer at the above mentioned temperature.

Sampling was done at 1, 2, 4 and 8 weeks in order to verify DS of DA over the time. In each sampling time, the aliquot of the DA-CMCS-conjugate was incubated with 1 mL HCl (0.1N) for 30 min to allow the cleavage of the amide linkage polymer-DA and, afterwards, the resulting mixture was centrifuged (16,000 × g, 45 min, Eppendorf 5415D, Hamburg, Germany).

In the supernatant the DA content was determined by HPLC as described in Section 2.4.

*2.6. In vitro neurotransmitter release from conjugates **2** and **3** in Simulated Nasal Fluid*

The neurotransmitter DA release in SNF [22] (pH 6.0, without enzymes) from *N,O*-CMCS-DA or *O*-CMCS-DA conjugates was carried out starting from a weighted amount of conjugate corresponding to 1-1.2 mg of DA and dispersing it in 2.5 mL of SNF containing 0.05% (v/v) of DMSO and thermostated at 37 ± 0.1°C in an agitated (40 rpm/min) water bath (Julabo, Milan, Italy). At scheduled time points, 0.25 mL of the receiving medium were withdrawn and replaced with 0.25 mL of fresh medium Then, each sample was centrifuged at 16,000 × g for 45 min, (Eppendorf 5415D, Germany), and the amounts of the neurotransmitter delivered were quantified in the resulting supernatants by HPLC, as above described, and plotted against the time. All the release experiments in SNF were carried out in triplicate.

*2.7. Self-aggregation of CMCS-DA conjugates **2** and **3** to form nanosized structures*

Dilute stock suspensions of conjugates **2** and **3** were prepared by dispersion of 2 mg of each conjugate in 200 μL of PBS (pH 7.4). Centrifugation of the samples at 13,200 rpm for 45 min (Eppendorf 5415D, Germany) allowed to discard the pellet and isolating the corresponding supernatant from which 25 μL were dropped onto carbon-coated copper grids and then stained with 1% (w/v) phosphotungstic acid solution for 1 min. Afterwards, the grids were rinsed with deionized water and left to dry under air overnight. Then, TEM observations of the resulting nanoparticles (NPs) were performed in order to obtain their morphology and an average TEM size. TEM images of both conjugates were recorded on a JEOL Jem1400 microscope (Tokyo, Japan) operating at an accelerating voltage of 120 kV. Particle size data arising from TEM analysis were also compared with the ones acquired according to Photon Correlation Spectroscopy (PCS) of the Zetasizer NanZS (ZEN 3600, Malvern, UK) apparatus after treatment with a probe sonication with a Vibra-cell sonicator (Sonics and Materials, U.K.) for 15 min at the output of energy equal to 750W in an ice water bath. The particle size and polydispersion (PDI) values were measured at 25 °C after dilution in double distilled water (1:1, v/v). For ζ-potential measurements laser Doppler anemometry technique was adopted (ZetasizerNanoZS, ZEN 3600, Malvern, UK) after dilution 1:20 (v.v) with KCl (1 mM, pH 7.0).

2.8. In vitro evaluation of antioxidant activity: Assay of DPPH radical scavenging activity

The in vitro antioxidant activity of the pure polysaccharides, *O*-CMCS-DA and *N,O*-CMCS-DA and the two corresponding conjugates (*N,O*-CMCS-DA **2** and *O*-CMCS-DA **3**) was evaluated using the DPPH test reported in literature slightly edited [32]. Firstly, ethanol was used as solvent for DPPH

test to obtain a stock solution at the concentration of 0.001% w/v and, then, diluted to 8 x 10^{-4}% (w/v). Dispersion of 5 mg of each sample in 0.5 mL of double distilled water was reacted with 2.5 mL of the diluted DPPH solution for 60 min at room temperature in the dark. The corresponding absorbances were recorded at the wavelength of 514 nm by using PerkinElmer Lambda Bio 20 spectrophotometer (PerkinElmer, Milan, Italy). Blanks were obtained by filling the cuvettes with 0.5 mL of ethanol and 2.5 mL of the 8 x 10^{-4}% (w/v) solution in DPPH. For all formulations under investigation, antioxidant activity (AA) was calculated from Equation (2) and expressed in percentages:

$$AA\ (\%) = (1 - As/Ab) \times 100 \qquad (2)$$

where As is the sample absorbance, and Ab the absorbance of the radical. All the experiments were carried out in triplicate.

However, it is now accepted that the results obtained by Equation (2) are useful only for qualitative but not for accurate quantitative evaluations which should be made considering the IC_{50} values defined as the concentration of the sample that caused 50% inhibition of DPPH radical formation [33].

2.9. Cytotoxicity evaluation in SH-SY5Y cell model line

SH-SY5Y cells were grown as previously described [29]. Briefly, cells were plated in a 96-well plate (BD, USA) at a density of 1×10^4 per well in 100 µL of complete medium and incubated overnight to allow cell attachment. Then, the culture medium was replaced with 100 µL of fresh medium containing different dilutions of *N,O*-CMCS-DA conjugate **2** (final concentration of dopamine: 18.75 µM and 4 µM, corresponding to 1336 µg/mL and 334 µg/mL) and *O*-CMCS-DA conjugate **3** (final concentrations of dopamine: 75 µM, 18.75 µM, 4 µM, corresponding to 11.5 µg/mL, 2.9 µg/mL, 0.7 µg/mL). Volumes of *O*-CMCS without DA were chosen to obtain the same CMCS amounts of the *O*-CMCS-DA conjugate **3** (11.5 µg/ml, 2.9 µg/ml, 0.7 µg/ml). Under these conditions cells were grown at 37 °C for 24 h. 1% Triton-X100-treated cells were used as a positive control. After treatments, cell viability was evaluated by MTT (3-(4,5-dimethylthiazol-2-yl)-2,5 diphenyl tetrazolium bromide), as previously described [23]. The cell viability was calculated as follows: % viability = [(Optical density {OD} of treated cell − OD of blank)/(OD of vehicle control − OD of blank) × 100], considering untreated cells as 100%.

2.10. Uptake of amide conjugates by SH-SY5Y cells

SH-SY5H cells were plated at the number of 80,000 per each well of a 24-well plate. Cells were incubated with 500 µL of fresh medium containing different dilutions of *O*-CMCS-DA conjugate **3** (final concentrations of dopamine: 75 µM, 18.75 µM, 4 µM, corresponding to 11.5 µg/mL, 2.9 µg/mL, 0.7 µg/mL) and *N,O*-CMCS-DA conjugate **2** (final concentration of dopamine: 75 µM, 18.75 µM and 4 µM, corresponding to 5344 µg/mL, 1336 µg/mL and 334 µg/mL). After 2.5 or 24 h, each well was treated with 0.05% trypan blue in PBS (in order to quench extracellular fluorescence), trypsinized, resuspended in 0.5 mL of PBS, and analysed by the BD FACSLyric™ Flow Cytometry (BD Biosciences, Franklin Lakes, NJ, USA). Fluorescence for FITC was measured at the wavelength of 488 nm, determining the percentage of FITC-positive cells after setting the gating on 99% (excluding cell debris) and by subtracting the fluorescence of untreated control cells. Ten thousand cells were examined in each experiment, evaluating the percentage of positive cells for FL1H fluorescence and the relative mean fluorescence per cell (MFI).

2.11. Statistics

Statistical analyses were carried out by Prism v. 5, GraphPad Software Inc., USA. Results were expressed as mean ± SD. Multiple comparisons were based on one-way analysis of variance (ANOVA) with Bonferroni or Tukey post hoc test and differences were considered significant when $p < 0.05$.

3. Results

[Insert Scheme 1]

*3.1. Synthesis and structural characterization of the amide conjugates **2** and **3***

EDC mediated coupling reaction between *N,O*-CMCS or *O*-CMCS and DA was used to prepare *N,O*-CMCS-DA amide conjugate **2** and *O*-CMCS-DA amide conjugate **3**, respectively (Scheme 1). In particular, the condensation reaction was carried out by stirring the reagents in aqueous buffered medium at pH 6.0 for 48 h at r. t. and the reaction products were purified by dialysis in distilled water for three days and lyophilisation. Conjugates **2** and **3** were structurally characterized by spectroscopic methods i.e., FT-IR and ^{1}H NMR. In the FT-IR spectrum of *N,O*-CMCS-DA amide conjugate **2** a characteristic absorption band centered at 1629 cm^{-1} was present and it was attributed to the carbonyl groups of the conjugate **2** (Figure 2a). In the FT-IR spectrum of *O*-CMCS-DA amide conjugate **3**, the splitted band at 1639 cm^{-1} and 1617 cm^{-1} was diagnostic of the amide carbonyl group (Figure 2b). Notably, in the FT-IR spectra of both *N,O*-CMCS-DA conjugate **2** and *O*-CMCS-DA conjugate **3**, no absorption band at 1730 cm^{-1} occurs suggesting that in these chitosan derivatives the carboxymethyl substituent is present in –COONa form [26].

[Insert Figure 2 revised]

In Figure 3, the ^{1}H NMR spectrum of the polysaccaride *O*-CMCS in D_2O (Figure 3a), showed multiplets from 3.91 to 3.27 ppm that were assigned to protons H3, H4, H5, H6 and the signal at 4.41 to methylene protons H7, in accordance with Du and Hsieh's peak attribution [34]. In Figure 3b, the ^{1}H NMR spectrum of the reaction product after functionalization of *O*-CMCS with DA is reported. Two new sets of signals, located at 6.26, 6.41, 6.51, 6.59, 6.66 ppm, were shown corresponding to the aromatic protons of DA, covalently-bonded to the polymer by an amide bond, probably due to two conformers of *O*-CMCS-DA conjugate **3**. The signals at 6.26 and 6.41 ppm belong to two aromatic protons of the majority signal set, those at 6.51 and 6.59 ppm belong to the minority one, while the third aromatic dopamine proton gives a single signal, for both conformers, to 6.66 ppm.The percentage of monomeric units substituted with DA (*DA-subst*) was determined comparing the integral of the signal at 6.66 ppm with that of the multiplets from 3.83 ppm to 3.22 ppm, which takes into account the H3, H4, H5, 2 x H6 protons, using the Equation: $DA\text{-}subst = I_{H\text{-}Ar} \times 5 / I_{H3,H4,H5,H6}$, where $I_{H\text{-}Ar}$ is intensity of the signal for the aromatic proton at 6.66 ppm and $I_{H3,H4,H5,H6}$ is intensity of the signal for H3, H4, H5 and both H6 protons, and it turns out to be 11%.

[Insert Figure 3]

Similarly, in Figure 4, the ^{1}H NMR spectra *of N,O*-CMCS, conjugate **2** (Figure 4a), in D_2O and after its functionalization with DA (Figure 4b) are shown. In this case, comparing the integral of the signals of the aromatic protons (6.50-6.64 ppm) with that of the multiplets 3.71-3.28 ppm (corresponding to H3, H4, H5, H6 protons [34]), the percentage of incorporated DA turns out to be 7%, calculated by the equation *DA-subst* = $I_{H\text{-}Ar}$ x 5 / $I_{H3,H4,H5,H6}$ x 3, where $I_{H\text{-}Ar}$ is the sum of the intensity of the signal for the aromatic protons and $I_{H3,H4,H5,H6}$ is intensity of the signal for H3, H4, H5 and both H6 protons. However, the analysis of the ^{1}H-NMR spectrum does not allow to distinguish between DA bound in position 2 and 6 of the six-term ring.

[Insert Figure 4]

The amounts of DA covalently bound to *N,O*-CMCS-DA and *O*-CMCS-DA amide conjugates **2** and **3**, respectively, were also determined by chemical means following the procedures reported in Section 2.2.3. From titration data focusing on quantification of -COOH groups, the DS% of *N,O*-CMCS-DA conjugate **2** was 5.36% corresponding to 536 μg (-COO derivatized)/10 mg *N,O*-CMCS-DA conjugate **2**. The DS% of *O*-CMCS-DA conjugate **3** was 12.65% corresponding to 1.265 mg (-COO derivatized)/10 mg *O*-CMCS-DA conjugate **3**. From hydrolysis under strong acidic conditions the DS% values were found equal to 2.3 ± 0.8% for *N,O*-CMCS-DA conjugate **2** and 6 ± 0.9% for *O*-CMCS-DA conjugate **3**. Comparing these data it appears that the DS% values of conjugates **2** and **3** measured by spectroscopic (^{1}H-NMR spectrum) and titration methods are in good agreement, while those obtained by hydrolysis under strong conditions are underestimated enough. This outcome may suggest that the conditions used for such hydrolysis under strong acidic conditions (mixture at pH 1 stirred at r.t. for 3 h) are not appropriate to obtain complete hydrolysis of the starting conjugate.
As for the FITC-*N,O*-CMCS-DA and FITC-*O*-CMCS DA amide conjugates the measured DS% values of the neurotransmitter were 0.7 ± 0.05% for the former conjugate and 2.2 ± 0.9% for the latter conjugate, respectively. The labelling efficiency referred to FITC (mg FITC/mg FITC-DA-conjugate) for the FITC-*N,O*-CMCS-DA and FITC-*O*-CMCS DA amide conjugates were 13 ± 0.4% and 5 ± 0.6%, respectively.

3.2. Thermal analysis

Thermal analysis on the herein examined conjugates included both studies of TGA and DSC.

3.2.1. Thermo-Gravimetric Analysis (TGA)

TGA thermograms and derivative traces are reported in Figure 5 panel (a) and in the relevant inset, respectively, whereas all the main events are summarized in Table 1.

[Insert Figure 5]

In all the analysed samples for TGA, excluding DA, the water content was in the range of 10-13%, which is typical for polysaccharides. DA degraded under one thermal event centred at 327°C, with a residue at 600°C of 29%. Pure *N,O*-CMCS polymer exhibited two main decompositions peaks at 295°C and 307.4°C, while the residue at 600°C was equal to 51% (Figure 5), as also reported in a previous work [35]. As far as pure *O*-CMCS is concerned, a single sharp decomposition step was recorded, centred at 290°C, corresponding to a weight loss of 30.7%, while the residue at 600°C was equal to 57.2%. Finally, as far as the two conjugates **2** and **3** are concerned, after a first step relevant to the moisture/volatiles loss, a broad decomposition step, centred at 307.7°C and 304.9°C (weight losses of 30.7%, and 56.3% respectively) occurred for *N,O*-CMCS-DA and *O*-CMCS-DA, respectively. The residue at 600°C was equal to 26.8% and 30.5% and for *N,O*-CMCS-DA conjugate **2** and *O*-CMCS-DA conjugate **3**, respectively.

3.2.2. Differential Scanning Calorimetry (DSC)

In Figure 5 panel (b), DSC thermal curves of different polymers/conjugates were shown. For both polymers *N,O*-CMCS and *O*-CMCS, (i.e., Figure 5 panel (b), curves b and d, respectively), a semi-crystalline solid state was deduced from DSC thermograms referring to both polymers with melting point of 153°C and 159°C for *N,O*-CMCS and *O*-CMCS, respectively. An amorphous state was observed for both *N,O*-CMCS-DA conjugate **2** and *O*-CMCS-DA conjugate **3** (Figure 5, panel (b), curves c and e), with the disappearance for both of them of the melting point peak of the corresponding polymer. Furthermore, none of the conjugates showed the melting point peak, as such or shifted, of the pure neurotransmitter DA, confirming the existence of an amorphous solid state for these CMCS conjugates (Figure 5 panel (b), curves c and e).

[Insert Table 1]

3.3. Storage Stability of DA-CMCS-conjugates at T= -20°C

To estimate the storage stability of conjugates herein studied, both powders of *N,O*-CMCS-DA conjugate **2** and *O*-CMCS-DA conjugate **3** were stored in a freezer at T = -20°C up to eight weeks and the DS% over the time are shown in Figure 6 panel (a). We chose to use the method of hydrolysis under strong conditions because a faster determination of DS% takes place, even though we knew that in this way an underestimated value of DS% is deduced. In particular, *O*-CMCS-DA conjugate **3** reduced DS %, starting from one week where DS% collapsed to 40% and after 8 weeks 32% was found (Figure 6 panel (a)). Moreover, in the corresponding HPLC chromatograms, the peak of DA maintained its shape, typical retention time value and no further peaks appeared. In contrast, for *N,O*-CMCS-DA conjugate **2**, HPLC chromatograms showed an enlarged peak with an increase of few min in the retention time value than in the case of intact DA and such behaviour occurred since one week of storage (Figure 6 panel (a)).

3.4. In vitro drug release from conjugates

In Figure 6 panel (b) the in vitro release profiles of *N,O*-CMCS-DA conjugate **2** and *O*-CMCS-DA conjugate **3** in SNF (pH 6.0 without enzymes) are shown. While after 2 days only about 14% of the neurotransmitter was delivered from conjugate **2**, DA was released in a greater extent from the amide **3** in the SNF receiving medium (about 24% after 2 days). These DA release percentages, however, are greater than those observed for *N,O*-CMCS-DA conjugate **2** previously prepared in organic solvent by us (about 5% after 2 days) [23]. Notably, it should be considered that under the conditions

used (pH 6.0 without enzymes) during release test of the *N,O*-CMCS-DA conjugate **2** further degradation products of the neurotransmitter were detected as additional HPLC peaks showed in the corresponding chromatograms since 3 days up to 14 days [36]. For *O*-CMCS-DA conjugate **3**, such additional peaks appeared only when HPLC chromatograms were recorded from 10 to 14 days.

A deeper understanding of DA release data can be obtained using the approach reported by Juriga et al. [37] who pointed out that the release kinetic of polymer-DA conjugates is depending on the water solubility of these macromolecular compounds with different underlying release mechanisms. In particular, they demonstrated that, if the polymer-DA conjugate is poorly soluble in water or buffer solution, the DA cleavage from the conjugates involves two main steps: diffusion from the solid surface to the saturated solution and drug cleavage by chemical reaction (e.g., hydrolytic cleavage of the conjugate linkage). Thus, the DA release mechanism in this heterogeneous environment is the result of diffusion coupled with chemical reaction. In such case, the release of neurotransmitter can be appropriately described, for very short time or very slow cleavage reactions, considering the diffusion of DA from the solid surface as rate determining step. In other words, the dominant release mechanism in this first case is the Fickian diffusion. The diffusion contribution may be expressed by the Higuchi equation [i.e., increase of DA concentration released $C_T = K_H \times t^{1/2}$] where K_H is the Higuchi parameter which can be used for comparative kinetic purposes. This approach has been used by us to evaluate the DA release from the ester *N,O*-CMCS-DA **1** and the amide *N,O*-CMCS-DA **2** prepared in organic solvent medium [21]. On the other hand, whether the polymer-DA conjugate is soluble in water or buffer solution, the DA release takes place in homogeneous environment as the result of consecutive cleavage reactions. In this second case, the dominant release mechanism is the cleavage of the DA-polymer conjugate linkage. In both cases, decomposition of polymer-DA conjugates provides free DA which, unlike the amide CMCS-DA conjugates prepared by us, is unstable and slowly is converted into even polymeric substances such as melanin and its derivatives. Juriga et al suggested that, in the case of polymer-DA conjugate soluble in water or buffer solution, the increase of DA concentration may be described by first order reaction kinetic [37]. We do not know what is, actually, the aqueous solubility of conjugates **2** and **3** and, hence, whether they should be considered poorly- or very-soluble in water. In such circumstances, to interpret the DA release data from the amide conjugates *N,O*-CMCS-DA **2** and *O*-CMCS-DA **3** herein prepared in aqueous environment, we used both the approaches, considering them poorly or soluble enough in water. By plotting the increase of DA concentration released in natural logarithm scale (i.e., ln C_T) as function of time, straight lines are obtained. The slope of these straight lines, determined by linear regression, provides the first order rate constant k_1 from which the corresponding half-life ($t_{1/2}$= ln 2/k_1) can be calculated. The half-life values can be employed to compare the release features of different samples. In Figure 6 panel (c) the dependence of the increase of DA concentration released (ln C_T) as function of time for amide conjugates *N,O*-CMCS-DA **2** and *O*-CMCS-DA **3** is shown and in Table 2 the corresponding half-life is reported. Alternatively, by plotting the measured percentages of DA released in SNF from conjugates **2** and **3** as function of the square root of the time straight lines are obtained. The slope of these straight lines, determined by linear regression, provide the corresponding K_H values, which can be used for comparative kinetic purposes between the two conjugates and also showed in Table 2. Even though these calculations are based on a limited number of data points, a certain trend may be deduced. It is evident from the results reported in Table 2, indeed, that conjugate **3** provides a DA release quicker and in greater extent than conjugate **2** since the k_1 or K_H values of the former are higher than the corresponding of the latter. It in both the circumstances *i.e.,* whether they should be considered poorly- or, alternatively, very-soluble in water.

[Insert Figure 6 and Table 2 revised]

3.5. CMCS-DA conjugates can self-assemble to form nanosized structures

An interesting property of the CMCS-DA conjugates herein studied is that they can self-assembly to form nanosized structures. Thus, by dispersing each conjugate (2 mg) in 200 μL of PBS (pH 7.4) followed by centrifugation and by dropping 25 μL of the resulting supernatant onto grids for TEM and then stained with phosphotungstic acid, TEM analysis clearly demonstrated the nanostructured assembly of conjugates with NP formation. Figure 7(a) and 7(b) show NPs obtained from *N,O*-CMCS-DA conjugate **2** and *O*-CMCS-DA conjugate **3**, respectively. In particular, from conjugate **3** smaller and spherical NPs were obtained, whereas from conjugate **2** larger particles (average TEM size of 187 ± 41 nm) probably due to the fusion of individual particles (see the inset of Figure 7(a)) were detected. On the other hand, besides a negligible amount of microsized structures, by PCS analysis a bimodal distribution was detected in both cases with a little quantity having a particle size < 100 nm and a prevalent one with a particle size > 100 nm (Figure 7(c) and 7(d)).

In Table 3, the hydrodynamic diameters, polydispersity and zeta potential values of conjugates **2** and **3** self-assembled into NPs determined by Zetasizer NanoZS, ZEN 3600 instrument are shown.

[Insert Figure 7]

[Insert Table 3]

*3.6 In vitro antioxidant activity of conjugates **2** and **3***

The antioxidant activity of *N,O*-CMCS-DA conjugate **2** and *O*-CMCS-DA conjugate **3** was studied according to a slightly modified spectrophotometric assay based on the use of 2,2-diphenyl-1-picrylhydrazyl (DPPH) free radical enabling us to assess the ability of studied chemical substances to act as free radical scavengers [32, 38]. In this assay, antioxidants are able to reduce the stable DPPH radical (purple) to non-radical form DPPH-H (yellow). Polymers as such, namely *N,O*-CMCS and *O*-CMCS in our hands showed negligible DPPH radicals scavenging activity since they did not produce any yellow mixture. Instead, the DA conjugates **2** and **3** resulted to be in vitro capable to elicit DPPH radicals scavenging activity evidenced by yellow mixture formation and, hence, possess an antioxidant effect. On the other hand, even the neurotransmitter DA is endowed with radical scavenging ability which is reported to be 86% at 0.1 mM [39]. Thus, it can be stated that the DPPH radical scavenging activity of starting polymer and corresponding conjugates herein studied decreased in the following rank order: DA > *O*-CMCS-DA conjugate **3** > *N,O*-CMCS-DA conjugate **2** >>>> *O*-CMCS ~ *N,O*-CMCS.

3.7. MTT assay

In order to verify the cyto/biocompatibility of conjugates **2** and **3** with the target neuronal cells, SH-SY5Y cells were treated with *N,O*-CMCS or *O*-CMCS based conjugates at the indicated concentrations. *O*-CMCS was used also as a formulation not carrying DA. None of these formulations was cytotoxic, although a nonsignificant decrease in cell viability was observed with 75 μM of *N,O*-CMCS-DA conjugate **2** and *O*-CMCS-DA conjugate **3** (Figure 8).

[Insert Figure 8 revised]

3.8. Uptake studies

For uptake studies fluorescent *O*-CMCS-DA conjugate **3** or *N,O*-CMCS-DA conjugate **2** were prepared by covalent linkage of FITC (see Materials and Methods). Cell uptake was studied in SH-SY5Y cells following incubation for either 2.5 or 24 h. Fig. 9 illustrates the cytofluorimetric gating (panels a and c) and overlay analysis (panels b and d) made on the total population that have been used for cells incubated with *N,O*-CMCS-DA conjugate **2** only as an example. Overlay of gated cells demonstrated that cells took up FITC-conjugated conjugate in a dose- and time-dependent manner (Figure 9b and d). Figure 10 shows these data as histograms. As expected, the uptake was a time-dependent process with more conjugates internalised at 24 h than at 2 h. Specifically, after 2.5 h there was a steep increase of percentages of FITC-positive cells with both conjugates, reaching ~34% and ~39% with *N,O*-CMCS-DA conjugate **2** and *O*-CMCS-DA conjugate **3**, respectively (Figure 10a). At 24 h of incubation, the percentage of FITC-positive cells arose to ~66% with *O*-CMCS-DA conjugate **3** and ~40% with *N,O*-CMCS-DA conjugate **2** at the highest concentration of 75 μM (Fig. 10b). MFI showed also a dose-dependent increase at 2.5 h, in particular with *N,O*-CMCS-DA conjugate **2** (Figure 10c); however, there was not an increment at 24 h, except for *O*-CMCS-DA conjugate **3** at 75 μM (Figure 10d). Overall, these data indicate that the two conjugates are taken up by a high number of cells in a time-dependent fashion although the average number of conjugates remained similar, with the notable exception of *O*-CMCS-DA conjugate **3** at the highest DA concentration.

[Insert Figure 9 revised]

[Insert Figure 10 revised]

4. Discussion

There is great interest for developing new and more effective therapeutic strategies as disease-modifying treatments for PD based on polymeric and lipid nanocarriers able to cross the BBB and to combat this rapidly rising in incidence and harmful disease. In this context, we are involved in a project aimed at developing polymer-DA conjugates which should possess the advantage of limited premature leakage of cargo (i.e., DA) during manipulations and administration due to the presence of a covalent chemical bond between polymeric backbone and neurotransmitter. The polymer we studied was *N,O*-CMCS, a water-soluble derivative of chitosan, endowed with several properties such as biocompatibility, biodegradability, mucoadhesion and non-toxicity [40]. We have previously described the synthesis by using DMF as solvent of the ester and amide conjugates **1** and **2**, respectively, as well as the high internalization of conjugate **2** by OECs (Figure 1) [22, 23]. The main aim of the present work was to develop a synthetic procedure of the amide conjugates **2** and **3** (Figure 1) carried out in aqueous medium in order to minimize the toxicity potential of the resulting conjugates as well as to follow eco-friendly procedures of synthesis in pharmaceutical laboratories. In addition, a further aim was to evaluate the effect of the carboxymethyl substituent position onto glucose nucleus of chitosan in order to gain insights into this structural modification. To this end, we included in this study also the polymer O-CMCS characterized by the presence of the carboxymethyl substituent exclusively on the primary –OH group in position-6 of the parent polymer chitosan.

We succeeded in reaching these goals following a modified reported procedure based on carbodiimide (EDC) chemistry [28]. As for the EDC mediated coupling reaction between *N,O*-CMCS or *O*-CMCS and DA to prepare the amide conjugates **2** and **3**, the coupling reagent EDC can react with the carboxyl groups of the carbohydrate polymers to form an *O*-acylisourea intermediate which, in turn,

provides the required amide conjugate by reaction with the NH_2 group of the neurotransmitter as outlined in Scheme 1.

When the backbones of *N,O*-CMCS and *O*-CMCS were subjected to the amidification with DA in water as solvent, the yield values of the corresponding conjugates were 37% and 24% for *N,O*-CMCS-DA conjugate **2** and *O*-CMCS-DA conjugate **3**, respectively. It should be noted that the amide conjugate *N,O*-CMCS-DA **2** previously prepared employing organic solvent (DMF) was obtained in 70% yield [23]. On the other hand, comparing the yields in water as solvent, it resulted that conjugate **3,** even though prepared in lower yield, it is characterized by a higher DS% (12.65% vs 5.36% determined by potentiometric titration for **3** and **2**, respectively). This result could be rationalized considering that in *O*-CMCS the carboxymethyl group substituent on the primary –OH group in position-6 of the glucose nucleus is available for the reaction with EDC and NH_2 group of the neurotransmitter more than that occurs for the carboxymethyl group substituents of *N*,*O*-CMCS polymer.

The thermal stability of DA, *N,O*-CMCS, *O*-CMCS, and corresponding conjugates with DA was investigated by TGA to give a quantitative measure of their mass changes on increasing the temperature (Figure 5). Both the developed DA-conjugates from TGA thermograms evidenced thermal stability (up to about 190°C) which are acceptable for pharmaceutical applications [41]. In details, from TGA curves (Figure 5a), the main thermal events ascribable to both the chitosan derivatives under investigation could consist of deacetylation and decomposition of the parent chitosan's main chains [42]. Moreover, it can be hypothesized that the cleavage of substituent groups in the carboxymethylated derivatives fell in the same temperature range (270-330°C). In any case, comparing with unmodified chitosan, the thermal stability of chitosan derivatives slightly decreased, as also reported [43]. While in the case of pure substances, a sharp weight loss was observed, starting at higher temperatures, in the case of conjugates a slow weight loss occurred at lower temperatures. Indeed, broader peaks are observed in DTGA profiles of both the DA-conjugates, probably due to the overlapping of the decomposition steps relevant to CMCS (*N,O*- and *O*-) moieties and DA. Overall, TGA has been already employed to determine the thermostability of delivery systems targeting brain diseases, as reported in literature [35, 44] and information arising from such methodology has been combined with data obtained from DSC analysis. DSC thermograms reported in Figure 5b evidenced the amorphous state of both *N,O*-CMCS-DA **2** and *O*-CMCS-DA **3**, without any endothermal/esothermal event occurring in the range of temperatures explored, whereas the thermogram of pure *N,O*-CMCS showed an endothermic peak at 150°C and the thermogram of *O*-CMCS showed an endothermic peak at 153°C.

Some information on the physical stability of *N,O*- and *O*-CMCS-DA conjugates on storage at -20°C can be gained from Figure 6 panel (a). As can be seen, conjugate **2** possess higher stability under storage at T= -20°C than *O*-CMCS-DA conjugate **3**. Moreover, a further different behaviour noted between the two conjugates refers to the shape and retention time of the peak corresponding to the neurotransmitter in HPLC chromatograms. This peak maintained its shape, typical retention time value and no further peaks appeared in the case of *O*-CMCS-DA conjugate **3** suggesting that no DA autoxidation occurred during storage frame time. Instead, for *N,O*-CMCS-DA **2**, HPLC chromatograms showed an enlarged peak with a little increase in retention time of DA signal together with the apparent increase of DS % occurring since four up to eight weeks. It may be probably due to DA autoxidation induced by air oxygen which was demonstrated to be a very slow process unlike the aerobic and anaerobic DA autoxidation in solution [45].

Consistent enough with the physical stability on storage data were also those from in vitro DA release from conjugates (Figure 6 panel (b)). The general trend showed in both release profiles, indeed, was of a prompt DA release (burst effect) within the first two days followed by a sustained release period. However, the bust effect noted for conjugate **3** was more intense than that showed by conjugate **2**, just as deduced by physical stability on storage data and, moreover, unlike that occurs for *O*-CMCS-DA, it was noted the complete disappearance of the neurotransmitter in the release profile of *N,O*-CMCS-DA **2**. This last outcome may support the above made hypothesis to explain the apparent increase of DS % of conjugate **2** occurring since four up to eight weeks of storage.

Comparing the release kinetic features of the amide conjugates **2** and **3** here prepared in homogeneous environment with those of poorly-soluble *N,O*-CMCS-DA amide conjugate previously prepared in organic solvent by us [23], it can be concluded that all these conjugates may be suitable for sustained neurotransmitter release applications. However, taking into account also the mentioned greater (Figure 6) and quicker (Table 2) DA released from the amide **3**, this last conjugate seems interesting delivery system for further developments. In particular, it should be of interest to evaluate the potential of conjugate **3** both to restore acceptable levels of the neurotransmitter in the brain of parkinsonian patients and to avoid the adverse effects observed after long-term administration of L-DOPA [6].

Several recent literature suggestions pointed out the self-aggregation of phenolic compounds conjugated with polysaccharides including *N,O*- or *O*-CMCS [33, 46, 47]. It prompted us to verify whether also the conjugates **2** and **3** prepared in aqueous medium could similarly self-assembly into nanoscale structures as NPs. We succeeded in this task as demonstrated by TEM analysis after dispersion of each conjugate in PBS (pH 7.4) and following the procedure reported in Section 2.7. However, a different behaviour between the two conjugates was noted. In detail, while from conjugate **3** smaller and spherical NPs were observed by PCS (average size of 292 ± 2 nm), from conjugate **2** larger particles (average size of 459 ±7 nm) were detected. Moreover, by comparing the average diameters observed by TEM it was noted that they were smaller than the corresponding deduced by PCS (i.e., 187 ±7 nm by TEM compared with 459 ±7 nm by PCS). This discrepancy is a well-documented outcome in the literature and it has been ascribed to the procedure involved in preparation of samples for which, due to solvent effect, the diameter measured by PCS (hydrodynamic diameter) results larger than that determined by TEM. Furthermore, by deeply examining TEM pictures, we have deduced that nanosized structures were formed by both conjugates **2** and **3**, namely they could spontaneously self-assembly once dispersed in aqueous medium. In our case, as for the self-assembly process of *N,O*- or *O*-CMCS-DA conjugates **2** and **3**, it can be rationalized taking into account that both these conjugates may be considered amphiphilic polymers just as occurs for other phenolic compounds conjugated with polysaccharides [33, 46, 47]. In both conjugates, indeed, hydrophobic domains can be envisaged due to specific π–π- as well as hydrogen bonding-interactions between the catechol moieties of these conjugates (Figure S1). These hydrophobic domains may form the internal core of polymeric micelles with an external shell constituted by CMCS hydrophilic moieties [47]. It should be noted that classical polymeric micelles are prepared starting from amphiphilic polymers which self-assembly in aqueous environment leading to a core-shell structure. In this arrangement, the hydrophobic part constitutes a place where hydrophobic drugs are encapsulated, while the hydrophilic outer shell enables that the micelles are unrecognized by the reticuloendothelial system and hence allows to protect the hydrophobic part from the biological invasion. In this context, recently several amphiphilic CS derivatives have been prepared and self-assembled in aqueous medium to give polysaccharide based polymeric micelle delivery systems, exploiting the hydroxyl- and amine-

groups occurring in the molecules of CS and its derivatives [48-50]. Comparing the hydrophobic domains of the classical polymeric micelles with those proposed for the self-assembly process of *N,O*- or *O*-CMCS-DA conjugates **2** and **3**, it is evident a certain difference between the two types considered and it may lead to important practical consequences. Thus, for instance, it may be possible that the micelles arising from polysaccharide based conjugates **2** and **3** suffer from major thermodynamic and kinetic instability in comparison with that observed for classical polymeric micelles and it remains to be checked.

Hence, the self-assembly process of conjugates **2** and **3** may involve polymeric micelle formation in DA-grafted CMCSs. The observed better quality of NPs from conjugate **3** in terms of size may be due to the uniform introduction of the CH_2-CO-NH-$(CH_2)_2$-Aryl-substituent on the C-6 hydroxyl of the glucose nucleus which allows the formation of regular and more effective π–π interactions between the mentioned aromatic regions than those occurring in conjugate **2** (Figure S1). In this last conjugate, indeed, the mentioned Aryl-substituents occur either at C-6 hydroxyl group or at the NH_2 moiety, making the mentioned interactions even at long-range and, hence, less regular and effective hydrophobic domains. Hence, it can be stated that the position of the carboxymethyl substituent on the CMCS backbone is quite important in determining the features of the resulting nanocarrier. A peculiar property of micelles is that they are stable at concentration higher than the Critical Micellar Concentration (CMC) while they disassemble by dilution at concentration below the CMC. In our case, however, even the disassembled conjugates **2** and **3** may be nano-structured leading to NP formation. It is already known, indeed, that grafted chitosans bearing aryl-groups can form polymeric NPs [51]. Hence, besides polymeric micelles, conjugates **2** and **3** may form polymeric NPs as nanosized structures. Considering that often polymeric micelles are smaller than 100 nm in size, at present it cannot be excluded that particles in little amount with a particle size < 100 nm detected in size distribution plots (Figure 7 (c) and 7 (d)) are constituted by polymeric micelles, while those in predominant amount with a particle size > 100 nm are represented by NPs. The negative zeta potentials of these nanocarriers (Table 3) are consistent with the absence of any absorption at 1730 cm^{-1} in FT-IR spectra of both conjugates suggesting the presence of free carboxymethyl substituents in –COONa form. Moreover, the observed PDI values suggest a satisfactory polydispersion. However, further characterization and evaluation of such nanocarriers as delivery systems of the neurotransmitter is in progress and the results of these studies will be reported in due course.

As mentioned in introduction section, mitochondrial disruptions and oxidative stress have been suggested to play an important role in the loss of DAergic neurons occurring in parkinsonian patients and such processes are mediated by ROS (reactive oxygen species) and free radicals like H_2O_2 and OH^- [7]. It prompted us to evaluate the significant antioxidant potential of conjugates **2** and **3** measured by DPPH, unlike the starting polymers *N*,*O*-CMCS and *O*-CMCS. This is also supported by a literature report showing that the DPPH scavenging activity of *O*-CMCS is only 2.98% at 2.5 mg/mL [33]. Following the literature hints reported for phenolic compounds conjugated with polysaccharides, *N*,*O*- or *O*-CMCS-DA could react with DPPH radical by donating hydrogen atom to form stable DPPH-H and *N*,*O*- or *O*-CMCS-DA radicals. Next, *N*,*O*- or *O*-CMCS-DA radical could be further withdrawn hydrogen atom to form stable *N*,*O*- or *O*-CMCS-DA quinone compounds as shown in Figure S2 [52]. Hence the DPPH radical scavenging activity of *N*,*O*- or *O*-CMCS-DA conjugates **2** and **3** may be mainly due to the catechol moieties occurring in these macromolecular substances and, therefore, possess an antioxidant effect with the latter conjugate at a higher extent than the former.

For uptake studies, fluorescent conjugates were obtained and for both FITC-*O*-CMCS-DA conjugate **3** and FITC- *N*,*O*-CMCS-DA conjugate **2** the DS in the dye FITC was found to be equal to 5 and 13 μg FITC/mg of fluorescent conjugate, namely significantly lower than the previously studied FITC-*N*,*O*-CMCS-DA **1** exhibiting 100 μg FITC/mg of FITC-*N*,*O*-CMCS-DA [23]. However, while in our previous work, FITC-*N*,*O*-CMCS-DA **1** was taken up by ~70% of OECs already at 2 h, neuroblastoma cells were less permissive to uptake at 2.5 h, reaching a good level of internalisation only at 24 h. Whether these results are due to less FITC molecules associated with conjugates or to a different cell line, it is difficult to discern. The lower MFI (~8000 verso ~2000 arbitrary units) may indicate that the lower FITC content may have given these results. Nevertheless, the therapeutic dose of DA (i.e. 75 μM, corresponding to 11.5 μg/mL, with Tang et al. [53] showing that DA-carrying nanoparticles was effective in alleviating motor symptoms in a rat model of PD at the dose of ~ 7.4 μg/mL) was taken up by a good number of cells, (i.e. up to 66% with *O*-CMCS-DA **3**), indicating that further experiments would clarify if these percentages allows for an efficacious arrival of DA into the relevant neuronal cells of the subcortical nuclei.

Overall, it seems that *N*,*O*- or *O*-CMCS-DA conjugates **2** and **3** may constitute an example of the so called "multifunctional nanomedicines" that combine multiple biological functions into a single nanosystem and whose usefulness in brain diseases has been recently evidenced [54]. Thus, conjugates **2** and **3** can provide neurotransmitter DA useful for "dopamine replacement strategy" and an antioxidant effect which limits the ROS production.

As chitosan derivatives, conjugates **2** and **3** as such or in nanostructured form incorporated into a number of nanoformulations such as hydrogel should possess, in our opinion, a good potential for nose-to-brain delivery due to their mucoadhesive properties. This last feature combined with the ability of these chitosan derivatives to act as penetration enhancers by temporarily opening intercellular tight junctions allow to obtain a longer residence time of the formulation in contact with nasal mucosa increasing so the transport through this last barrier [12]. About the behaviour of the conjugates **2** and **3** in vivo, we suppose that the transport of the conjugate directly to the brain from the nasal cavity may occur using the olfactory and/or trigeminal nerves as above mentioned exploiting two pathways namely the intracellular and the extracellular mechanism as discussed in the papers of Crowe and colleagues [12, 55] to whom the reader is referred to. Briefly, the intracellular pathway involves endocytosis of conjugate by olfactory nerve endings, while according to the extracellular mechanism, the conjugate is transported directly into the cerebral spinal fluid by first passing through the paracellular cleft, lamina propria, then through the perineural space to the subarachnoid space of the brain. It is possible that during all these transport phases, the amide linkage between the neurotransmitter and polymer backbone can be broken due to hydrolytic reactions and free DA is released in sustained manner producing the corresponding pharmacological effects. Alternatively, it cannot ruled out that the intact conjugate, even in nanostructured form, may access brain and next undergoes the breakage of the amide bond. Finally, it is also possible the conjugate is taken up by target neuronal cells in which DA release could happen. To assess these aspects, more studies must be done.

5 Conclusions

We succeeded to conjugate the primary amino group of neurotransmitter DA with the –COOH function of *N*,*O*-CMS or *O*-CMCS leading to amide conjugates **2** and **3** in aqueous environment following eco-friendly procedures of synthesis trying to minimize the toxicity potential of the

conjugates obtained. From a structural point of view, conjugates **2** and **3** were characterized by spectroscopic means (i.e., FT-IR and ^{1}H-NMR) and percentage of substitution degree. Thermal analysis showed that **2** and **3** are endowed with thermal stability and an amorphous state was observed for both, unlike the starting polymers *N*,*O*-CMS and *O*-CMCS. Interestingly, it was found that CMCS-DA conjugates may self-assembly to form polymeric micelles and/or NPs, these last supported by TEM observations. The better quality in size of NPs from conjugate **3** may be due to more efficient π–π- and hydrogen bonding- interactions between aromatic regions than those occurring in conjugate **2.** Moreover, DA release from conjugate **3** was quicker and in greater extent in the SNF receiving medium as well as its uptake increased of ~66% with *O*-CMCS-DA conjugate **3** at the highest concentration of 75 μM compared with~40% for conjugate **2**. Hence, the obtained results indicate that the position of the carboxymethyl group on the CMCS backbone plays an important role in determining the features of the resulting nanocarrier confirming so our starting hypothesis. Further characterization and evaluation of such NPs as DA delivery systems are in progress and the results will be reported in due course. Besides this, a further interesting conclusion is that conjugates **2** and **3** show antioxidant activity, with the latter conjugate at a higher extent than the former, as demonstrated by DPPH radical scavenging assay. Thus, such new examples of chitosan-based nanocarriers to be used by intranasal administration possess promising properties for brain delivery as "multifunctional nanomedicines" [54, 56].

5. Author contribution section

Sante Di Gioia: Writing—review and editing; supervision, **Giuseppe Fracchiolla**: Investigation and methodology **Stefania Cometa:** Investigation; **Filippo Perna**: Investigation and methodology; **Andrea Francesca Quivelli**: Investigation and software; **Giuseppe Trapani**: Supervision; **Valeria Daniello:** Investigation; **Concetta Nobile:** Investigation; **Md Niamat Hossain**: Investigation; **Adriana Trapani**: Conceptualization, investigation; writing—original draft preparation, writing—review and editing; funding acquisition and Supervision; **Massimo Conese**: Conceptualization, methodology, supervision; writing—original draft preparation, writing—review and editing.

Declaration of competing interests

The authors declare that they have no known competing financial interests or personal relationships that could have appeared to influence the work reported in this paper.

Acknowledgement

A.T. would like to acknowledge Dr. Sergio Cellamare (University of Bari, Aldo-Moro, Italy) and Dr. Alessandra Quarta (University of Salento, Italy) for their technical help. S.D.G and M.C. would like to thank Dr. Nicoletta Mangialetto (Hematology Unit, Policlinico Riuniti of Foggia, Foggia, Italy) for her help with cytofluorimetric analysis.

References

[1] A.D. Gitler, P. Dhillon, J. Shorter, Neurodegenerative disease: models, mechanisms, and a new hope, Dis Model Mech 10(5) (2017) 499-502.

[2] Y. Esmaeili, Z. Yarjanli, F. Pakniya, E. Bidram, M.J. Los, M. Eshraghi, D.J. Klionsky, S. Ghavami, A. Zarrabi, Targeting autophagy, oxidative stress, and ER stress for neurodegenerative disease treatment, J Control Release 345 (2022) 147-175.
[3] C. Spuch, O. Saida, C. Navarro, Advances in the treatment of neurodegenerative disorders employing nanoparticles, Recent Pat Drug Deliv Formul 6(1) (2012) 2-18.
[4] M. Pandya, C.S. Kubu, M.L. Giroux, Parkinson disease: not just a movement disorder, Cleve Clin J Med 75(12) (2008) 856-64.
[5] E. Wollmer, S. Klein, A review of patient-specific gastrointestinal parameters as a platform for developing in vitro models for predicting the in vivo performance of oral dosage forms in patients with Parkinson's disease, Int J Pharm 533(1) (2017) 298-314.
[6] K.R. Chaudhuri, A. Rizos, K.D. Sethi, Motor and nonmotor complications in Parkinson's disease: an argument for continuous drug delivery?, J Neural Transm (Vienna) 120(9) (2013) 1305-20.
[7] C. Rodriguez-Nogales, E. Garbayo, M.M. Carmona-Abellan, M.R. Luquin, M.J. Blanco-Prieto, Brain aging and Parkinson's disease: New therapeutic approaches using drug delivery systems, Maturitas 84 (2016) 25-31.
[8] V. Bourganis, O. Kammona, A. Alexopoulos, C. Kiparissides, Recent advances in carrier mediated nose-to-brain delivery of pharmaceutics, Eur J Pharm Biopharm 128 (2018) 337-362.
[9] M. Conese, R. Cassano, E. Gavini, G. Trapani, G. Rassu, E. Sanna, S. Di Gioia, A. Trapani, Harnessing Stem Cells and Neurotrophic Factors with Novel Technologies in the Treatment of Parkinson's Disease, Curr Stem Cell Res Ther 14(7) (2019) 549-569.
[10] C. Riccardi, F. Napolitano, D. Montesarchio, S. Sampaolo, M.A.B. Melone, Nanoparticle-Guided Brain Drug Delivery: Expanding the Therapeutic Approach to Neurodegenerative Diseases, Pharmaceutics 13(11) (2021).
[11] D. Lee, T. Minko, Nanotherapeutics for Nose-to-Brain Drug Delivery: An Approach to Bypass the Blood Brain Barrier, Pharmaceutics 13(12) (2021).
[12] T.P. Crowe, W.H. Hsu, Evaluation of Recent Intranasal Drug Delivery Systems to the Central Nervous System, Pharmaceutics 14(3) (2022).
[13] J.A. Falcone, T.S. Salameh, X. Yi, B.J. Cordy, W.G. Mortell, A.V. Kabanov, W.A. Banks, Intranasal administration as a route for drug delivery to the brain: evidence for a unique pathway for albumin, J Pharmacol Exp Ther 351(1) (2014) 54-60.
[14] Z. Wang, G. Xiong, W.C. Tsang, A.G. Schatzlein, I.F. Uchegbu, Nose-to-Brain Delivery, J Pharmacol Exp Ther 370(3) (2019) 593-601.
[15] G. Trapani, M. Franco, A. Trapani, A. Lopedota, A. Latrofa, E. Gallucci, S. Micelli, G. Liso, Frog intestinal sac: a new in vitro method for the assessment of intestinal permeability, J Pharm Sci 93(12) (2004) 2909-19.
[16] A. Ancona, M. Sportelli, A. Trapani, R.A. Picca, C. Palazzo, E. Bonerba, F. Mezzapesa, G. Tantillo, G. Trapani, N. Cioffi, Synthesis and Characterization of Hybrid Copper-Chitosan Nano-antimicrobials by Femtosecond Laser-Ablation in Liquids, Material Letters 136 (2014) 397-400.
[17] A. Singh, H.L. Kutscher, J.C. Bulmahn, S.D. Mahajan, G.S. He, P.N. Prasad, Laser ablation for pharmaceutical nanoformulations: Multi-drug nanoencapsulation and theranostics for HIV, Nanomedicine 25 (2020) 102172.
[18] T.T. Nguyen, H.J. Maeng, Pharmacokinetics and Pharmacodynamics of Intranasal Solid Lipid Nanoparticles and Nanostructured Lipid Carriers for Nose-to-Brain Delivery, Pharmaceutics 14(3) (2022).
[19] T. Kurano, T. Kanazawa, A. Ooba, Y. Masuyama, N. Maruhana, M. Yamada, S. Iioka, H. Ibaraki, Y. Kosuge, H. Kondo, T. Suzuki, Nose-to-brain/spinal cord delivery kinetics of liposomes with different surface properties, J Control Release 344 (2022) 225-234.
[20] R. Maher, A. Moreno-Borrallo, D. Jindal, B.T. Mai, E. Ruiz-Hernandez, A. Harkin, Intranasal Polymeric and Lipid-Based Nanocarriers for CNS Drug Delivery, Pharmaceutics 15(3) (2023).
[21] V. De Leo, S. Ruscigno, A. Trapani, S. Di Gioia, F. Milano, D. Mandracchia, R. Comparelli, S. Castellani, A. Agostiano, G. Trapani, L. Catucci, M. Conese, Preparation of drug-loaded small unilamellar liposomes and evaluation of their potential for the treatment of chronic respiratory diseases, Int J Pharm 545(1-2) (2018) 378-388.

[22] R. Cassano, A. Trapani, M.L. Di Gioia, D. Mandracchia, R. Pellitteri, G. Tripodo, S. Trombino, S. Di Gioia, M. Conese, Synthesis and characterization of novel chitosan-dopamine or chitosan-tyrosine conjugates for potential nose-to-brain delivery, Int J Pharm 589 (2020) 119829.
[23] S. Di Gioia, A. Trapani, R. Cassano, M.L. Di Gioia, S. Trombino, S. Cellamare, I. Bolognino, M.N. Hossain, E. Sanna, G. Trapani, M. Conese, Nose-to-brain delivery: A comparative study between carboxymethyl chitosan based conjugates of dopamine, Int J Pharm 599 (2021) 120453.
[24] N. Denora, V. Laquintana, A. Trapani, A. Lopedota, A. Latrofa, J.M. Gallo, G. Trapani, Translocator protein (TSPO) ligand-Ara-C (cytarabine) conjugates as a strategy to deliver antineoplastic drugs and to enhance drug clinical potential, Mol Pharm 7(6) (2010) 2255-69.
[25] X.-G. Chen, H.-J. Park, Chemical characteristics of O-carboxymethyl chitosans related to the preparation conditions, Carbohydrate Polymers 53(4) (2003) 355-359.
[26] V.K. Mourya, N. Inamdara, N. Ashutosh Tiwari, Carboxymethyl Chitosan And Its Applications, Advanced Materials Letters 1(1) (2010) 11-33.
[27] D. Mandracchia, A. Trapani, G. Tripodo, M.G. Perrone, G. Giammona, G. Trapani, N.A. Colabufo, In vitro evaluation of glycol chitosan based formulations as oral delivery systems for efflux pump inhibition, Carbohydr Polym 166 (2017) 73-82.
[28] C. Fan, J. Fu, W. Zhu, D.A. Wang, A mussel-inspired double-crosslinked tissue adhesive intended for internal medical use, Acta Biomater 33 (2016) 51-63.
[29] A. Trapani, F. Corbo, G. Agrimi, N. Ditaranto, N. Cioffi, F. Perna, A. Quivelli, E. Stefano, P. Lunetti, A. Muscella, S. Marsigliante, A. Cricenti, M. Luce, C. Mormile, A. Cataldo, S. Bellucci, Oxidized Alginate Dopamine Conjugate: In Vitro Characterization for Nose-to-Brain Delivery Application, Materials (Basel) 14(13) (2021).
[30] A. Trapani, F. Corbo, E. Stefano, L. Capobianco, A. Muscella, S. Marsigliante, A. Cricenti, M. Luce, D. Becerril, S. Bellucci, Oxidized Alginate Dopamine Conjugate: A Study to Gain Insight into Cell/Particle Interactions, J Funct Biomater 13(4) (2022).
[31] A. Trapani, D. Mandracchia, G. Tripodo, S. Cometa, S. Cellamare, E. De Giglio, P. Klepetsanis, S.G. Antimisiaris, Protection of dopamine towards autoxidation reaction by encapsulation into non-coated- or chitosan- or thiolated chitosan-coated-liposomes, Colloids Surf B Biointerfaces 170 (2018) 11-19.
[32] M. Fir, L. Milivojevic, M. Prosek, A. Smidovnik, Properties Studies of Coenzyme Q10-Cyclodextrins complexes. , Acta Chim Slov. 56 (2009) 885.891.
[33] R. Bai, H. Yong, X. Zhang, J. Liu, J. Liu, Structural characterization and protective effect of gallic acid grafted O-carboxymethyl chitosan against hydrogen peroxide-induced oxidative damage, Int J Biol Macromol 143 (2020) 49-59.
[34] J. Du, Y.L. Hsieh, Nanofibrous membranes from aqueous electrospinning of carboxymethyl chitosan, Nanotechnology 19(12) (2008) 125707.
[35] A. Trapani, S. Cometa, E. De Giglio, F. Corbo, R. Cassano, M.L. Di Gioia, S. Trombino, M.N. Hossain, S. Di Gioia, G. Trapani, M. Conese, Novel Nanoparticles Based on N,O-Carboxymethyl Chitosan-Dopamine Amide Conjugate for Nose-to-Brain Delivery, Pharmaceutics 14(1) (2022).
[36] N. Umek, B. Gersak, N. Vintar, M. Sostaric, J. Mavri, Dopamine Autoxidation Is Controlled by Acidic pH, Front Mol Neurosci 11 (2018) 467.
[37] D. Juriga, I. Laszlo, K. Ludanyi, I. Klebovich, C.H. Chae, M. Zrinyi, Kinetics of dopamine release from poly(aspartamide)-based prodrugs, Acta Biomater 76 (2018) 225-238.
[38] A. Trapani, L. Guerra, F. Corbo, S. Castellani, E. Sanna, L. Capobianco, A.G. Monteduro, D.E. Manno, D. Mandracchia, S. Di Gioia, M. Conese, Cyto/Biocompatibility of Dopamine Combined with the Antioxidant Grape Seed-Derived Polyphenol Compounds in Solid Lipid Nanoparticles, Molecules 26(4) (2021) 916.
[39] D. Hadjipavlou-Litina, G.E. Magoulas, S.E. Bariamis, D. Drainas, K. Avgoustakis, D. Papaioannou, Does conjugation of antioxidants improve their antioxidative/anti-inflammatory potential?, Bioorg Med Chem 18(23) (2010) 8204-17.
[40] Z. Shariatinia, Carboxymethyl chitosan: Properties and biomedical applications, Int J Biol Macromol 120(Pt B) (2018) 1406-1419.
[41] M.I. Yoshida, E.C. Gomes, C.D. Soares, A.F. Cunha, M.A. Oliveira, Thermal analysis applied to verapamil hydrochloride characterization in pharmaceutical formulations, Molecules 15(4) (2010) 2439-52.

[42] S.F. Wang, L. Shen, Y.J. Tong, L. Chen, I.Y. Phang, P.Q. Lim, T.X. Liu, Biopolymer chitosan/montmorillonite nanocomposites: Preparation and characterization, Polymer Degradation and Stability 90(1) (2005) 123-131.
[43] M. Ziegler-Borowska, D. Chełminiak, H. Kaczmarek, A. Kaczmarek-Kędziera, Effect of side substituents on thermal stability of the modified chitosan and its nanocomposites with magnetite, Journal of Thermal Analysis and Calorimetry 124(3) (2016) 1267-1280.
[44] S. Cometa, M.A. Bonifacio, G. Trapani, S. Di Gioia, L. Dazzi, E. De Giglio, A. Trapani, In vitro investigations on dopamine loaded Solid Lipid Nanoparticles, J Pharm Biomed Anal 185 (2020) 113257.
[45] M. Salomaki, T. Ouvinen, L. Marttila, H. Kivela, J. Leiro, E. Makila, J. Lukkari, Polydopamine Nanoparticles Prepared Using Redox-Active Transition Metals, J Phys Chem B 123(11) (2019) 2513-2524.
[46] J. Liu, J.F. Lu, J. Kan, Y.Q. Tang, C.H. Jin, Preparation, characterization and antioxidant activity of phenolic acids grafted carboxymethyl chitosan, Int J Biol Macromol 62 (2013) 85-93.
[47] F.Q. Hu, L.N. Liu, Y.Z. Du, H. Yuan, Synthesis and antitumor activity of doxorubicin conjugated stearic acid-g-chitosan oligosaccharide polymeric micelles, Biomaterials 30(36) (2009) 6955-63.
[48] Y. Xu, N. Liang, J. Liu, X. Gong, P. Yan, S. Sun, Design and fabrication of chitosan-based AIE active micelles for bioimaging and intelligent delivery of paclitaxel, Carbohydr Polym 290 (2022) 119509.
[49] Y. Han, J. Pan, N. Liang, X. Gong, S. Sun, A pH-Sensitive Polymeric Micellar System Based on Chitosan Derivative for Efficient Delivery of Paclitaxel, Int J Mol Sci 22(13) (2021).
[50] H. Shi, N. Liang, J. Liu, S. Li, X. Gong, P. Yan, S. Sun, AIE-active polymeric micelles based on modified chitosan for bioimaging-guided targeted delivery and controlled release of paclitaxel, Carbohydr Polym 269 (2021) 118327.
[51] R.R. Gadkari, S. Suwalka, M.R. Yogi, W. Ali, A. Das, R. Alagirusamy, Green synthesis of chitosan-cinnamaldehyde cross-linked nanoparticles: Characterization and antibacterial activity, Carbohydr Polym 226 (2019) 115298.
[52] J. Liu, C.G. Meng, Y.H. Yan, Y.N. Shan, J. Kan, C.H. Jin, Protocatechuic acid grafted onto chitosan: Characterization and antioxidant activity, Int J Biol Macromol 89 (2016) 518-26.
[53] S. Tang, A. Wang, X. Yan, L. Chu, X. Yang, Y. Song, K. Sun, X. Yu, R. Liu, Z. Wu, P. Xue, Brain-targeted intranasal delivery of dopamine with borneol and lactoferrin co-modified nanoparticles for treating Parkinson's disease, Drug Deliv 26(1) (2019) 700-707.
[54] P. Faria, C. Pacheco, R.P. Moura, B. Sarmento, C. Martins, Multifunctional nanomedicine strategies to manage brain diseases, Drug Deliv Transl Res 13(5) (2023) 1322-1342.
[55] T.P. Crowe, M.H.W. Greenlee, A.G. Kanthasamy, W.H. Hsu, Mechanism of intranasal drug delivery directly to the brain, Life Sci 195 (2018) 44-52.
[56] C. Pacheco, F. Sousa, B. Sarmento, Chitosan-based nanomedicine for brain delivery: Where are we heading?, Reactive and Functional Polymers 146 (2020) 104430.

Captions to Figures and Tables

Figure 1. Chemical structures of ester and amide *N,O*-CMCS-DA conjugates **1** and **2** and amide *O*-CMCS-DA **3**.

Scheme 1. Synthetic pathway followed to obtain *N,O*-CMCS-DA amide conjugate **2** and *O*-CMCS-DA amide conjugate **3**

Figure 2. (a) FT-IR spectrum of pure DA (blue); *N,O*-CMCS (green); *N,O*-CMCS-DA amide conjugate **2** (pink). (b) FT-IR spectrum of pure DA (blue); *O*-CMCS (green); *O*-CMCS-DA amide conjugate **3** (pink).

Figure 3. (a) ^{1}H NMR spectrum of *O*-CMCS in D_2O with 1% of HCl with identification of the main signals; (b) ^{1}H NMR spectrum of *O*-CMCS-DA conjugate **3** in D_2O with identification of the main signals.

Figure 4. (a) ^{1}H NMR spectrum of *N, O*-CMCS in D_2O with 1% of HCl with identification of the main signals; b) ^{1}H NMR spectrum of *N,O*-CMCS-DA conjugate **2** in D_2O with identification of the main signals.

Figure 5. Panel (a): TGA traces of DA black line), *N,O*- CMCS (red line), *O*-CMCS (blue line), and as well as the relevant conjugates with DA, i.e., *O*-CMCS (green line) and *O*-CMCS-DA (violet line) (in the inset, the relevant derivative traces are shown). Panel b): DSC thermograms of a) pure DA; b) *N,O*-CMCS; c) *N,O*-CMCS-DA conjugate **2**; d) *O*-CMCS; e) *O*-CMCS-DA conjugate **3**. Colour codes in panel b) are the same of panel a).

Table 1. Water/volatiles content, main temperature of decomposition (Td) with the relevant weight losses percentages and residues at 600°C of DA, *N,O*-CMCS, *O*-CMCS and as well as the relevant conjugates with DA.

Figure 6. Storage stability of DA conjugates. Panel (a): Variations of DS (%) over the time of conjugates **2** (red bars) and **3** (blue bars) after storage in a freezer at -20 °C up to eight weeks. Panel (b): Cumulative DA released in SNF from amide conjugate **2** (red line) and **3** (blue line). Panel (c): Plot of DA concentration released in natural logarithm scale (i.e., ln C_T) as function of time for amide conjugates *N,O*-CMCS-DA **2** (red line) and *O*-CMCS-DA **3** (blue line). Panel (d): Plot of DA concentration released as function of the square root of the time.

Table 2. First order rate constant k_1 and half-life $t_{1/2}$ of DA release from amide conjugates **2** and **3** considered as soluble enough in water. Experimental Higuchi parameters (K_H) in the alternative case of release from amide conjugates **2** and **3** considered as poorly soluble in water.

Figure 7. Particle size analysis of conjugates. Panel (a): from *N,O*-CMCS-DA conjugate **2** few and large particles (average TEM size of 187 ± 41 nm) were obtained probably due to the fusion of individual particles (see the yellow dotted spheres in the inset, whose size is around 24 nm); panel (b): from *O*-CMCS-DA conjugate **3** small and spherical NPs with an average TEM size of 5.8 ± 1.0 nm were detected; panel (c) size distribution plot of *N,O*-CMCS-DA conjugate **2** measured by PCS; panel (d) size distribution plot of *O*-CMCS-DA conjugate **3** measured by PCS.

Table 3. Properties of NPs obtained by conjugates **2** and **3**. Results are mean of 6 determinations ±SD.

Figure 8. Cytotoxicity of CMCS based formulations. SH-SY5Y were challenged with *N,O*-CMCS-DA conjugate **2** or *O*-CMCS-DA conjugate **3** at the indicated DA concentrations of 4.7, 18.75, and 75 μM, while control *O*-CMCS was used at the same final polymer concentrations of *O*-CMCS-DA conjugate **3**. Cells were then assayed for vitality by the MTT assay. Controls are untreated cells (100% of vitality), whereas 1% Triton X-100 (Triton) was used as positive control. **** $p < 0.0001$ Triton vs. untreated. Data are the results of two-three experiments each carried out in eight wells.

Figure 9. Gating strategy and fluorescence intensity overlay of SH-SY5Y cells incubated with FITC-*N,O*-CMCS-DA conjugate **2**. The whole population of controls (cells not incubated with conjugates) was gated (P1) at 2.5 h (a) and 24 h (c) and this gate was used to evaluate for fluorescence intensity overlay at these time points after incubation with FITC-*N,O*-CMCS-DA conjugate **2** at different DA concentrations (b and d). A marker (P2) was positioned on the third decade (10^3) to separate control cells (red curve) from cells incubated with 4.7 μM (blue curve), 18.75 (yellow curve), and 75 μM (green curve).

Figure 10. Uptake of *O*-CMCS-DA conjugate **3** and *N,O*-CMCS-DA conjugate **2**. SH-SY5Y cells were incubated with different doses of *O*-CMCS-DA conjugate **3** and *N,O*-CMCS-DA conjugate **2** according to DA concentration (shown in μM) for 2.5 h (a,c) or 24 h (b,d) and then evaluated for percentage of positive fluorescent cells (a,b) and relative mean fluorescence (MFI) (c,d) by flow cytometry. Data are expressed as the mean ± SD of three experiments, each conducted in duplicate. *$p<0.05$, **$p<0.01$ and ***$p<0.001$ indicate statistical differences *vs.* untreated cells.

Figure S1. Schematic representation of π–π interactions for *O*-CMCS-DA **3** (panel (a)) and *N*,*O*-CMCS-DA **2** conjugates (panel (b)).

Figure S2. The antioxidant mechanism for *O*-CMCS-DA **3** scavenging DPPH radical. A similar pathway can be proposed for *N,O*-CMCS-DA conjugate **2**.

Figure

Click here to access/download;Figure;Figure 1 JPEG.jpg

Figure

Click here to access/download;Figure;Scheme 1.JPG

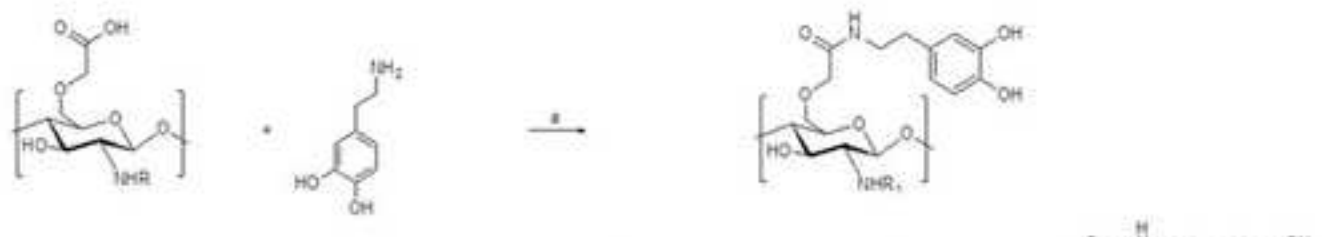

R = CH_2COOH (*N,O*-CMCS)
R = H (*O*-CMCS)

(*N,O*-CMCS-DA) R_1 = H, $COCH_3$

2

(*O*-CMCS-DA) R_1 = H, $COCH_3$

3

a) EDC, 48 h,

EDC

Figure

Click here to access/download;Figure;Figure 2 revised.jpg

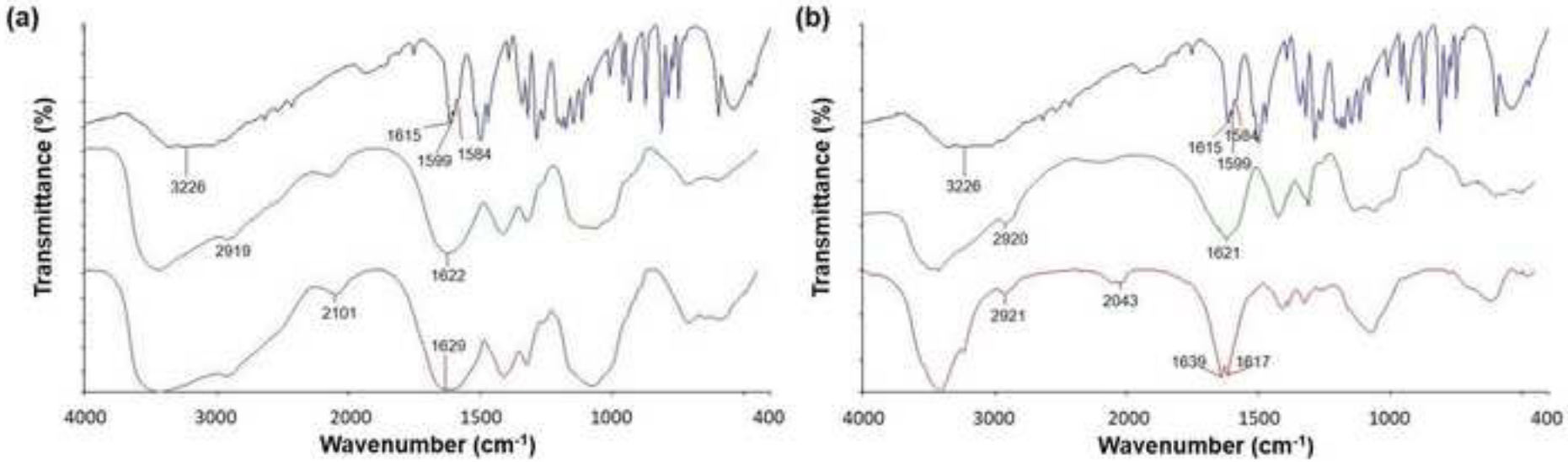

Figure

Click here to access/download;Figure;Figure 3a.jpg

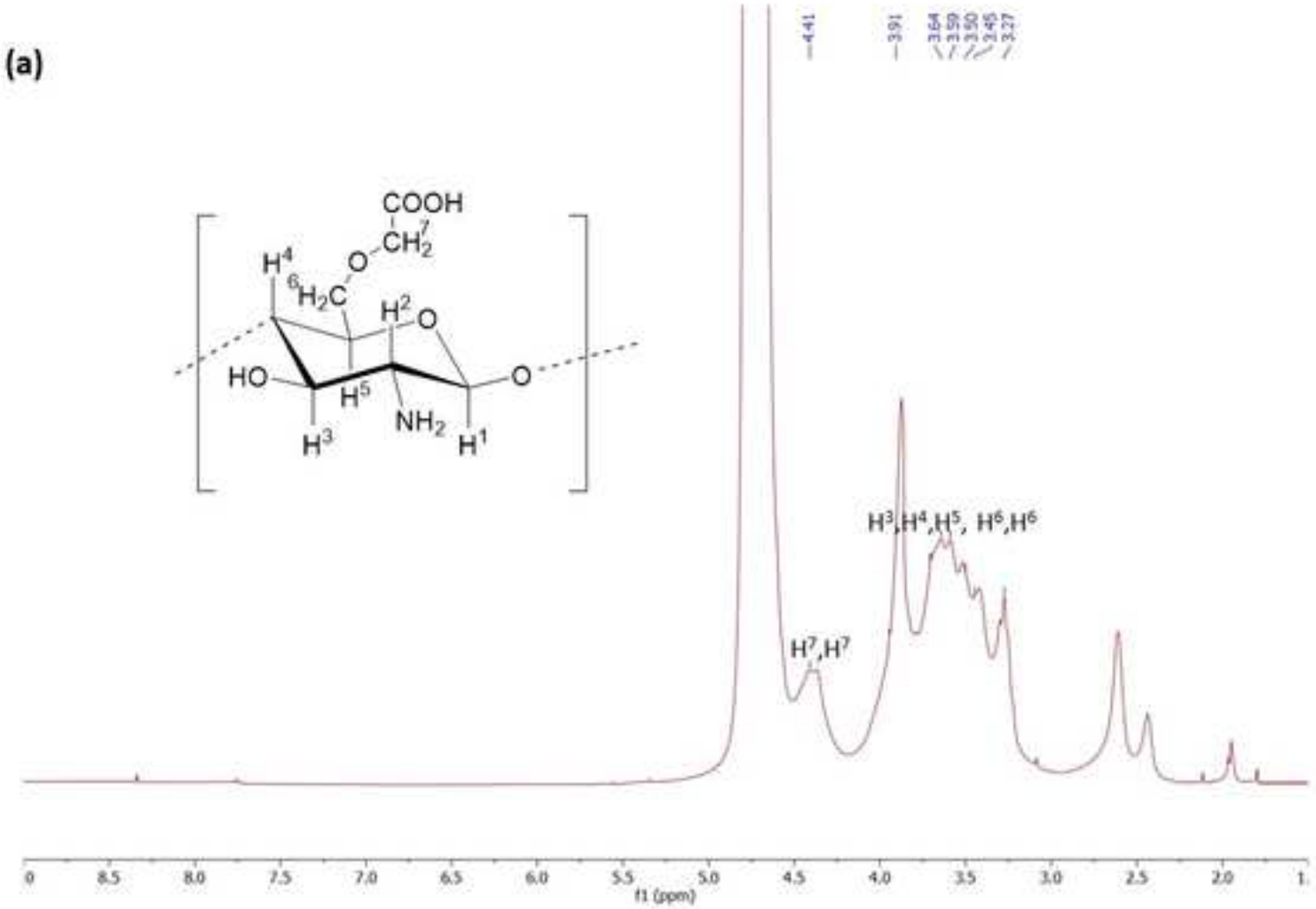

Figure

Click here to access/download;Figure;Figure 3b.jpg

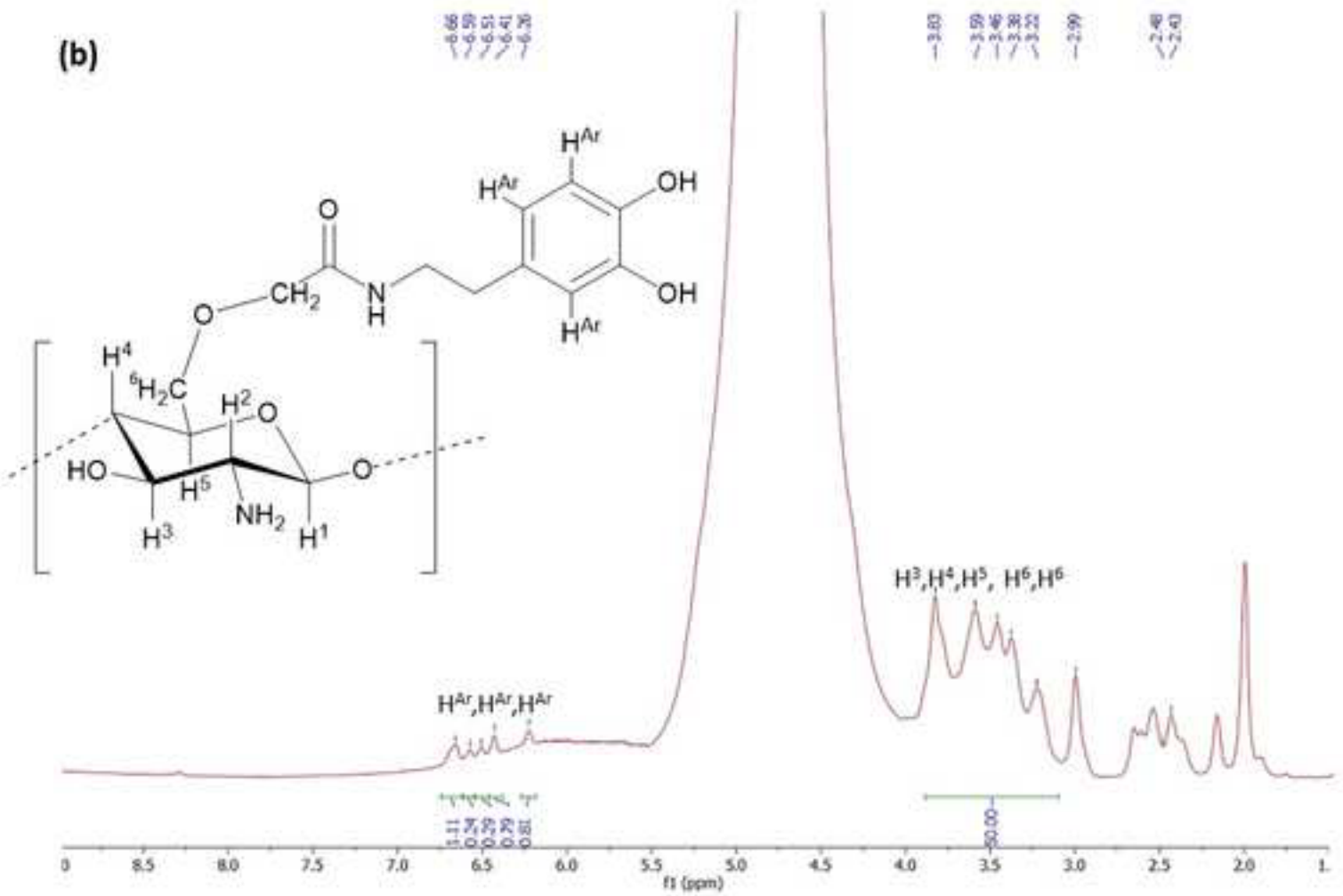

Figure

Click here to access/download;Figure;Figure 4a.jpg

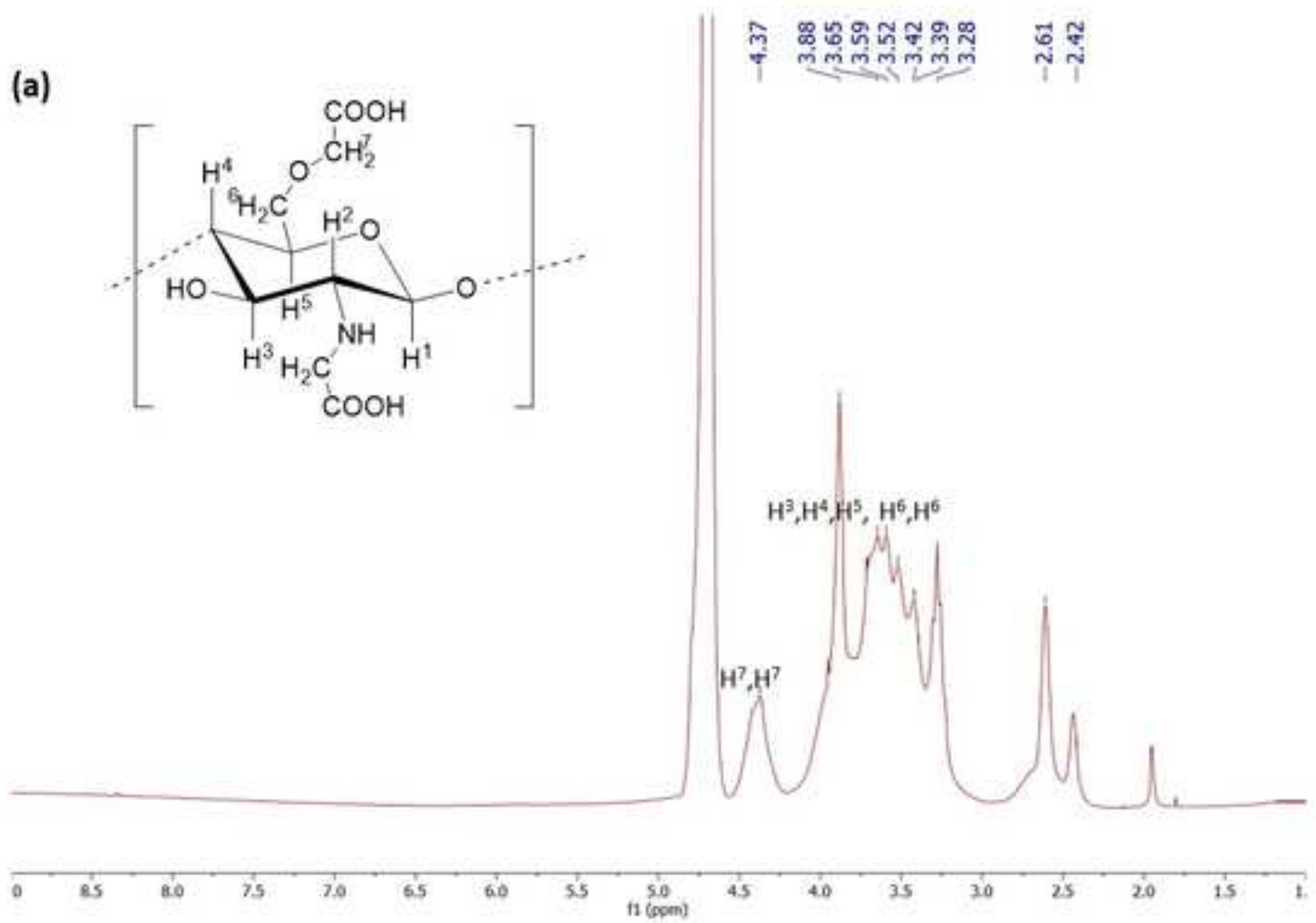

Figure

Click here to access/download;Figure;Figure 4b.jpg

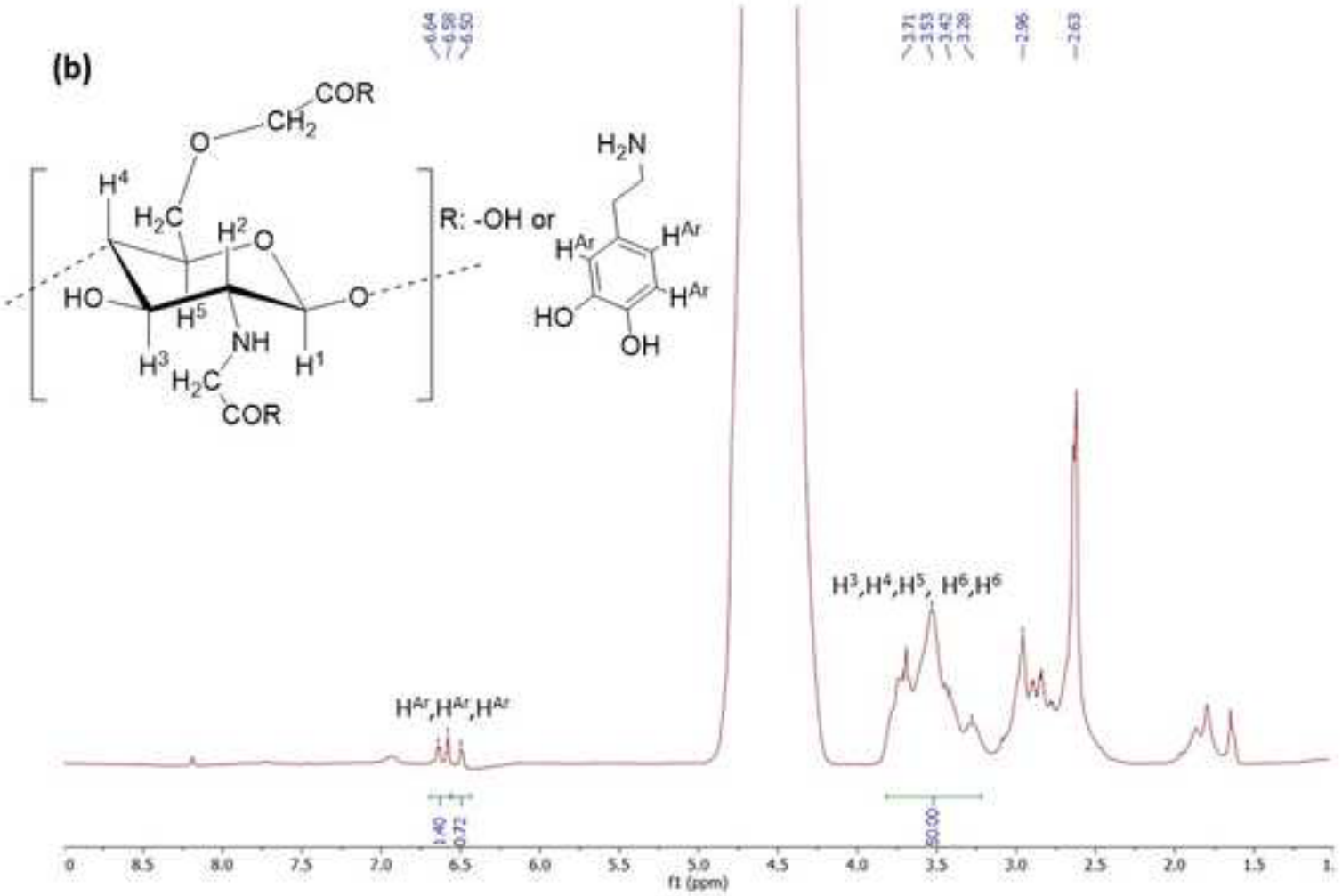

Figure

Click here to access/download;Figure;Figure 5 JPEG.jpg

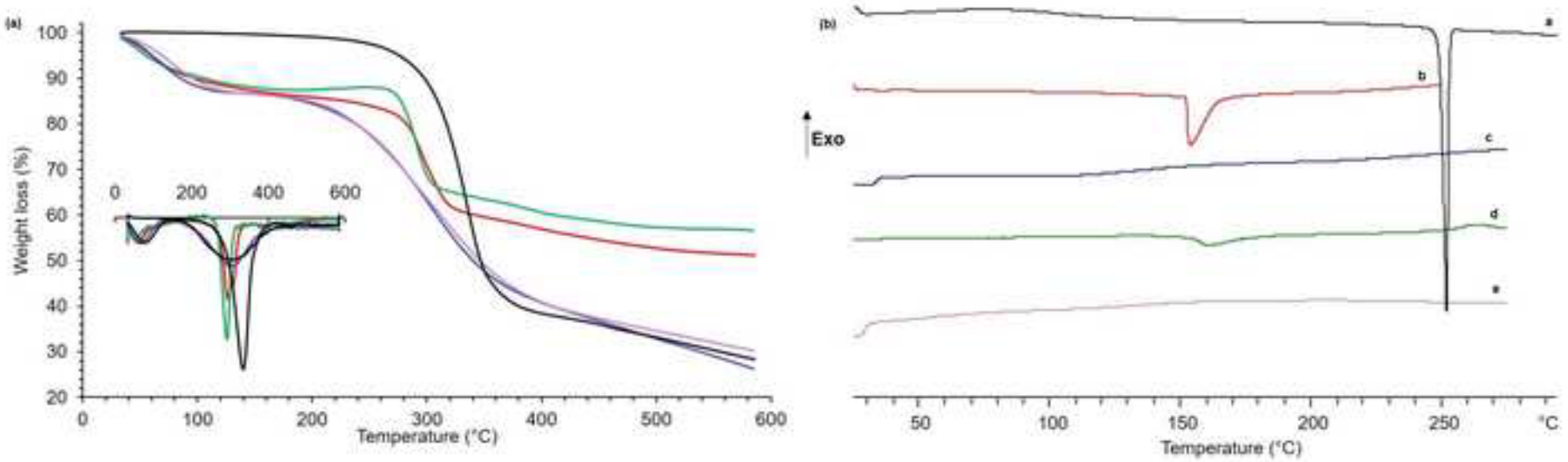

Figure

Click here to access/download;Figure;Figure 6 revised.jpg

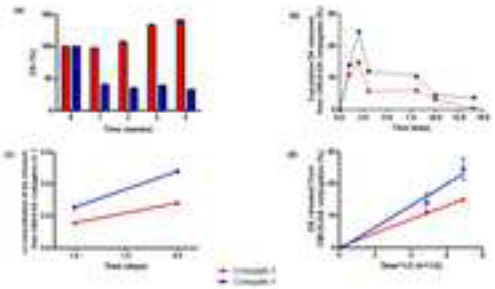

Figure

Click here to access/download;Figure;Figure 7 JPEG.jpg

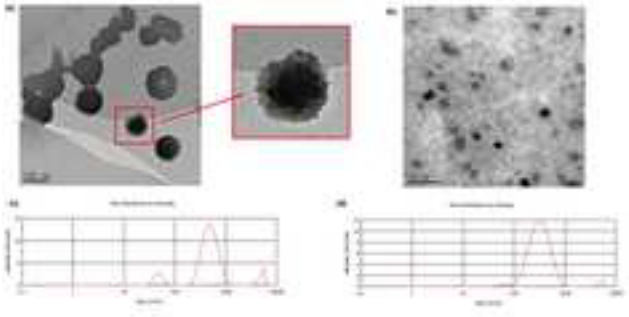

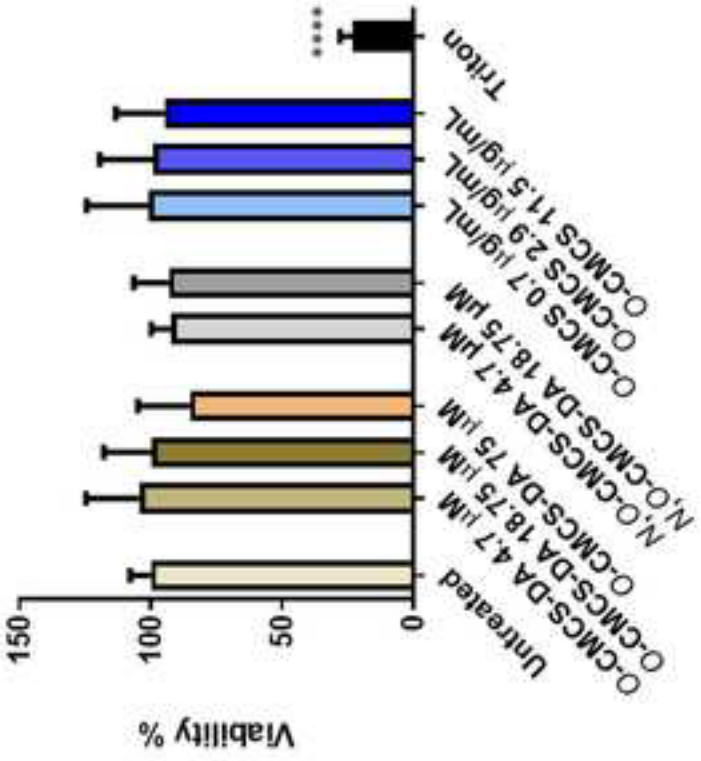

Figure

Figure

Click here to access/download;Figure;Figure 9 revised.tif

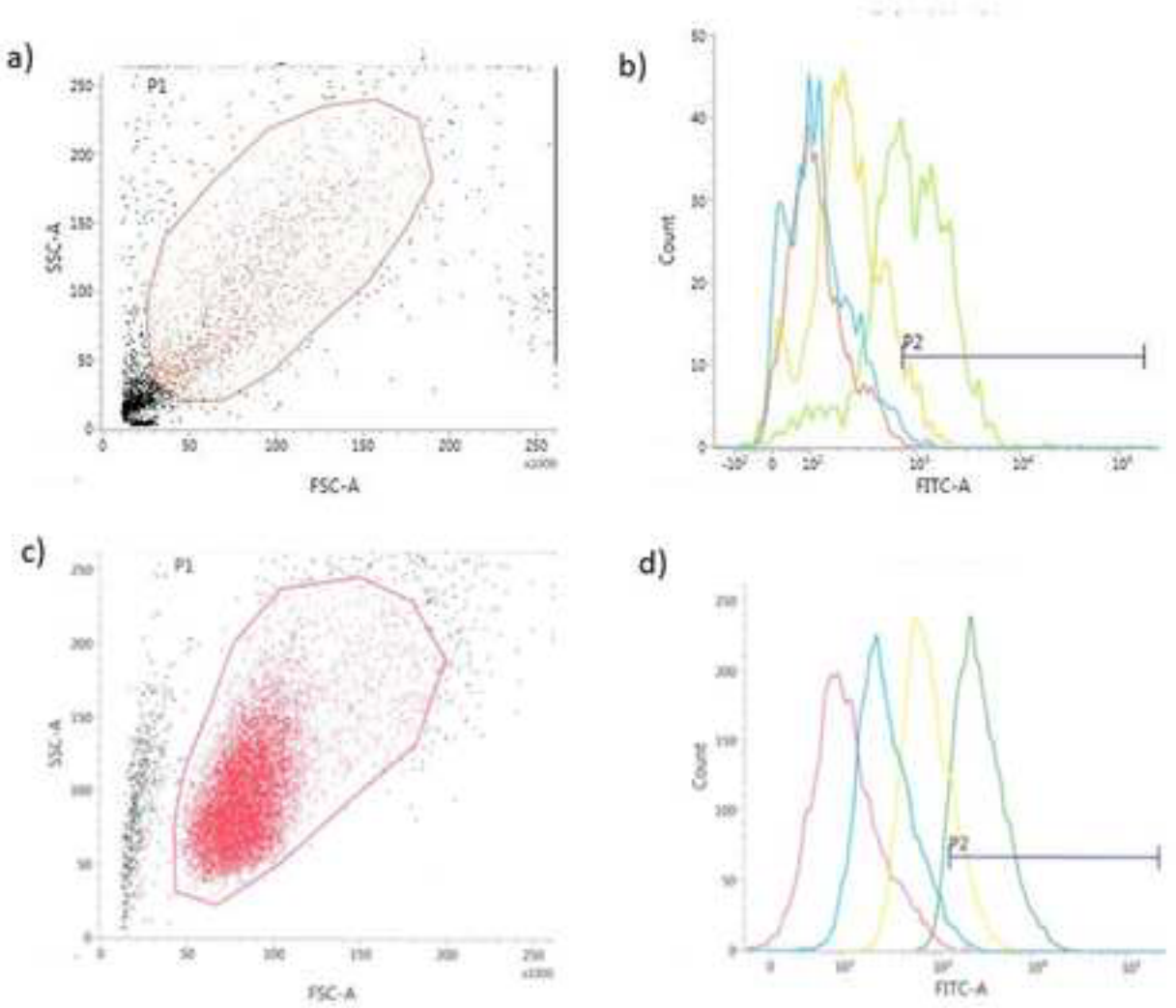

Figure

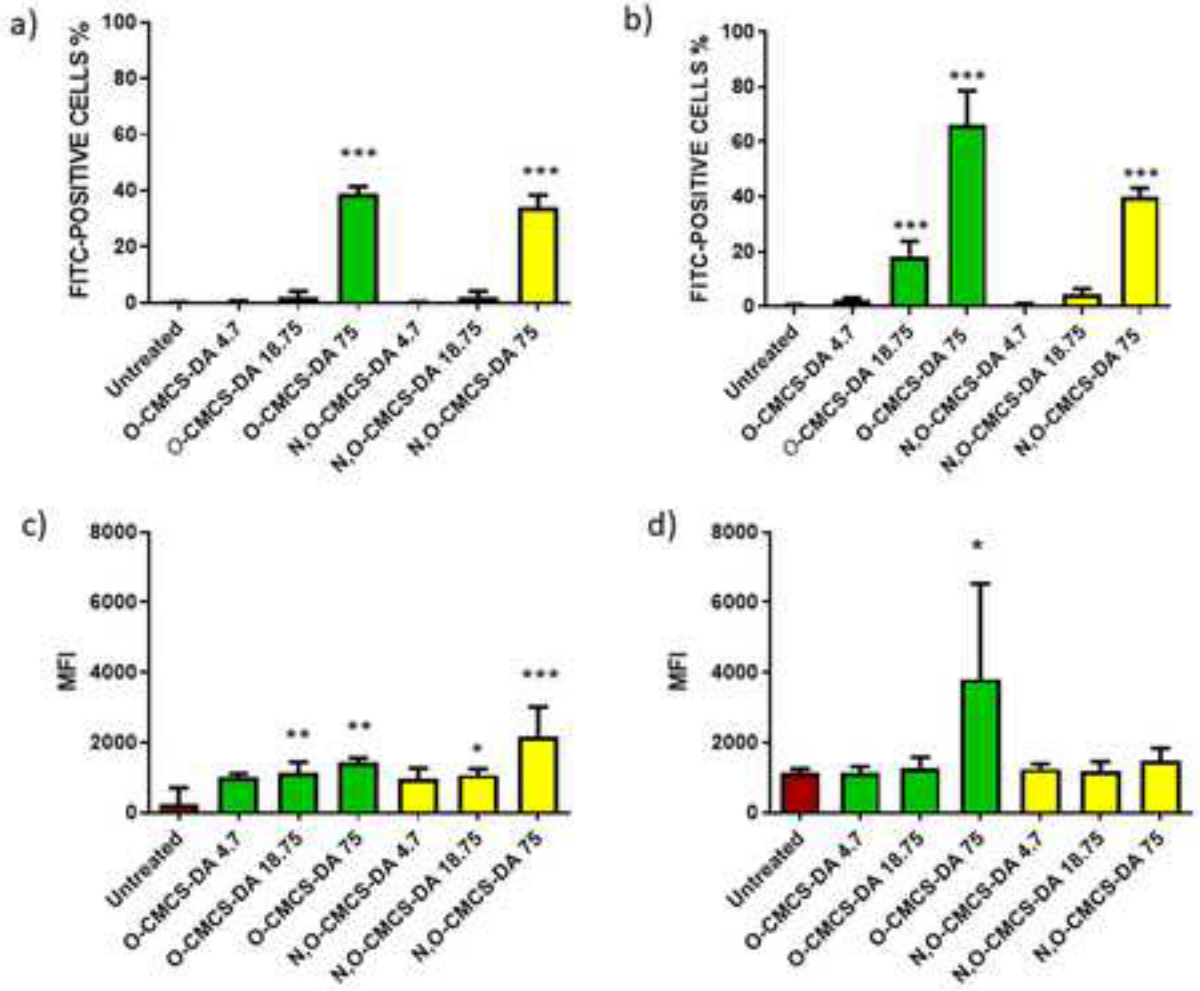

Figure

Click here to access/download;Figure;Figure S1 JPEG.jpg

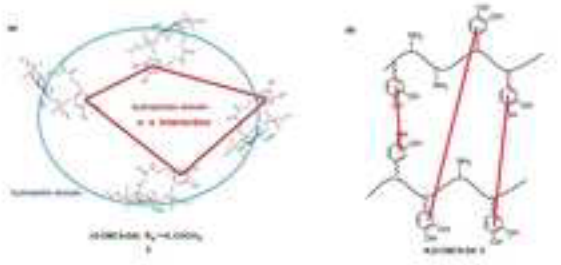

Figure

Click here to access/download;Figure;Figure S2 JPEG.jpg

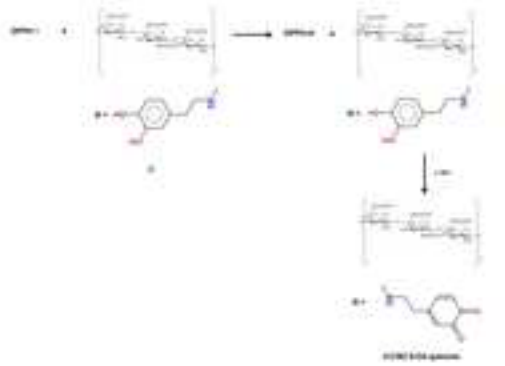

Table 1. Water/volatiles content, main temperature of decomposition (T_d) with the relevant weight losses percentages and residues at 600°C of DA, *N,O*-CMCS, *O*-CMCS and as well as the relevant conjugates with DA

Sample	**Water/volatiles (%)**	**T_d (°C)/weight loss (%)**	**Residue at 600°C (%)**
DA	-	327°C/71%	29%
N,O-CMCS	10.6%	295°C/17.5% 307.4°C/8.9%	51%
O-CMCS	12%	290°C/30.7%	57.2%
N,O-CMCS-DA **2**	12.7%	307.7°C/30.7%	26.8%
O-CMCS-DA **3**	13%	304.9°C/56.3%	30.5%

Table 2.

Conjugate	k_1 [day^{-1}]	$t_{1/2}$ [day]	$t_{1/2}$ [h]	K_H [% of DA released x $h^{-1/2}$]
N,O-CMCS-DA **2**	0.3129	2.2	52.8	2.169 ± 0.05698
O-CMCS-DA **3**	0.5626	1.2	28.8	3.414 ± 0.5314

Table 3. Properties of NPs obtained by conjugates **2** and **3.** Results are mean of 6 determinations±SD.

Formulation	Size (nm)	PDI	Zeta potential (mV)
NPs from *N,O*-CMCS-DA conjugate **2**	459±7	0.31-0.35	-2.2±0.2
NPs from *O*-CMCS-DA conjugate **3**	292±2	0.20-0.26	-14.6±0.3

Due to the sensitive nature of the questions asked in this study, survey respondents were assured raw data would remain confidential and would not be shared.
Data not available / The data that has been used is confidential

August 18, 2023

Prof Adriana Trapani

Declaration of interests

☐The authors declare that they have no known competing financial interests or personal relationships that could have appeared to influence the work reported in this paper.

☒The authors declare the following financial interests/personal relationships which may be considered as potential competing interests:

None reports writing assistance was provided by University of Bari Department of Pharmacy and Pharmacology. Adriana Trapani reports a relationship with University of Bari Department of Pharmacy and Pharmacology that includes: employment.